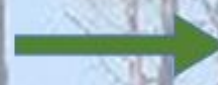


+



+



Daniela Fabíola de Matos Cecílio

# Treatment of an effluent polluted with Cr(III) by adsorption onto chemically modified agro-industrial waste

Master thesis in the scientific area of chemical engineering submitted to the Department of Chemical Engineering, Faculty of Science and Technology, University of Coimbra

September 2016



UNIVERSIDADE DE COIMBRA



Daniela Fabíola de Matos Cecílio

**Treatment of an effluent  
polluted with Cr(III) by  
adsorption onto agro-industrial  
waste chemically modified**

Master Thesis in the scientific area of Chemical Engineering and submitted  
to the Department of Chemical Engineering, Faculty of Science and  
Technology, University of Coimbra

Supervisor(s) :

Professor Doctor Licínio Manuel Gando de Azevedo Ferreira  
Professor Doctor Margarida Maria João de Quina

Host institutions:

CIEPQPF - Research Centre for Chemical Processes Engineering and Forest  
Products, Department of Chemical Engineering, Faculty of Sciences and  
Technology of the University of Coimbra

Coimbra  
2016



UNIVERSIDADE DE COIMBRA



*“Start by doing what’s necessary;  
then do what’s possible;  
and suddenly you are doing the impossible!”  
Francis of Assis*



## Acknowledgements

First of all, I'll thank my mother. I have the best mother of the world and don't tell me otherwise. I wanted to succeed and I worked hard to make you proud. I hope I did. You are the best. To my grandmother, thank you so much for everything. To my father, thank you for all the support and for believing that I could do it.

Aline, you are special. You deserve the best luck in the universe. Someday, you'll be a renowned Chemical Engineer, I know you will, and nothing will make me more proud than to say that I was, one day, your apprentice. This is not a "goodbye"; this is more a "see you later". You became someone dear that I didn't expect to find in these six months. Don't give up, keep smiling and... chromium is an amazing heavy metal, just misunderstood. :)

To my second family on B.10: Carolina and Vanessa. Thank you for all the support, all help and good moments. It was essential at some points when everything seemed to go wrong, it really made me maintain my courage to continue. I wish you all the luck in the world. To Giovanni and Joana, my companions in this journey to become Masters, I wish you all the luck. To Décio Lima, you are an adopted brother of B.10. You are a "big man". I wish you all the luck with your ionic liquids and don't give up on chromium. Chromium is good. To my sister Joana Cardoso for always being there, all those coffees, you will go far and I wish to be there to help you and wish you the best.

To all teachers who contributed for this day. Thank you for your teachings and orientation. It was necessary for this work to be what it is. Thank you to Professor Licínio Ferreira and Professor Margarida Quina for all the time and patience in orientating and helping to finish a Master Thesis that I'm proud off.

A special thanks to my friends. Sorry for having spoken only on Cr(III), adsorption and dissertation for the last months. It's over now. Thank you Mónica, Dina, Eliana, Ângela, Luis, Rúben, Rodrigo, Samarra, Sofia, Diana, Daniela and all of those that are not mentioned in here but they were always there. Your support and your smiles were really important. I'm very grateful for everything. You made my days brighter, even when they seemed too dark.

Another special thanks to FAAS (flame atomic absorption spectroscopy) for the happiest and saddest moments in this 6 months. With you I learnt that we could play God and break all the conservation of mass rules and that the only limits are the ones that we impose to ourselves.

Well... it's time to end a cycle and start a new adventure in the pursuit of my dreams. Let's end this, for I need a new challenge.





## Abstract

The adsorption process is one of the most used treatments to remove heavy metals from wastewater. Chromium is a contaminant which occurs frequently in effluents of tanneries, electroplating and dyeing. The hexavalent and trivalent states are the most stable forms of the metal in aqueous solution, and Cr (VI) is which exhibits higher level of toxicity causing thus damage to human and environmental health. The use of lignocellulosic waste as low cost adsorbents has been widely studied, however, this material has a low adsorption capacity. To overcome this problem, the material may be modified by physical and chemical treatments. In this work, the adsorption capacity of pine bark (*Pinus pinaster*) was improved by applying an acid and / or alkali treatment resulting in changes in the structural and chemical characteristics of the material. The treatment with different types of acid (citric acid, sulfuric, nitric, hydrochloric, phosphoric and acetic acid) did not improve the adsorption capacity of the material, so the study of this treatment was not pursued. In the alkali treatment (mercerization) was used NaOH solution. It was made a chemical and physical characterization of the adsorbent to evaluate the effects of mercerization and some differences in their properties before and after treatment were observed. The material was characterized by suitable analytical techniques, namely adsorption/desorption with N<sub>2</sub> at 77 K, SEM-EDS, point of zero charge method and acid-base titration for quantification of the active sites. Adsorption studies were performed, in batch mode, for different experimental conditions of the main operating variables, namely the contact time, pH and dosage adsorbent. From this study, it was concluded that the adsorption equilibrium of Cr (III) onto mercerised pine bark is reached in 3 h and the maximum amount of adsorbed Cr (III) occurs at pH = 5. In the tests performed to determine equilibrium isotherms, the effect of initial pH of the solution was evaluated. The equilibrium data were well fitted by the Langmuir model yielding a maximum adsorption capacity of 17.15 mg g<sup>-1</sup> at pH = 5. It was also proposed a new model based on the Langmuir modified equation to describe the equilibrium isotherms as function of initial pH of the solution. Finally, the application of a Box-Benken Design allowed to identify an optimal region of operation and infer the variables that most influence the Cr(III) removal efficiency.

Keywords: Adsorption; Trivalent chromium; Pine bark; Mercerization; Box-Benken Design.



## Resumo

O processo de adsorção é um dos tratamentos mais utilizados para remover metais pesados de efluentes. O crómio é um contaminante que ocorre frequentemente em efluentes de indústrias de curtumes, galvanoplastia e tinturarias. Os estados trivalente e hexavalente são as formas mais estáveis deste metal em solução aquosa, sendo o Cr(VI) o que apresenta maior grau de toxicidade para a saúde ambiental e humana. A utilização de resíduos lenhocelulósicos como adsorventes de baixo custo tem vindo a ser amplamente estudado, no entanto, estes materiais apresentam uma capacidade de adsorção baixa. Para ultrapassar este problema, este material pode ser modificado através de tratamentos físicos e químicos. Neste trabalho, a capacidade de adsorção da casca de pinheiro (*Pinus Pinaster*) foi melhorada aplicando um tratamento ácido e/ou alcalino do qual resultam alterações nas características estruturais e químicas do material. O tratamento com diferentes tipos de ácidos (ácido cítrico, sulfúrico, nítrico, clorídrico, fosfórico e acético) não melhorou as capacidades de adsorção do material, pelo que esta via de tratamento não foi prosseguida. No tratamento alcalino (mercerização) foi usado uma solução de NaOH. Foi feita uma caracterização química e física do adsorvente para avaliar os efeitos da mercerização, notando-se algumas diferenças nas suas propriedades antes e depois do tratamento. O material foi caracterizado pelas técnicas de adsorção/dessorção de N<sub>2</sub> a 77 K, SEM-EDS, ponto de carga nula e quantificação dos sítios ativos. Foram realizados estudos de adsorção em descontínuo para diferentes condições experimentais das principais variáveis operatórias, nomeadamente o tempo de contacto, o pH e a dosagem de adsorvente. Deste estudo concluiu-se que o equilíbrio de adsorção de Cr(III) em casca de pinheiro mercerizado é alcançado ao fim de 3 h e que a quantidade máxima de Cr(III) adsorvido ocorre a pH = 5. Nos ensaios realizados para a determinação de isotérmicas de equilíbrio foi avaliado o efeito do pH inicial da solução. Os dados de equilíbrio foram bem ajustados pelo modelo de Langmuir tendo-se obtido uma capacidade máxima de adsorção de 17,15 mg g<sup>-1</sup> a pH = 5. Foi também proposto um novo modelo baseado na equação modificada de Langmuir para descrever as isotérmicas de equilíbrio em função do pH inicial da solução. Por último, aplicou-se um desenho fatorial do tipo “Box-Benken Design” que permitiu identificar uma gama ótima de operação e inferir sobre as variáveis que mais condicionam a eficiência de remoção de Cr(III).

**Palavras-chaves:** Adsorção; Crómio trivalente; Casca de pinheiro; Mercerização; Box-Benken Design.



# List of contents

<i>List of contents</i> .....	<i>V</i>
<i>List of Figures</i> .....	<i>VII</i>
<i>List of Tables</i> .....	<i>IX</i>
<i>Nomenclature, Abbreviations, Symbols</i> .....	<i>XI</i>
<b>1. Introduction</b> .....	<b>1</b>
<b>1.1 Motivation</b> .....	<b>1</b>
<b>1.2 Objective</b> .....	<b>1</b>
<b>1.3 Organization of the dissertation</b> .....	<b>2</b>
<b>2. Fundamentals</b> .....	<b>3</b>
<b>2.1 Environmental pollution with heavy metals</b> .....	<b>3</b>
<b>2.2 Physico-chemical processes for the treatment of effluents contaminated with heavy metals</b> .....	<b>6</b>
2.2.1 Chemical precipitation .....	7
2.2.2 Coagulation and Flocculation .....	8
2.2.3 Electrochemical treatment .....	9
2.2.4 Membrane Filtration .....	9
2.2.5 Ion Exchange .....	9
<b>2.3 Adsorption Processes</b> .....	<b>10</b>
2.3.1 Fundaments of adsorption processes .....	10
2.3.2 Factors affecting adsorption processes .....	10
2.3.3 Adsorption Isotherms.....	12
2.3.4 Adsorption Kinetics .....	13
2.3.5 Adsorbent material.....	16
<b>2.4 Lignocellulosic Residues</b> .....	<b>16</b>
<b>3. State of the art</b> .....	<b>21</b>
<b>3.1 Chemical treatments of lignocellulosic materials</b> .....	<b>21</b>
3.1.1 Alkali treatment .....	21
3.1.2 Acid treatment.....	23
<b>3.2 Literature review</b> .....	<b>24</b>
<b>4. Methodologies</b> .....	<b>27</b>
<b>4.1 Materials and reagents</b> .....	<b>27</b>
<b>4.2 Adsorbent modification</b> .....	<b>27</b>
4.2.1 Mercerization .....	27
4.2.2 Acid treatment.....	28
<b>4.3 Adsorbent characterization</b> .....	<b>28</b>
4.3.1 Physical properties .....	28
4.3.2 Scanning Electronic Microscopy and Energy Dispersive Spectroscopy (SEM-EDS). .....	28
4.3.3 Surface actives sites by Boehm Titration method.....	28
4.3.4 Point of zero charge .....	30
<b>4.4 Adsorption studies</b> .....	<b>30</b>
4.4.1 Adsorption equilibrium isotherms .....	30
4.4.2 Effect of contact time.....	31
4.4.3 Effect of initial pH .....	31

<b>4.5</b>	<b>Modeling adsorption data .....</b>	<b>31</b>
4.5.1	Equilibrium isotherms.....	31
4.5.2	Design of experiments (DOE) .....	31
<b>5.</b>	<b>Results and discussion .....</b>	<b>33</b>
<b>5.1</b>	<b>Surface chemical modification.....</b>	<b>33</b>
5.1.1	Effect of particle size .....	33
5.1.2	Effect of chemical treatment – NaOH (mercerization).....	33
5.1.3	Effect of chemical treatment – Acids.....	35
<b>5.2</b>	<b>Characterization of adsorbent .....</b>	<b>36</b>
5.2.1	BET surface area, porosity and density .....	36
5.2.2	Scanning Electronic Microscopy and Energy Dispersive Spectroscopy (SEM-EDS).....	37
5.2.3	Determination of surface actives sites by Boehm Titration method.....	40
5.2.4	Point of zero charge .....	41
<b>5.3</b>	<b>Adsorption studies .....</b>	<b>43</b>
5.3.1	Effect of contact time.....	43
5.3.2	Effect of initial pH .....	44
5.3.3	Equilibrium adsorption isotherms.....	45
5.3.4	Design of experiments (DOE) .....	49
<b>6.</b>	<b>Conclusion and future work .....</b>	<b>52</b>
	<b>Bibliography .....</b>	<b>54</b>
<b>7.</b>	<b>Appendixes.....</b>	<b>I</b>
	<b>Appendix A - Different adsorption isotherm models and their assumptions .....</b>	<b>I</b>
	<b>Appendix B – Isotherm models adjust to adsorption data.....</b>	<b>IV</b>
	<b>Appendix C - State of the art (for other heavy metals).....</b>	<b>V</b>
	<b>Appendix D – Design of Experiments (DOE) .....</b>	<b>VII</b>
	<b>Appendix E – SEM-EDS results .....</b>	<b>VIII</b>
	<b>Appendix F - Quarterly report of “Águas de Coimbra” .....</b>	<b>IX</b>
	<b>Appendix G – Script of MATLAB used for the adsorption isotherm fitting.....</b>	<b>X</b>
	<b>Appendix H – mm to Mesh.....</b>	<b>XIII</b>
	<b>Appendix I - Physical properties of pine bar .....</b>	<b>XIV</b>
	<b>Appendix J - Effect of adsorbent dosage.....</b>	<b>XXII</b>

## List of figures

Fig. 2.1: Speciation of chromium at a given pH ( $[\text{Cr(III)}] = 1,0 \text{ ppm}$ ). Adapted from <sup>32</sup> .....	5
Fig. 2.2: Pourbaix diagram for chromium at $T=25 \text{ }^\circ\text{C}$ in an aqueous solution. $[\text{Cr(aq)}]_{\text{total}}=10^{-6} \text{ m}$ . Adapted from <sup>34</sup> .....	6
Fig. 2.3: Chemical precipitation process of heavy metals .....	8
Fig. 2.4: Coagulation and flocculation processes to remove heavy metals from contaminated effluents .....	8
Fig. 2.5: Representation of adsorption isotherms .....	12
Fig. 2.6: Steps of the adsorption process. Adapted from <sup>54</sup> .....	14
Fig. 2.7: Chemical composition of bark in comparison to chemical composition of wood (values approximated). Adapted from <sup>64</sup> .....	18
Fig. 2.8: A possible molecular structure of lignin. Adapted from <sup>68</sup> .....	19
Fig. 2.9: molecular structure of cellulose. Adapted from <sup>70</sup> .....	19
Fig. 2.10: <i>Pinus pinaster</i> bark .....	20
Fig. 3.1: Structure of cellulose chains. Adapted from <sup>76</sup> .....	22
Fig. 3.2: Mercerization (step 3) using a NaOH solution. Adapted from <sup>77</sup> .....	23
Fig. 3.3: Transformation of Cellulose I into Cellulose II during mercerization process. Adapted from <sup>73</sup> .....	23
Fig. 3.4: General process of esterification of cellulose using a catalyst and heat. Adapted from <sup>83</sup> .....	24
Fig. 5.1: Adsorption test to raw pine bark with different particle sizes (d in mm) .....	33
Fig. 5.2: Effect of concentration of NaOH solution for pine bark modification in its adsorption capacity (a) and in its efficiency (b) .....	34
Fig. 5.3: Effect of acid treatment in the adsorption capacity of Cr(III) (a) and in its removal efficiency (b) .....	35
Fig. 5.4: Images obtained by SEM of pine bark ( <i>Pinus pinaster</i> ) raw (a) and mercerized (b) (1000x) .....	38
Fig. 5.5: EDS of raw pine bark .....	38
Fig. 5.6: EDS of mercerized pine bark .....	39
Fig. 5.7: EDS of mercerized pine bark after adsorption of Cr(III) .....	40
Fig. 5.8: Active sites on raw and mercerized pine bark .....	40
Fig. 5.9: Point of zero charge pH for pine bark raw and mercerized .....	42
Fig. 5.10: Effect of contact time on Cr(III) removal .....	43
Fig. 5.11: Effect on pH on Cr(III) removal. ....	44
Fig. 5.12: Adsorption isotherms of Cr(III) on mercerized pine bark at $25 \text{ }^\circ\text{C}$ , for different initial pH values. Symbols represent the experimental data and the lines Langmuir model. ....	46
Fig. 5.13: Adsorption isotherms of Cr(III) on mercerized pine bark, at $25 \text{ }^\circ\text{C}$ , for different initial pH values. Symbols represent the experimental data and the lines Freundlich model. ....	46
Fig. 5.14: Pareto chart obtained after Box-Benken Design results .....	50
Fig. 5.15: Observed values in function of predicted values .....	50

Fig. 5.16: Surface response of the Box-Benken Design (a) the influence of $C_0$ and pH (b) the influence of temperature and pH.....	51
Fig. 5.17: Surface response of the Box-Benken design (a) influence of T and L/S relation (b) influence of T and $C_0$ .....	51
Fig. 5.18: Surface response of the Box-Benken Design. Influence of L/F and $C_0$ on removal efficiency.....	51



## List of tables

Table 2.1: Origin of heavy metals present in effluents and their effects to human health when in high concentration. ....	4
Table 2.2: Advantages and disadvantages of the different physico-chemical treatments of effluents contaminated with heavy metals. ....	7
Table 2.3 - Difference between physical and chemical adsorption.....	10
Table 2.4: Chemical composition of pine barks (values in % of material). ....	18
Table 3.1: Adsorption of Cr(III) on lignocellulosic residues without treatment.....	25
Table 3.2: Adsorption of Cr(III) on lignocellulosic residue pre-treated.....	25
Table 4.1: Inputs for the Box-Benken design.....	32
Table 5.1: Physical properties of raw pine bark and mercerized pine bark.....	37
Table 5.2: Langmuir and Freundlich model and adjust parameters .....	47
Table 5.3: Data information for the new model proposal.....	48
Table 5.4: Limits of the window of search .....	48



## Nomenclature, Abbreviations, Symbols

BBD	Box-Benken design
C	Concentration ( $\text{mg L}^{-1}$ or ppm)
$C_0$	Initial concentration of adsorbate ( $\text{mg L}^{-1}$ )
$C_e$	Concentration of the adsorbate on equilibrium ( $\text{mg L}^{-1}$ or ppm)
Cell-OH	Hydroxyl groups of cellulose
$C_f$	Final adsorbate concentration ( $\text{mg L}^{-1}$ or ppm)
Cr(III)	Trivalent chromium
Cr(VI)	Hexavalent chromium
DOE	Design of experiments
EDS	Energy dispersive spectroscopy
FAAS	Flame atomic absorption spectroscopy
$k_1$	Rate constant of the pseudo-first order model ( $\text{min}^{-1}$ )
$k_2$	Rate constant of the pseudo-second order model ( $\text{g (mg min)}^{-1}$ )
$k_F$	Freundlich isotherm constant ( $\text{mg}^{1-(1/n)} \text{L}^{1/n} \text{g}^{-1}$ )
$k_L$	Langmuir isotherm constant ( $\text{L mg}^{-1}$ )
L/S	Liquid-to-solid rate
$\text{M(OH)}_x$	Hydroxide species precipitated
$\text{M}^+$	Cation formed by the dissolution of heavy metal
$m_{\text{dried bark}}$	Weight of a sample of dried bark used in that specific experiment (g)
n	Freundlich isotherm constant
Na-cell	Sodium cellulose complexes
$N_B$	Concentration of the standardized solution of NaOH ( $\text{Eq L}^{-1}$ )
PZC	Point of zero charge
q	Adsorption capacity ( $\text{mg g}^{-1}$ )
$q_e$	Equilibrium adsorption capacity ( $\text{mg g}^{-1}$ )
$Q_{\text{max}}$	Maximum adsorption capacity ( $\text{mg g}^{-1}$ )
$q_t$	Adsorption capacity at a given time t ( $\text{mg g}^{-1}$ )
R	Carboxyl groups introduced by an acid solution
$R_{\text{eff}}$	Removal efficiency (%)
$R_L$	Dimensionless constant
SEM	Scanning electronic microscopy
t	Time (min)
TAS	Total acid sites ( $\text{mEq g}^{-1}$ )
TBS	Total basic sites ( $\text{mEq g}^{-1}$ )
V	Volume of titration solution used (mL)
$V_{\text{al}}$	Volume of the sample used for titration (mL)
$V_{\text{Am}}$	Total volume of standardized solution of NaOH used in titration of the sample (mL)
$V_B$	Total volume of standardized solution of NaOH used in titration of the reference (mL)
$V_S$	Volume of the solution (mL)
$V_T$	Total volume of neutralizing solution used in the experiment (mL)
$\text{X(OH)}^-$	Hydroxide species
$\phi$	Diameter of particle pores (mm)



# 1. Introduction

## 1.1 Motivation

The presence of heavy metals in industrial wastewater is one of the main concerns nowadays for threatening the public health and the environment if discharged without adequate treatment. This concern is due to the fact that these pollutants are very toxic, bioaccumulative characteristics and harmful<sup>1</sup>.

Chromium is frequently found in effluents from electroplating industries, leather tanning, metal finishing and chromate preparations. It can appear in two principal forms: trivalent chromium (Cr(III)) and hexavalent chromium (Cr(VI)). The latter form is of greater concern because of its carcinogenic properties<sup>2-5</sup>.

There are several methods to remove heavy metals from wastewater, such as chemical precipitation, coagulation-flocculation, ion-exchange, membrane filtration and adsorption. However, most of these treatments are expensive, require high maintenance costs, produce toxic sludge or have large consumption of chemicals. Adsorption process is often considered one of the best technologies<sup>1,6-8</sup>.

Adsorption can remove most of pollutants, the metal can be recovered by desorption and the adsorbent can normally be reused. However, it can require a high initial investment since for adsorbing a specific metal, a specific resin or activated carbon is required. To surpass this difficulty, it has been studied the use of agro-industrial residues, also known as lignocellulosic residues, as potential low-cost adsorbent. Those lignocellulosic residues have a low capacity for the removal of heavy metals as result of their chemical composition. To enhance this characteristic, the material can be subjected to physical treatment, such as grinding, or to chemical treatment with an acid or alkali solutions<sup>6,8-10</sup>.

One of the most abundant agro-industrial residues in Portugal is pine bark (*Pinus pinaster*) which has only been used as a soil fertilizer after its decomposition, or as fuel. It could be, therefore considered for low cost adsorbent<sup>11,12</sup>.

## 1.2 Objective

This study will be focused on the removal of Cr(III) from contaminated effluents by adsorption using a low-cost lignocellulosic residue, pine bark, chemically modified with alkali and acid solutions.

With this objective in mind, it will be made firstly a characterization (physical, morphological and chemical), before and after modification of the adsorbent. Then it will be

studied the effect of various parameters, such as effect of contact time, pH and adsorption equilibrium isotherms. After that it will be developed a model that relates the equilibrium adsorption capacity of the adsorbent as a function of pH, one of the most important parameters of adsorption processes. Flame atomic absorption spectroscopy (FAAS) will be used as analytical method to analyze the concentration of chromium on the solution before and after adsorption.

Statistical methods will be employed to understand the influence of the experimental parameters on adsorption processes using a design of experiments (DOE).

### **1.3 Organization of the dissertation**

This dissertation is organized in six main chapters. The first is introduction where it will be explained the problematic in study, the objective and the organization of the work. Then it would be made a brief overview of the fundamentals (Chapter 2) about heavy metals, waste water treatments, adsorption processes and lignocellulosic residues. In Chapter 3 it will be made a state of the art about the different chemical treatments of lignocellulosic residues and a literature review about the adsorption of Cr(III) onto lignocellulosic materials. Chapter 4 will be focused on explaining the methodologies used in this work while in Chapter 5 results will be exposed and discussed. For last, Chapter 6 are the conclusions and some appointments and suggestions for future works.

## 2. Fundamentals

### 2.1 Environmental pollution with heavy metals

In the recent years, there has been a major concern toward the impact of anthropogenic activities in nature, namely the ones caused by heavy metals. If contaminated effluents are discharged without treatment, they can cause severe problems on the environment and human health<sup>13-15</sup>.

With the increase of industrialization, effluents contaminated with heavy metals increased as well, and studies for investigating and creating new cost-effective methods for the treatment of those effluents are being strongly encouraged<sup>16,17</sup>.

In general, the term “heavy metal” refers to a group of metal and metalloids with atomic density higher than  $6 \text{ g cm}^{-3}$ . Heavy metals do not only appear as resultant of industrial activity, but they can also occur naturally on earth’s crust as rock formations or as ore minerals. Following this definition, metals such as cadmium (Cd), nickel (Ni), lead (Pb), copper (Cu), mercury (Hg), zinc (Zn) and chromium (Cr) are classified as heavy metals and they are also commonly associated with high toxicity and adverse effects in nature<sup>8,18</sup>.

Heavy metals are characterized by being non-biodegradable, like any other metal, and easily enter the food chain. If they are in aquatic environments, water supply or the biosystems living there can be strongly affected. Although, some of those metals are vital for the organism in small doses, in higher concentration they can induce various diseases and disorders. In Table 2.1, it can be seen the origins of effluents contaminated with heavy metals and their effects on human health<sup>7,8,15,19,20</sup>.

Heavy metals have been found in aqueous effluents originated from industries such as mining, refining ores, fertilizers industries, tanneries, metal pigment, battery manufacture, petroleum refining and production of pesticides. Chromium is one common contaminant in industrial effluents, and very difficult to remove<sup>14,21,22</sup>.

Table 2.1: Origin of heavy metals present in effluents and their effects to human health when in high concentration.

<b>Metal</b>	<b>Origin</b>	<b>Effect</b>
Cd	Fertilizers, metalliferous mining, electronics, pigments, plastic, refining.	Carcinogenic, weight loss, hypertension, renal disturbances, bone lesions.
Cr	Electroplating, textile dyeing, tanneries, steel manufacturing.	Lung tumor, mutagenic agent, severe diarrhea.
Cu	Electroplating, metallurgical industries (alloys and steels), paints.	Lethargy, weakness, anorexia, gastrointestinal tract damage.
Hg	Electronics, batteries.	Neurobehavioral disorders, renal disturbances, corrosive to skin, eyes, muscles.
Ni	Paint formulation, electroplating, and mineral processing, steam electric power plants.	Lung cancer, allergic responses, chronic bronchitis.
Pb	Pigments, electroplating, manufacturing of batteries, fertilizer.	Brain damage, anaemia, anorexia, kidney damage.
Zn	Batteries, paints, pigments, fertilizers, mining.	Gastrointestinal distress, diarrhea, nausea.

Chromium was discovered in 1798, by a French chemist named Nicholas Louis Vanquelin, due to the large range of colors this element could produce in a solution. Its name derives from the Greek word *chroma*, which means color. One example of the range of colors this element can take can be found on the gemstones, such as emerald and ruby, which own their colors green and red, respectively<sup>23</sup>.

This heavy metal is also one of the most abundant element of earth being usually found in the form of ferric chromite ore,  $\text{FeCr}_2\text{O}_4$ . It can also be found in the form of crocoite,  $\text{PbCrO}_4$ , and chrome ochre,  $\text{Cr}_2\text{O}_3$ <sup>23,24</sup>.

Chromium exists in both natural water and industrial effluents. For example, drinking water should have a concentration of no more than  $0,05 \text{ mg L}^{-1}$  of chromium. In Portugal, the concentration of chromium advised to have in drinking water can be found on Decreto de Lei n.º 306/2007 de 27 de Agosto de 2007.

Chromium has many oxidation states but the most stable ones are trivalent chromium (Cr(III)) and hexavalent chromium (Cr(VI))<sup>14,24</sup>. It is important to understand that these two oxidation states have different chemical, biological and environmental properties and thus they must be treated differently. For instance, Cr(III) is less toxic than Cr(VI) for about 1000 times, it has less mobility in the environmental compartments\* and is essential in normal carbohydrate, lipid and protein metabolism. Contrarily, Cr(VI) is very toxic for the human health, and in general considered carcinogenic agent<sup>1,24-29</sup>.

\* Considering that there are four major environmental compartments or conceptual spheres: atmosphere, hydrosphere, lithosphere and biosphere.



The form in which the Cr(VI) appear in nature or in effluents depends mainly on the pH and concentration. It can appear in its neutral or anionic form as chromate ( $\text{CrO}_4^{2-}$ ), chromic acid ( $\text{HCrO}_4^-$ ) or as dichromate ( $\text{Cr}_2\text{O}_7^{2-}$ )<sup>30</sup>.

On the other hand, Cr(III) usually appears in the form of stable complexes or in its the cationic form depending on the pH of the medium, redox potential and reactions, hydrolysis or adsorptions<sup>30-32</sup>.

Without complexation agents, Cr(III) can appear as a moderately strong acid that is deprotonated with the increase of pH as it can be seen at Eq. 2.1 to Eq. 2.3<sup>32</sup>.

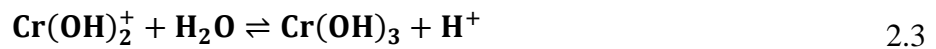
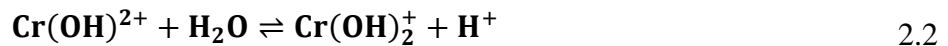
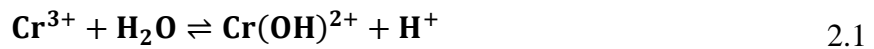


Fig. 3.1 shows the speciation of chromium as function of pH. At pH below 4, Cr(III) appears as  $\text{Cr}^{3+}$ . With the increasing of the pH, from 4 to 6, the most common form is  $\text{Cr}(\text{OH})^{2+}$ , and above pH 6 it can occur precipitation of the chromium in the form of  $\text{Cr}(\text{OH})_3$ . Cr(III) has an amphoteric behavior becoming soluble again at high pH (pH > 10) in the form of  $\text{Cr}(\text{OH})_4^-$ . This comportment can be observed on Eq. 2.4. and in Fig. 2.1 below<sup>30-32</sup>.

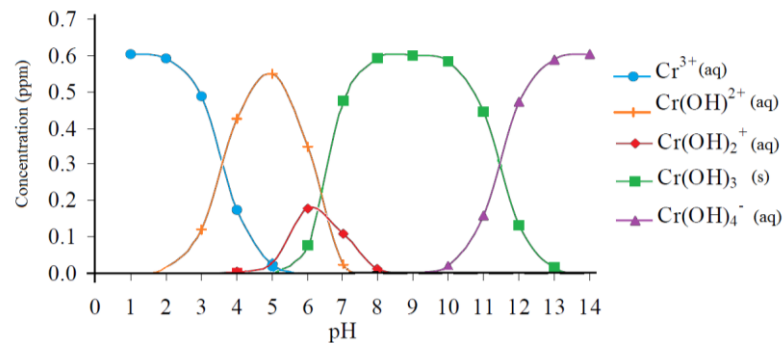
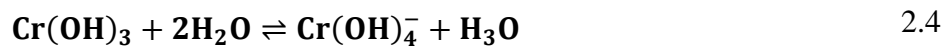


Fig. 2.1: Speciation of chromium at a given pH ( $[\text{Cr}(\text{III})] = 1,0 \text{ ppm}$ ). Adapted from <sup>32</sup>

Another way to understand in which form chromium will appear depending on the pH is analyzing a Pourbaix diagram, Fig.2.2, in diluted aqueous solutions, in the presence of air and in the absence of any other complexing agent than  $\text{H}_2\text{O}$  or  $\text{HO}^-$ . In this potential-pH diagram, it can be seen how chromium reacts in aqueous solutions. It is very important to consider this diagram for chromium, because it helps to understand in which form this heavy metal will appear in an aqueous solution at a given pH<sup>33,34</sup>.

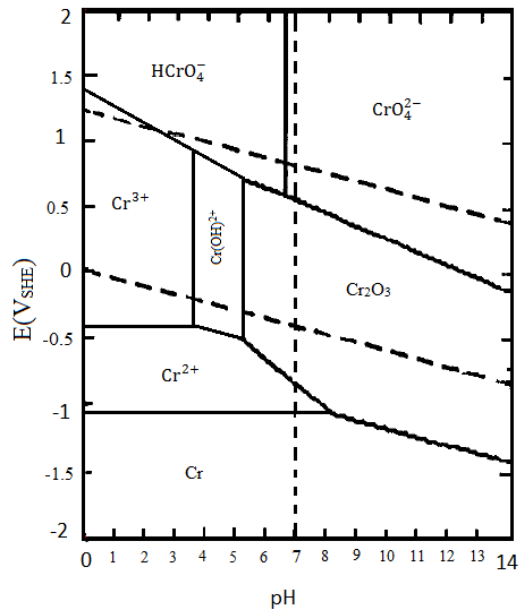


Fig. 2.2: Pourbaix diagram for chromium at T=25 °C in an aqueous solution.  $[\text{Cr}(\text{aq})]_{\text{total}}=10^{-6}$  m. Adapted from<sup>34</sup>.

When treating effluents contaminated with heavy metals, the selection of the best methodology can become a difficult and complex task. Some factors should be taken into account such as: chemical composition of the effluent, pollutant to be removed, operating costs of the treatment, available space for the construction of treatment facilities, waste disposal constraints and desired water quality at the end of the treatment<sup>35</sup>.

## 2.2 Physico-chemical processes for the treatment of effluents contaminated with heavy metals

There are several processes to treat contaminated effluents, such as chemical precipitation, coagulation, electrolysis, ion exchange, membrane filtration, flotation and adsorption. Advantages and disadvantages associated to those treatments are indicated in Table 2.2<sup>1,6,8,10,19,20,36</sup>.

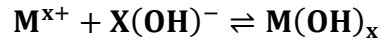
Adsorption has been considered as the best solution for removing heavy metals from wastewaters due to the fact that the metals can be recovered again. Moreover, it is a less expensive technique when compared to others, does not consume many chemicals during the process, has high removal efficiency and can remove most of the heavy metals.

Table 2.2: Advantages and disadvantages of the different physico-chemical treatments of effluents contaminated with heavy metals.

<b>Treatment method</b>	<b>Advantages</b>	<b>Disadvantages</b>
Chemical precipitation	<ul style="list-style-type: none"> <li>• Low capital cost</li> <li>• Simple operation</li> <li>• Not metal selective</li> </ul>	<ul style="list-style-type: none"> <li>• Contaminated sludge production</li> <li>• Extra operational cost for sludge disposal</li> <li>• High maintenance costs</li> <li>• Slow metal precipitation</li> <li>• Initial solution pH</li> </ul>
Coagulation-flocculation	<ul style="list-style-type: none"> <li>• Good sludge settling and dewatering</li> <li>• Shorter time to settle out</li> </ul>	<ul style="list-style-type: none"> <li>• High operational cost</li> <li>• Large consumption of chemicals (coagulants/flocculants)</li> <li>• Increase of sludge production</li> </ul>
Electrochemical treatment	<ul style="list-style-type: none"> <li>• Metal selective</li> <li>• Pure metals can be retrieved</li> <li>• No consumption of chemicals</li> </ul>	<ul style="list-style-type: none"> <li>• High investment cost</li> <li>• High running cost</li> <li>• Initial solution pH and current density</li> </ul>
Ion Exchange	<ul style="list-style-type: none"> <li>• High regeneration of the metal</li> <li>• High selectivity</li> <li>• Less sludge volume produced</li> <li>• Less time consuming</li> </ul>	<ul style="list-style-type: none"> <li>• High maintenance costs</li> <li>• High initial capital costs</li> <li>• Can require pretreatment of the effluent before using ion exchange resin</li> <li>• Ion exchange resins are not available for all heavy metals</li> </ul>
Membrane filtration	<ul style="list-style-type: none"> <li>• Less chemicals consumption</li> <li>• Less solid waste produced</li> </ul>	<ul style="list-style-type: none"> <li>• High initial and running costs</li> <li>• Low flow rates</li> <li>• Membrane fouling</li> </ul>
Flotation	<ul style="list-style-type: none"> <li>• Low operational costs</li> <li>• Shorter hydraulic reaction time</li> <li>• Better removal of small particles</li> </ul>	<ul style="list-style-type: none"> <li>• It is needed subsequent treatments to improve the removal efficiency of heavy metal</li> </ul>
Adsorption	<ul style="list-style-type: none"> <li>• Most of metals can be removed</li> <li>• High efficiency</li> <li>• Relatively less costly materials</li> <li>• Fast kinetics</li> <li>• Less sludge production</li> </ul>	<ul style="list-style-type: none"> <li>• Performance of the adsorbent depends on the adsorbate</li> <li>• Can require chemical treatment of the adsorbent to enhance its adsorption capacity</li> </ul>

### 2.2.1 Chemical precipitation

Chemical precipitation is one of the most used methods in wastewater treatment to remove heavy metals. The strategy is to increase the pH of the effluent that causes the heavy metal to precipitate in its hydroxide form. This new form is insoluble and easy to remove by filtration, for example. The general reaction of chemical precipitation can be seen in Eq. 2.5 and by the Fig. 2.3<sup>8,37</sup>.



2.5

where  $M^{x+}$  is the cation in the solution, the  $X(OH)^-$  the hydroxide species added to the solution and the  $M(OH)_x$  the hydroxide precipitated.

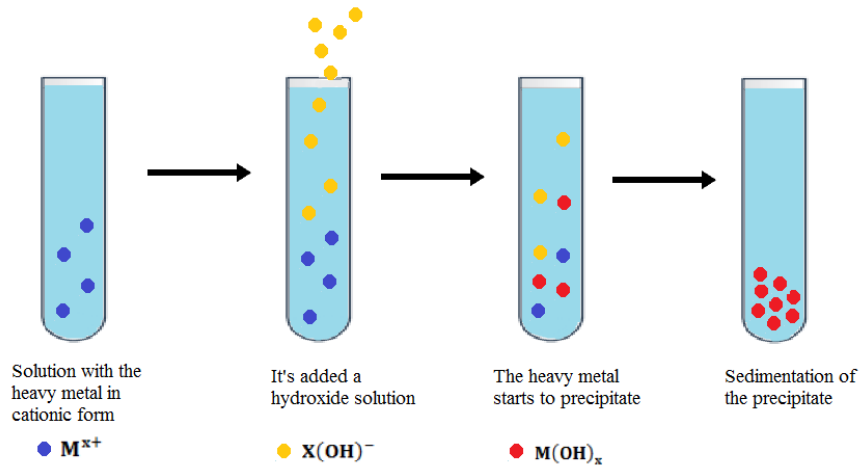


Fig. 2.3: Chemical precipitation process of heavy metals

### 2.2.2 Coagulation and Flocculation

This methodology for treating effluents consists in adding a coagulant that will destabilize colloidal particles in the solution which will result in sedimentation. To increase the particle size, in views of helping sedimentation, coagulation can be followed by flocculation where the unstable particles form bulky floccules that will settle faster. For this to happen, ferric/alum salts or polymeric agents are added to overcome the repulsive forces between the particles acting as coagulant and pH is adjusted as well. This treatment can be seen in Fig. 2.4<sup>6,8</sup>.

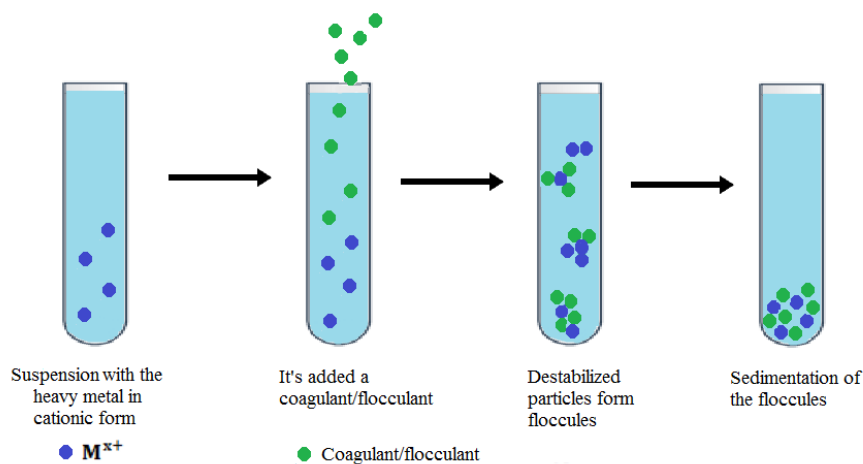


Fig. 2.4: Coagulation and flocculation processes to remove heavy metals from contaminated effluents

### 2.2.3 Electrochemical treatment

Electrochemical treatment consists on removing the metal ions from the solution using an electrode. This is a good method when the objective is recovering the metal in its elemental state, however it consumes much electricity and it is necessary a large capital investment <sup>38</sup>.

This treatment can be subdivided in other treatments like electrocoagulation, electroflotation and electrodeposition, depending on how the electricity is applied. For example, in electroflotation, the metal is separated from the liquid phase when it floats to the surface by tiny bubbles of hydrogen and oxygen gases generated from water electrolysis. On the other hand, electrocoagulation uses coagulants formed by dissolving electrically ion from the electrodes <sup>38,39</sup>.

### 2.2.4 Membrane Filtration

The process of membrane filtration is a physical treatment of wastewaters contaminated with heavy metals. The fact that makes this treatment interesting is that all of the water can be reutilized <sup>39</sup>.

This method is based on the fact that there is a semipermeable membrane, of rigid material or flexible films, that is permeable to certain constituents of the mixture allowing their removal from the effluent. It is a process pressure-driven and can be classified after the separation size range of particles that is meant to retain on the membrane as microfiltration, ultrafiltration, nanofiltration, dialysis, electrodialysis or reverse osmose <sup>40,41</sup>.

### 2.2.5 Ion Exchange

Ion exchange is the oldest chemical method used in water treatment. It is used for demineralization of water, to remove components from effluents before they are discharged and can be used to catalyze specific reactions or in chromatography <sup>40</sup>.

Ion exchange can be explained as the exchange of equivalent numbers of similarly charged ions between an immobile phase and a liquid surrounding it. The rate of this exchange can be driven by the necessity to maintain electroneutrality and by concentration difference in the two phases <sup>40</sup>.

Nowadays, there are multiple ion exchange resins in the market used for removing heavy metals from wastewater, some of them with high selectivity. Normally resins have high adsorption efficiency and they can be reused several times (due to regeneration). Nevertheless, they are very expensive and very selective <sup>1,8,42</sup>.

## 2.3 Adsorption Processes

Adsorption is a process in which components present on a fluid phase (liquid or gas), known as adsorbate, are selectively transferred to insoluble and rigid particles, known as adsorbents, suspended in vessels or packed in columns.

The fluid-solid adsorption is the type of treatment most popular for removing heavy metals from contaminated wastewater. In this case, the adsorbate is the effluent contaminant and the adsorbent is the resin or a low-cost adsorbent, like corncob or a tree bark <sup>43</sup>.

In the recent years, adsorption processes have been implemented for removing heavy metal from wastewater<sup>8</sup>.

### 2.3.1 Fundamentals of adsorption processes

Adsorption can be classified as physical or chemical depending on the forces involved. Physical adsorption occurs when there are only weak intermolecular forces involved, like Van der Waal forces (dispersion-repulsion) and electrostatic forces comprising polarization, dipole, and quadrupole interactions. Chemisorption or chemical adsorption occurs when there is formation of a chemical bond between the solute and the adsorbent <sup>44</sup>.

Table 2.3, high lights the differences between physical and chemical adsorption<sup>40,44,45</sup>.

Table 2.3 - Difference between physical and chemical adsorption

	<b>Physical adsorption</b>	<b>Chemical adsorption</b>
Forces involved in adsorption	Weak forces (Van der Waals, electrostatic)	Strong forces (ion binding)
Regeneration	Easy	Difficult
Layer	Monolayer or multilayer	Monolayer only
Heat of adsorption	Low (< 2 or 3 times latent heat of evaporation)	High (> 2 or 3 times latent heat of evaporation)
Specificity	Non specific	Highly specific
Temperature of adsorption	Only significant at relatively low temperature	Possible over a wide range of temperature
Velocity of adsorption	Rapid	Slow

The process of adsorption is always accompanied by releasing of energy in the form of heat. This happens because when the component in the solution (the adsorbate) moves to the adsorbent, it loses degrees of freedom resulting in the reduction of free energy <sup>40</sup>.

When the adsorbent is from a biological origin, the process is called bioadsorption <sup>46</sup>.

### 2.3.2 Factors affecting adsorption processes

There are several factors that may affect the adsorption process<sup>44,47,48</sup>:

- *pH*. The pH of the solution is determinant variable due to the fact that it affects not only the adsorbent but also heavy metals present in the effluent. In the case of adsorption of

Cr(III) in lignocellulosic residue, the pH of the solution will influence the speciation of chromium and the dissociation of active functional groups (hydroxyl, carboxyl and phenolic groups) of the adsorbent. At low pH, the functional groups on lignocellulose residues are protonated resulting on repulsive forces between the adsorbent and the cationic specie of Cr(III). As the pH of the solution increases, the protonation of the functional groups decreases favoring the adsorption of this heavy metal.

- *Surface area and porosity of the adsorbent.* The higher the surface area, the more favorable will be the adsorption. That is why most of the adsorbents are highly porous.

- *Temperature.* In general, increasing of temperature will help to enhance the adsorption process through the increasing the surface activity and kinetic energy achieving and equilibrium more quickly. Still, it is important to notice that high temperatures may damage the adsorbent.

- *Ionic strength and competing ions.* Other ions present on the solution may influence the adsorption by competing with the adsorbate for binding sites changing its activity or forming complexes with it.

- *Initial pollutant concentration.* A higher initial pollutant concentration will increase the driving-force of the adsorption process, helping to overthrow the mass transfer resistances per adsorbent mass weight.

- *Adsorbent dosage.* A higher dosage of adsorbent will lead to an increase of removal efficiency, but the quantity of adsorbed pollutant per unit weight of adsorbent is diminished.

- *Adsorbent particle size.* Small adsorbent particles increase surface area and thus promoting adsorption. However, small particles will face difficulties in a column process due to clogging. This is a parameter to have attention too because it will also determine if it is necessary to have in mind the diffusion processes during the mathematical modulation of the adsorption process.

- *Agitation speed.* Increasing the agitation speed will minimize the mass transfer resistance. Still, agitation speed higher than necessary can damage the structure of the adsorbent. So, this is a parameter to adjust when optimizing the adsorption process;

Understanding the comportment of the adsorbent and the adsorbate, as well as how the factors explained above would affect them, will allow the optimization of the process to remove the pollutant from wastewater with less effort and cost.

### 2.3.3 Adsorption Isotherms

Quantification of the interactions between adsorbate and adsorbent is fundamental to better understand this phenomenon. For that, it is used adsorption isotherms that shows the equilibrium relationship between the adsorbate present in the fluid phase and the concentration of it in the adsorbent particles at a given temperature <sup>41</sup>.

Typical adsorption isotherms, Fig. 2.5, show information to select the best concentration to a given adsorbate.

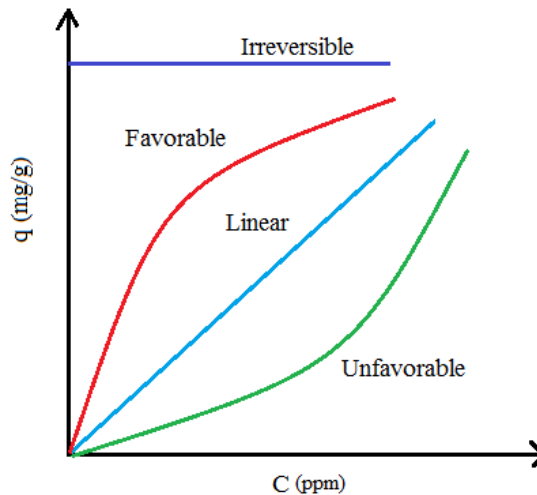


Fig. 2.5: Representation of adsorption isotherms

Linear isotherms show that as the concentration (C) of the adsorbate increases the amount of adsorbed (q) also increases in a proportional way. A favorable isotherm corresponds to a high uptake even at low concentration in the fluid. An isotherm that is concave upward are unfavorable because a relatively low solid loadings are obtained<sup>41,49</sup>.

The simplest isotherm that was originally designed for chemisorption, on a set of distinct localized adsorption sites, is the Langmuir isotherm. Other theoretical models designed to describe more complex isotherms are deviations from Langmuir isotherm or Freundlich model<sup>44,45</sup>.

Langmuir isotherm is based on several assumptions such as <sup>44,50</sup>:

1. There is a fixed number of well-defined localized sites on the adsorbent where the adsorbate is adsorbed;
2. Each site can only hold one molecule of adsorbate (monolayer adsorption);
3. All sites are energetically equivalent;
4. The adsorbed molecules have no interaction with molecules on neighboring sites;
5. The strength of the intermolecular attractive force decreases with the increase of distance;

The Langmuir model is represented by the following Eq. 2.6 <sup>44,51,52</sup>



$$q_e = \frac{Q_{max} \times K_L \times C_e}{1 + K_L \times C_e} \quad 2.6$$

where  $q_e$  is the adsorption capacity at equilibrium ( $\text{mg g}^{-1}$ ),  $C_e$  the equilibrium concentration of the adsorbate ( $\text{mg L}^{-1}$ ),  $Q_{max}$  is the maximum monolayer coverage capacity or maximum adsorption capacity ( $\text{mg g}^{-1}$ ) and  $K_L$  the Langmuir isotherm constant ( $\text{L mg}^{-1}$ ). In this case a dimensionless constant,  $R_L$ , can be defined by Eq. 2.7<sup>50</sup>.

$$R_L = \frac{1}{1 + K_L C_0} \quad 2.7$$

where  $C_0$  is the adsorbate initial concentration ( $\text{mg L}^{-1}$ ) and  $K_L$  is the Langmuir constant that is related to the energy of adsorption.  $R_L$  is sometimes referred as the separation factor and it<sup>41,50</sup>:

- $0 < R_L < 1$  – the adsorption is favorable;
- $R_L > 1$  – the adsorption is unfavorable;
- $R_L = 1$  – the adsorption is linear;
- $R_L = 0$  – the adsorption is irreversible.

Another very well-known model is the Freundlich equation, which describes multilayer adsorption, with interaction between adsorbed molecules. It can be represented by Eq. 2.8<sup>45,49,51,52</sup>.

$$q_e = K_f \times C_e^{1/n} \quad 2.8$$

where,  $q_e$  is the adsorption capacity ( $\text{mg g}^{-1}$ ),  $C_e$  the equilibrium concentration of the adsorbate ( $\text{mg L}^{-1}$ ),  $K_f$  is the Freundlich isotherm constant ( $\text{mg}^{1-(1/n)} \text{L}^{1/n} \text{g}^{-1}$ ) and  $n$  is another Freundlich isotherm constant that represents the adsorption intensity. Freundlich constants are empirical and they are dependent on many factors. The degree of non-linearity of the adsorption process can be found if the value of  $1/n$  varies between 0 and 1. If the ratio is equal to 1, the adsorption process is linear<sup>50</sup>.

Other isotherm models and their assumptions can be found in Table A.1 in Appendix A, most of them derived from Langmuir or Freundlich isotherm or a combination of the two<sup>50</sup>.

### 2.3.4 Adsorption Kinetics

Kinetics studies are very important in order to select the best operational conditions for the removal of the pollutant. It gives us information about the rate-controlling step which will help on process design<sup>47</sup>.

Heavy metal adsorption is in general fast normally within 60 min. After a rapid uptake in the first minutes, the adsorption reaches an equilibrium, normally after 2-6 h for cationic metals, like Cr(III) <sup>46,53</sup>.

These processes can be described in four fundamental steps, as it can be seen in Fig. 2.6.

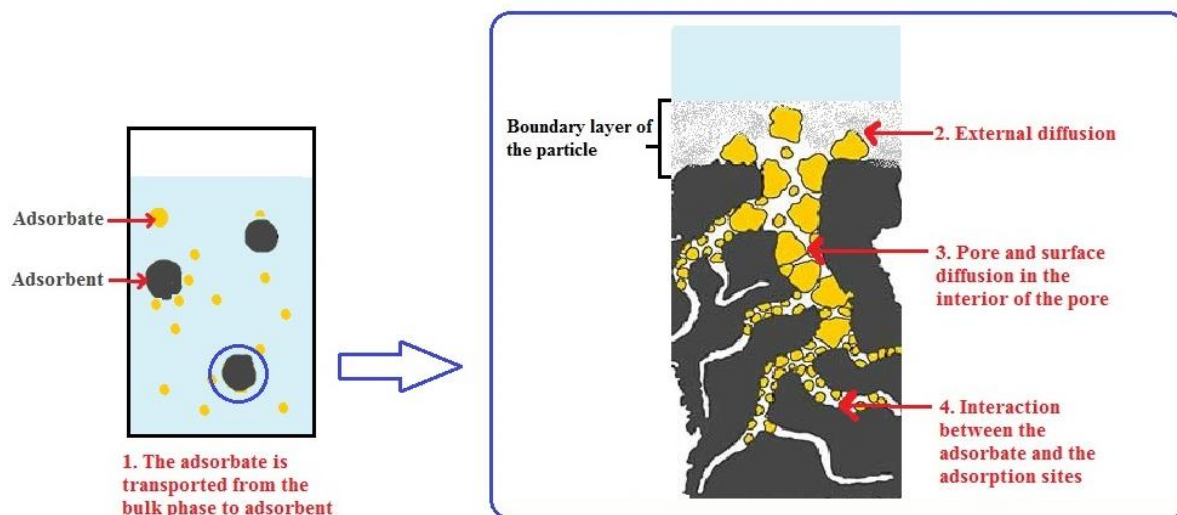


Fig. 2.6: Steps of the adsorption process. Adapted from <sup>54</sup>

1. The adsorbate is transported from the bulk liquid phase to the hydrodynamic boundary layer that involves the adsorbent particle.
2. The adsorbate particles go through the boundary layer that surround the particle. This external layer is known to create a resistance to mass transfer. This step is known as external diffusion or film diffusion.;
3. The adsorbate is transported to the interior of the adsorbent particle (intraparticle diffusion) by pore diffusion (diffusion through the liquid in the pore) and/or by surface diffusion (diffusion through the internal surface of the adsorbent);
4. There is energetic interaction between adsorbate molecules and the final adsorption sites completing the adsorption process.

To describe this phenomena, mathematical models have been developed under several conditions, for example, adsorptions at a given pH of the medium or temperature<sup>18,47</sup>.

Some factors may affect these kinetic models, as for example particle size, mass transfer coefficients, initial concentration, solute diffusivity and the maximum uptake capacity <sup>47</sup>.

In the literature, over than 25 models were proposed to describe the kinetic behavior during adsorption. However, each model has its own limitations derived from theoretical and specific experimental assumptions. In general, a kinetic model is based on mass transfer

equations, equilibrium relationships, and a mass balance of the system in study (diffusion processes). The most common considerations are: constant temperature; the adsorbate is completely mixed in the solution; the mass transfer, into and within the adsorbent, is considered as diffusion processes; the attachment onto the adsorbent surface is much faster than diffusional processes and, at last, the adsorbent is assumed to be spherical and isotropic<sup>51</sup>.

Normally, two kinetics equations are used to describe adsorption processes: pseudo-first- and second-order kinetic equations. The pseudo-first-order equation, also known as pseudo-first-order rate of Lagergren, Eq. 2.9<sup>47</sup>:

$$\frac{dq_t}{dt} = k_1(q_e - q_t) \quad 2.9$$

where  $q_e$  and  $q_t$  (mg/g) are the amount of solute adsorbed on the adsorbent at equilibrium and at a given time, respectively,  $t$  is the time (min) and  $k_1$  is the rate constant ( $\text{min}^{-1}$ ). This equation can be integrated considering the boundary condition,  $t = 0$  and  $q_t = 0$  to  $t = t$  and  $q_t = q_e$  resulting on Eq. 2.10 or in the linearized form Eq. 2.11<sup>55</sup>.

$$q_t = q_e(1 - e^{-k_1 t}) \quad 2.10$$

$$\ln(q_e - q_t) = \ln(q_e) - k_1 \cdot t \quad 2.11$$

The second-order kinetic equation assumes that the rate-limiting step is the last stage of the adsorption process, when the chemical sorption, between the adsorbate and the adsorbent, occurs. It also assumes that the sorption capacity of the adsorbent is proportional to the active sites occupied on the sorbent. This other model can be represented by the Eq. 2.12<sup>51,55</sup>.

$$\frac{dq_t}{dt} = k_2(q_e - q_t)^2 \quad 2.12$$

where  $k_2$  ( $\text{g} (\text{mg min})^{-1}$ ) is the rate constant of the pseudo second-order model.

Integrating the Eq. 2.12 considering the boundaries conditions of  $t=0$  and  $q_t=0$  to  $t=t$  and  $q_t = q_e$ , Eq. 2.13 can be obtained.

$$\frac{1}{q_t} = \frac{1}{k_2 q_e^2} + \frac{1}{q_e} \cdot t \quad 2.13$$

In both models described above, the considerations are reasonable if the adsorbent is weakly porous and the final adsorption step is the most important step in the adsorption process, and the film diffusion practically inexistent. If not, the models should take into account the diffusional steps becoming more complicated when applied to adsorption systems<sup>51</sup>.

### 2.3.5 Adsorbent material

An adsorbent can be natural or synthetic materials, on the form of irregular particles, extruded pellets or formed spheres. These materials must meet several requirements considering that adsorption process occurs due to differences in molecular weight, shape, or polarity between the adsorbent and the adsorbate. Those differences will lead the adsorbate to be held more strongly on a specific adsorbent in detriment of another<sup>40,41</sup>.

First of all, adsorbents can be characterized by surface properties and polarity. It is preferable for adsorbents to be highly porous providing a large surface area, and thus a high adsorption capacity.

The size and distribution of the pores on the particle are very important parameters due to the fact that adsorption cannot occur if the pores are too small to admit larger molecules of the adsorbate. The pores can be classified as macropores, if the diameter ( $\Phi$ ) is higher than 50 nm, mesopores ( $2 < \Phi < 50$  nm) and micropores ( $\Phi < 2$  nm)<sup>41,49,52</sup>.

Surface polarity is also a very important parameter. Polar adsorbents are called “hydrophilic”, as for example, zeolites, porous alumina or silica gel. On the other hand, nonpolar adsorbents are called “hydrophobic”. Carbonaceous adsorbents and polymer adsorbents are typically hydrophobic adsorbents, and those have more affinity with oil than water<sup>41,52</sup>.

Moreover, it is also desirable that an adsorbent material can be easily regenerated and resilient, not losing its capacity as adsorbent through continual recycling. It should be also mechanically strong enough to withstand the bulk handling and vibration that are a feature of any industrial unit<sup>40</sup>.

For choosing an adsorbent for the treatment of wastewaters contaminated with heavy metals, it is significant to know, beforehand, the properties of the heavy metal that is planned to remove (solubility, ion size...) and the properties of the wastewater intended to treat (pH, ionic charge, solutes present in the effluent that could compete with the heavy metal for the active sites in the adsorbent...) <sup>16</sup>. Nowadays, agro-industrial wastes, such as lignocellulosic residues, has been used as biological adsorbent for heavy metals<sup>8,16,20,56</sup>.

## 2.4 Lignocellulosic Residues

Agro-industrial residues or lignocellulosic residues, are being studied as low-cost adsorbent for heavy metal wastewaters treatment. They are eco-friendly materials with

promising uptakes capacities, generate few sludge, are available and they valorize materials that would be considered wastes otherwise <sup>44,57</sup>.

Most of investigated materials, as low-cost adsorbents, are shells and/or stone of fruits, such as olive and cherry stones or almonds and peanut shells; wastes resulting from production of cereals (rice, coffee, etc.), olive cakes, sugar cane bagasse or algae. Those residues have mechanical resistance, can be milled and sieved into small particles, are porous, have a great superficial area and have a natural adsorption property that can be enhanced through physical or chemical treatment. Bark is one of many lignocellulosic residues that is highly complex in their chemical composition and highly heterogeneous, but with potential to be used as adsorbent for removal of heavy metals<sup>8,16,17,20,25,56,58-60</sup>.

Bark is one of the major biomass feedstock that has been under valorized. Nowadays, most of the bark is considered a solid residue in wood processing industries and its applications has been mainly as biofuel through burning, or used in small scale markets, like horticulture. Even though bark is a low-cost material, it is rich in chemicals and bio-polymers whose applications are multiple and are still being explored. The chemical composition of barks is very complex and it depends on the environmental conditions in which the tree grew, which part of bark is considered (outer bark or a more internal bark) and which specie are being studied (hardwood or softwood). Still, the chemical constituents of the bark can be classified in four principal groups<sup>61,62</sup>:

- *Polysaccharides*: cellulose, hemicellulose...;
- *Lignin and polyphenols*;
- *Hydroxyl acid complexes*
- *Extractives*: fats, oils, resin acids, waxes....

There are several approaches to quantify the different constituents of the bark, due to the fact that some constituents are soluble in certain solvents, and for comparison purposes it matters which method was used to characterize the bark. An approximate composition for wood and bark can be found in Fig. 2.7, regarding the four main groups <sup>63,64</sup>.

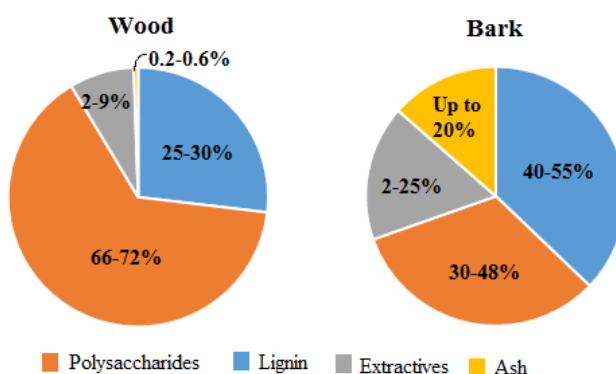


Fig. 2.7: Chemical composition of bark in comparison to chemical composition of wood (values approximated). Adapted from<sup>64</sup>.

In Table 2.4, it can be seen an example of chemical composition for different pine barks (*Pinus Pinaster* and *Pinus sylvestris*) that are in accordance with the average composition presented in Fig. 2.7<sup>61,62</sup>.

Table 2.4: Chemical composition of pine barks (values in % of material).

	<i>Pinus sylvestris</i>	<i>Pinus pinaster</i>
Extractives	18.8	11.4
Lignin	33.7	43.7
Polysaccharides (Cellulose, hemicellulose)	37.6	41.7
Ash	4.6	3.2

Extractives are considered a nonstructural wood constituents composed of low-molecular weight compounds that are formed by the tree through a secondary metabolism, after mechanical damage or attack by fungi or insects. Those extractives, which represent a minor fraction of the bark, are usually soluble in neutral organic solvents allowing their quantification for the chemical characterization of the material. This part of bark consists in fats, phenols, resins, waxes and other compounds. However, the values of each component of extractives varies from specie to specie, from environmental conditions where the tree had grown or which technique was used to quantify them<sup>62,63</sup>.

Lignin is the most abundant phenolic polymer in nature and the second most abundant natural raw material, being cellulose the first. This phenolic polymer is highly branched and amorphous, producing a random three-dimensional network, Fig. 2.8<sup>65-67</sup>.

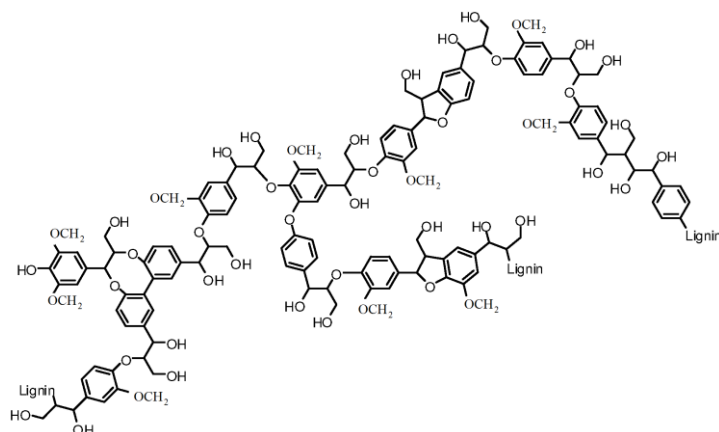


Fig. 2.8: A possible molecular structure of lignin. Adapted from<sup>68</sup>

The stiffness of the cell walls is also result of having lignin in its constitution, along with hemicellulose and cellulose. It also works as a shield against rapid microbial or fungal destruction of the cellulosic fibers. This macromolecule has high surface area ( $180 \text{ m}^2 \text{ g}^{-1}$ ) and various functional groups in its structure, such as: aliphatic and phenolic hydroxyl groups, methoxyl groups and carbonyl groups. The fact that there are so many functional groups in its structure, will help to bind heavy metals during the adsorption process<sup>56,62,65,69</sup>.

Cellulose is the most abundant and renewable polymer resource available on earth and the main constituent of wood. It is usually found on cell walls of woody plants combined with other polysaccharides, like hemicelluloses and lignin. The molecular structure of cellulose can be seen in Fig. 2.9. It is a homo-polymer of glucose comprising the repetition of  $\beta$ -D-glucopyranose units linked through glycosidic linkage (between the OH groups of the C4 and C1 carbons –  $\beta$ -1,4-glucan) and intra-molecular and intermolecular hydrogen bonds<sup>8,48,57,63,69</sup>.

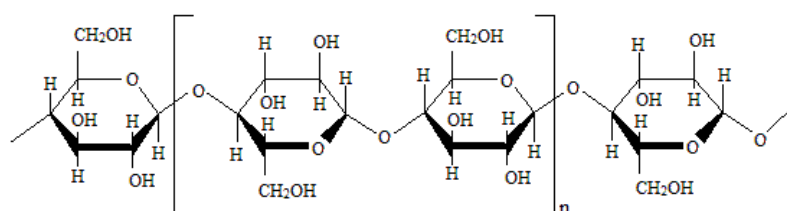


Fig. 2.9: molecular structure of cellulose. Adapted from<sup>70</sup>

Cellulose molecules are highly ordered (crystalline), even though there are some places less ordered (amorphous), and they are normally aggregated in the form of microfibrils. There are several types of cellulose due to the changes in the lattice of this bio-polymer by chemical or physical treatment. The cellulose I is the common cellulose in nature. Cellulose II results of the treatment of cellulose I with a strong alkali solution (mercerization). This type of cellulose is very important and used for making cellulose derivatives. Cellulose III and IV are product of chemical treatments or heating of cellulose I and II<sup>62,63,65,67</sup>.

Hemicellulose, is a heteropolymer comprised repetitions of different monosaccharide units mainly of glucose and xylose. However, it can also have units of mannose, galactose or other sugars. Hemicellulose has short branches of sugar units attached, which explain its amorphous. Though crystalline parts have already been found in form of microfibrils. The amorphous nature of this constituent allows the OH content of the cell wall to be more accessible, to react more readily and be less thermally stable than cellulose or lignin. This fact is interesting when studying ways to modify the properties of the bark for adsorption processes<sup>62,63,65,67</sup>.

Ash content comprises the inorganic part of the bark. Typically, there are a higher percentage of inorganics on bark than on wood of a tree. The major inorganic elements are Na, K, Ca, Mg, Mn, Zn and P. They are absorbed through the roots and its composition depends on the environment and place where the tree grew. The fact that there are more inorganics on bark will also affect its surface pH (normally 3,4-3,5) which is important to adsorption processes that occur mostly on the surface of the adsorbent material<sup>62,63</sup>.

One of those lignocellulosic residues and very common in Portugal is pine bark (*Pinus Pinaster*)

### **Pine (*Pinus pinaster*) bark**

*Pinus pinaster*, as seen in Fig 2.10, is a specie of pine very common in Portugal, occupying 30% of the national forestry area in 2000, and being one of the most important native species<sup>71</sup>.

Currently, this natural resource is explored mostly for pulp industry, wood panels, carpentry and furniture. Another sub product of this resource is the pine bark, which still represents 20-40% of the torus of pine tree. This bark is normally decomposed and used as soil fertilizer or used as bio combustible through burning<sup>11,12</sup>.

A way to valorize this sub product can be through its use as low-adsorbent to treat effluents contaminated with heavy metals.



Fig. 2.10: *Pinus pinaster* bark



### 3. State of the art

#### 3.1 Chemical treatments of lignocellulosic materials

Lignocellulosic residues have a natural capacity to remove some heavy metals, due to their functional groups on surface. However, their uptake capacity is very low and their physical stability is very variable. To overcome those problems a physical and/or chemically treatment to the adsorbent can be made. Physical treatment consists on subjecting the lignocellulosic residue to high temperature, milling and grinding operations or microwave irradiation treatments. Chemical treatments, on the other hand, uses diluted acids, alkali solutions, or gases to change the structure of the residue or its surface properties<sup>8,10,20,72</sup>.

Recent studies proved that chemical treatments are advantageous comparatively with physical pretreatments. Thus chemical modification of the adsorbent will be the focus of this study in order to enhance the adsorption of Cr(III)<sup>72</sup>.

There are two approach for chemical modification of the residue. The first is the direct modification of molecular structure of cellulose (one of the constituents of lignocellulosic residue) with the introduction of chelating or metal binding functionalities through different reactions, like mercerization, esterification, etherification, halogenation or oxidation<sup>8,10,20</sup>.

The second approach is through grafting, where selected monomers are grafted and added main chains of polymers in order to introduce metal binding capacities or functionalization of grafted polymer chains by chelating agents<sup>8,10,20</sup>.

##### 3.1.1 Alkali treatment

Alkali treatment, also known as mercerization, is a chemical treatment where strong alkali solutions, normally sodium hydroxide (NaOH), is put into contact with a lignocellulosic residue. This will change the crystallinity of cellulose structures present on the material, increase the specific surface area and make the hydroxyl groups more easily accessible<sup>8,10,20,63</sup>.

This alkali treatment comprises four stages: swelling, dissolution, mercerization and degradation. For the alkali treatment to succeed, the first two steps (dissolution and swelling) must occur allowing that all the material suffered the treatment. Both, swelling and the dissolution phenomenon have in common the fact that the forces between molecular chains are greater than the intermolecular forces between macromolecules of cellulose. Moreover, NaOH solutions can cause swelling and dissolution at the same time, depending on the initial structure of the material<sup>62,63,67,73,74</sup>.

During swelling phase, the structure of cellulose is maintained even though it suffers an increasing of weight due to absorption of the sodium ions and changes on its physical properties. On the other hand, throughout dissolution, a transition between one biphasic phase and a monophasic phase happens and the initial supramolecular structure of the cellulose is destroyed. Those two preliminary steps will increase the accessibility to hydroxyl groups allowing the cellulose to become more reactive for the next steps and will also affect the molecular and supramolecular structure<sup>63,67,73-75</sup>.

On a molecular level, inter and intramolecular bond are severed by strong interactions between hydroxyl and sodium hydrate groups. The solvation of sodium hydroxide ions acts as a way to separate cellulose chains through the interaction between cellulose and ions from the alkali solution<sup>73</sup>.

First, water molecules penetrate the most amorphous parts of cellulose where the hydrogen bonds are destroyed. This way, sodium hydroxide can enter on crystalline parts of cellulose and react with anhydroglucose hydroxyl groups (the anhydroglucose unit is identified in Fig. 3.1).

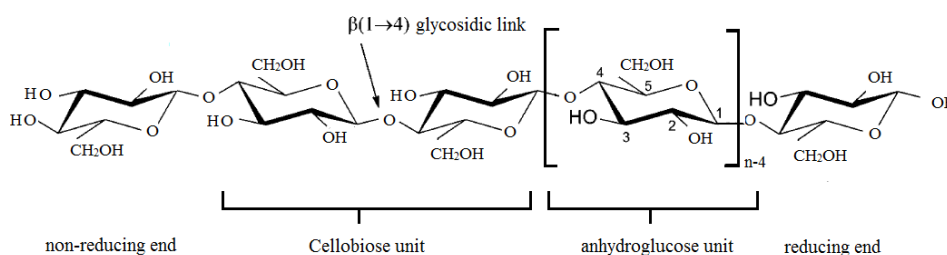


Fig. 3.1: Structure of cellulose chains. Adapted from<sup>76</sup>

Slowly, the initial stability of the structure is regained due to inter and intramolecular bonds that are restored through hydrogen bonds. Those are then replaced by additional bonds between hydrocellulose groups and Na<sup>+</sup> and OH<sup>-</sup> ions from the NaOH solution. This change on bonds and reactions between groups will change the crystallinity of cellulose and the crystalline and amorphous proportions in the material.

During this first two steps of mercerization, there are the formation of ternary complexes of cellulose-sodium-water that are commonly called sodium celluloses (Na-Cell), as it can be seen in Fig. 3.2 and they can appear in multiple conformations because they strongly depend on the concentration of alkali solution<sup>10,62,63,73,74</sup>.

In mercerization stage, the cellulose I (characterized for having parallel chains) is transformed in cellulose II (antiparallel chains) being this transformation irreversible since cellulose II is thermodynamically more stable than the latter form. During this phase, sodium hydroxide solution penetrates on the amorphous regions of cellulose leading to the formation

of the complexes mentioned above (sodium-cellulose or Na-cell), Fig. 3.2, which has an effect on the crystallinity and chain conformation<sup>10,63,73,74</sup>.

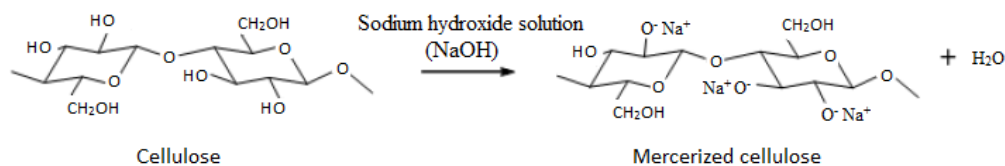


Fig. 3.2: Mercerization (step 3) using a NaOH solution. Adapted from<sup>77</sup>

The formation of cellulose with antiparallel chains is favored over its crystalline form decreasing crystalline regions on the material. As crystalline regions decrease, the alkali solution penetrates more on the material and then convert cellulose I to cellulose II with helical structure. The Fig. 3.3 illustrates the changes on crystallinity mentioned during this process<sup>8,10,20,63,73</sup>.

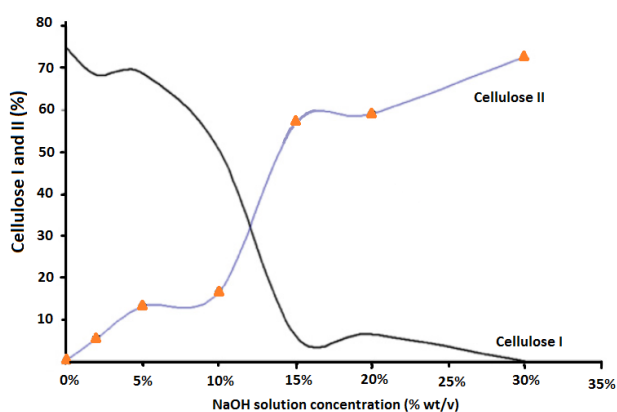


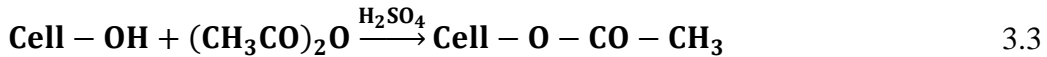
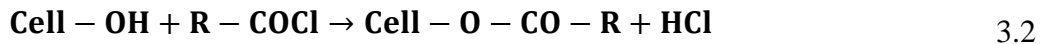
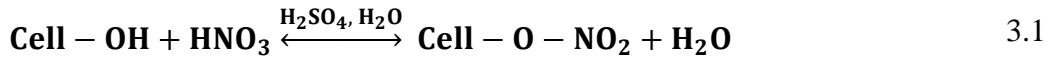
Fig. 3.3: Transformation of Cellulose I into Cellulose II during mercerization process. Adapted from<sup>73</sup>

Fig. 3.3 shows that the majority of transformations occurs with a NaOH concentration between 10-15%. At lower concentration, Cellulose I is predominant and only occurred swelling and dissolution, because there was no transformation on crystallinity. Whereas, when the concentration exceeds 15%, cellulose II is the major component and it is expected degradation of the material<sup>73</sup>.

### 3.1.2 Acid treatment

The acid treatment involves a reaction between a modifying agent (acid solution) and the hydroxyl groups presents on cellulose of the lignocellulosic residue after the swelling and dissolution step. The reaction between those groups are, normally, reactions characteristics of the alcohols, such as esterification and etherification<sup>20,63,78-82</sup>.

Esterification of cellulose occurs when the material is put into contact with an acid solution in the presence of a dehydrating agent, or with acid (or acyl) chlorides, or acids anhydrides, as it can be seen on Eq. 3.1, 3.2 and 3.3, respectively.



where Cell-OH in the representation of the hydroxyl groups of cellulose.

One example of esterification is the reaction with citric acid or succinic acid. In those reactions, heat and/or a catalyst is necessary to convert the acid to its anhydride state that will react with the hydroxyl groups of cellulose to form an ester linkage introducing carboxyl groups to the cellulose<sup>9,20,80,81,83</sup>.

A general process of esterification can be seen in Fig. 3.4 where R represents a carboxylic group introduced by the acid.

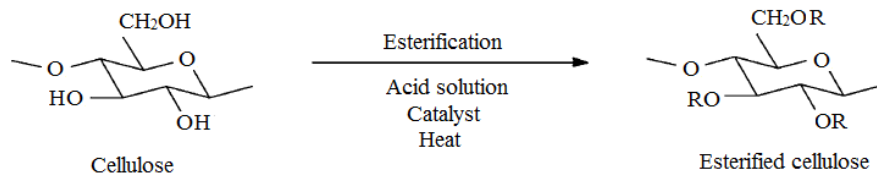


Fig. 3.4: General process of esterification of cellulose using a catalyst and heat. Adapted from<sup>83</sup>

The resulting ester can be classified depending on the acid solution used for the modification. If the modification was carried out using an inorganic acid (HCl, H<sub>2</sub>SO<sub>4</sub>...) the ester formed will be classified as esters from inorganic acids. On the other hand, if it was used an organic acid (citric acid, succinic acid...), the ester will be named ester from organic acids. Globally, the acid modification has the objective of increasing of carboxylic content of the material in order to increase their adsorption capacity, because the adsorption will mostly occur in those functional groups<sup>8,9,20,63,78,80-82</sup>.

### 3.2 Literature review

As seen before, lignocellulosic residues can be used as low-cost adsorbents. Their characteristics can even be improved through chemical or physical treatments. Having this in mind, it was done a research about what has already be studied in the field of adsorption of heavy metals on low-cost materials. This analysis is important because it will work as a stepping-stone on how to approach the problem and find a way to solve it.

First of all, it was noticed that there was much more investigation on the removal of other heavy metals than for Cr(III) through adsorption on lignocellulosic residues. Information collected to other heavy metals can be seen in Table C.1, C.2. and C.3 in the

Appendix C. The information about Cr(III) was divided into studies without treatment (raw material), Table 3.1, and studies with treatment (acid and alkali treatments), Table 3.2.

Table 3.1: Adsorption of Cr(III) on lignocellulosic residues without treatment

Adsorbent	Adsorbate	Q <sub>max</sub> (mg/g)	pH	T (°C)	Co (ppm)	L/S (mL/g)	Ref.
Coir pith	Co(II)	12,41	4,3	27	50	500	[ 84 ]
	Cr(III)	11,52	3,3				
	Ni(II)	15,72	5,3				
Sugar beet pulp	Cr(III)	10,04	5,5	20	10-156	400	[ 26 ]
Aspergillus Biomass	Cr(III)	23,60	5,0	28	400	10	[ 36 ]
	Cr(VI)	15,60	5,0				
	Ca	27,00	5,0				
	Ni	19,60	6,0				
	Fe	19,20	4,0				
Grain-less stalk of corn	Cr(VI)	7,10	0,8	20	66-1000	50	[ 85 ]
	Cr(III)	7,30	4,6				
Peat	Cr(III)	14,03	4,0	-	156	-	[ 86 ]
	Cr(VI)	30,15	2,0				
Biomass of Alfalfa ( <i>Medicago sativa</i> )	Cd(II)	7,10	5,0	-	33.7		[ 87 ]
	Cr(III)	7,70					
	Cr(VI)	0,00					
	Pb(II)	43,00					
	Zn(II)	4,90					
Wine processing waste sludge	Cr(III)	26,79	4,0	30	100	100	[ 88 ]
Peat	Cr(III)	20,80	4,0	25	200	1000	[ 89 ]
	Cu(II)	25,42	5,0				
	Cd(II)	31,47	7,0				
Carrot residues	Cr(III)	45,09	4,5	25	20-1350	100	[ 90 ]
	Cu(II)	32,74					
	Zn(II)	29,61					

Table 3.2: Adsorption of Cr(III) on lignocellulosic residue pre-treated

Adsorbent	Modifying agent	Adsorbate	Q <sub>max</sub> (mg/g)	pH	T (°C)	C0 (ppm)	L/S (mL/g)	Ref.
Corn cob waste	Raw	Cr(III)	34,45	4,5	-	450	1000	[ 91 ]
	HNO <sub>3</sub>		-	500				
	H <sub>2</sub> SO <sub>4</sub>		-	400				
				200				
Cork powder	Raw	Cr(III)	3,40	4,0	22	10	500	[ 92 ]
	CaCl <sub>2</sub>		3,20					
	NaCl		3,61					
	H <sub>2</sub> SO <sub>4</sub>		2,65					
	HCl		2,59					
Saltbush biomass ( <i>Atriplex canescens</i> )	Raw	Cr(III)	5,50	5,0	-	156	0.2	[ 5 ]
	HCl		7,10					
	NaOH		26,20					
Wheat straw	NaOH	Cr(III)	3,91	4,5	25	130	50	[ 93 ]

Rice bran	NaCl	Cr(III)	7,80	5,0	-	20	12.5	[ 94 ]
		Hg(II)	245,00			500		

Table 3.1 shows that the adsorption capacity of raw materials are in the range of 7,3 mg g<sup>-1</sup> to 45,09 mg g<sup>-1</sup>, and the pH used is normally in acidic range of 3,3 to 5,5. However, even with chemical treatment, the Cr(III) uptake capacity is very low. For example, the Q<sub>max</sub> for the removal of Hg(II) of Pb(II), even without treatment, is 245,00 mg g<sup>-1</sup> and 43,00 mg g<sup>-1</sup>, respectively.

After those studies, it was decided to use pine bark (*Pinus Pinaster*) due to the fact that it is one of the most available residue in Portugal without any important application nowadays. The studies have also used the most available residue in their countries as a potential low-cost adsorbent due economic reasons. It will be made an alkali and acid treatment to see if there are indeed an improvement on adsorption as indicated on those studies.

## 4. Methodologies

### 4.1 Materials and reagents

The lignocellulosic material used in this study was pine bark, species *Pinus pinaster* that was collected in North of Portugal, sub-region of Pinhal Litoral in the Tâmega's valley. In the laboratory the pine bark was washed with distilled water several times to remove the dirt, lichens and resin. Then it was dried in the oven at 60 °C during 24 h to remove superficial water. The bark was grinded in a Reischert MUHLER, model 5657 HAAN and sieved using JULABO model SW-21C automatic sieve to achieve adequate particle diameter. Then it was dried again at 80 °C for 24-48 h, to remove any remaining free water. Finally, the material was stored for further studies and considered as "raw".

The solutions of Cr(III) were prepared using chromium nitrate nonahydrated ( $\text{CrN}_3\text{O}_9 \cdot 9\text{H}_2\text{O}$ ) from Alfa Aesar and ultrapure water. For chemical modifications of pine bark, solutions of sodium hydroxide (NaOH), citric acid ( $\text{C}_6\text{H}_8\text{O}_7$ ), sulfuric acid ( $\text{H}_2\text{SO}_4$ ), nitric acid ( $\text{HNO}_3$ ), hydrochloric acid (HCl), phosphoric acid ( $\text{H}_3\text{PO}_4$ ) and acetic acid ( $\text{CH}_3\text{COOH}$ ) were used. All primary chemicals used were of analytical grade.

The pH was controlled with solutions of 0.01-0.1 mol L<sup>-1</sup> of NaOH or 0.01-0.1 mol L<sup>-1</sup> of HCl.

The laboratory glass material was washed with a solution of 10% (v/v) of nitric acid and then washed with distilled water to avoid contamination.

### 4.2 Adsorbent modification

#### 4.2.1 Mercerization

The alkali treatment of pine bark (raw) involved the addition of 900 mL of NaOH was added to 30 g of material previously milled and sieved. This suspension was stirred at room temperature for 16 h. Then it was filtered and washed with tap water and then with ultrapure water until pH constant. The material was dried in an oven at 80 °C for 48 h. *A priori*, the material was divided with sieves of 0.595-0.420, 0.420-0.297, 0.297-0.210, 0.210-0.149 and 0.149-0.088 mm<sup>†</sup>. For selecting the best range of particle sizes adsorption tests were conducting using 0.3 g of pine bark mixed with 30 mL of a chromium (III) solution (300 ppm) at room temperature. The best particle size fraction was mercerized with NaOH (10, 20 and 30% v/v)<sup>10,57</sup>.

---

<sup>†</sup> A conversion table between millimeters and mesh can be found on Appendix H

#### 4.2.2 Acid treatment

Acid treatment was performed with citric acid ( $C_6H_8O_7$ ), sulfuric acid ( $H_2SO_4$ ), nitric acid ( $HNO_3$ ), hydrochloric acid ( $HCl$ ), phosphoric acid ( $H_3PO_4$ ) and acetic acid ( $CH_3COOH$ ). For that, acid solutions were added to 30 g of pine bark previously milled and sieved (raw). The suspension was stirred at 60 °C for 2 h at 1200 rpm. Then, the mixture was filtered and washed with tap water and then with ultrapure water until pH constant. The modified pine bark was later dried at 80°C for 48 h<sup>95-97</sup>.

The best concentrations for each acid and particle size of raw material, were optimized through adsorption tests, using 0.3 g of adsorbent in contact with 30 mL of a Cr(III) solution (500 ppm) at room temperature and pH 5.

### 4.3 Adsorbent characterization

#### 4.3.1 Physical properties

Physical characterization of the adsorbent was carried out regarding surface area, average pore diameter and pore volume. Those parameters were assessed by  $N_2$  adsorption (micromeritics ASAP 2000). In addition, density was evaluated through helium pycnometry (micromeritics AccuPyc 1330). These analyses were performed in an external laboratory (Instituto Pedro Nunes (IPN) Coimbra).

#### 4.3.2 Scanning Electronic Microscopy and Energy Dispersive Spectroscopy (SEM-EDS)

Energy dispersive spectroscopy (EDS) combined with SEM was used to obtain elemental composition of the sample and images with specific amplifications. The heights of peaks observed in the spectrum indicate the magnitude of elemental concentration on the sample<sup>98,99</sup>.

The images of pine bark surface, raw and modified, were obtained by conventional SEM-EDS with a high resolution microscope in VEGA 3 SB of the TESCAN of the Physics Department, UC.

#### 4.3.3 Surface actives sites by Boehm Titration method

Boehm proposed a titration method to determine the various functional groups on the surface of the adsorbent, namely total acid sites (comprised by carboxylic, phenolic and lactonic sites) and the total basic sites. This method was adopted in this study<sup>100-105</sup>.

The concentration of total basic sites, TBS, on the surface of pine bark was determined by taking 1 g of the adsorbent and mixing it with 50 mL of NaOH 0.1 mol L<sup>-1</sup> in an Erlenmeyer at room temperature during five days. After that time, the mixture was filtered



and 40 mL sample was taken out and titrated with a standardized solution of 0.1 mol L<sup>-1</sup> HCl using phenolphthalein as indicator. The quantity of total basic site, TBS, s was then calculated using Eq. 4.1:

$$\text{TBS} = \frac{V_T \times N_B \times (V_B - V_{AM})}{V_{AI} \times m_{\text{dried bark}}} \quad 4.1$$

where:  $V_T$  is the total volume of neutralizing solution (HCl) used (mL);  $V_B$  and  $V_{AM}$  are the volume of standardized NaOH solution used during titration of the reference and the sample (mL), respectively;  $V_{AI}$  is the volume of the sample for the titration (mL),  $m_{\text{dried bark}}$  is the mass of dried bark used in this test (g) and  $N_B$  is the concentration of the NaOH solution (mEq mL<sup>-1</sup>).

The total acid sites, TAS, are comprise carboxylic (-COOH), phenolic (-OH) and lactonic (-COOR) sites, each of them determined with different neutralizing solutions. It is known that a sodium hydroxide (NaOH) solution will neutralize all the acid sites; on the other hand, a solution of sodium carbonate (Na<sub>2</sub>CO<sub>3</sub>) will neutralize the carboxylic and lactonic sites and a solution of sodium bicarbonate (NaHCO<sub>3</sub>) will neutralize only the carboxylic groups. Thus, 1 g of pine bark was added to an Erlenmeyer with 50 mL of one of the tree neutralizing solutions at room temperature during five days. The concentration of the neutralizing solutions was the following: 0.01 mol L<sup>-1</sup> of NaOH; 0.05 mol L<sup>-1</sup> of Na<sub>2</sub>CO<sub>3</sub> and 0.1 mol L<sup>-1</sup> of NaHCO<sub>3</sub>. After that time, the mixture was filtered and 40 mL of solution was taken.

To determine the concentration of total acid sites, it was added 10 mL of 0.1 mol L<sup>-1</sup> of HCl to the sample neutralized with NaOH. Then, it was titrated with a standardized solution of 0.1 mol L<sup>-1</sup> of NaOH using phenolphthalein as indicator. Then, TAS were determined using the Equation ( 4.2 ).

$$\text{TAS} = \frac{V_T \times N_B \times (V_{AM} - V_B)}{V_{AI} \times m_{\text{dried bark}}} \quad (4.2)$$

where:  $V_T$  is the total volume of the neutralizing solution used in adsorption (mL);  $V_B$  and  $V_{AM}$  are the volume of the standardized solution of NaOH used during titration of the reference and the sample (mL), respectively;  $N_B$  is the concentration of NaOH solution (mEq mL<sup>-1</sup>);  $V_{AI}$  is the volume of the sample for the titration (mL) and  $m_{\text{dried bark}}$  is the mass of dried bark used in this test (g).

The carboxylic and lactonic groups were determined using a solution of NaHCO<sub>3</sub> and Na<sub>2</sub>CO<sub>3</sub>. After filtration and removing a sample of 40 mL, it was added 15 mL and 10 mL, respectively, of 0.1 mol L<sup>-1</sup> of HCl to each sample and heated until boiling point. Then it was

left to cool down, until room temperature, and titrated with 0.1 mol L<sup>-1</sup> of a standardized solution of NaOH, using phenolphthalein as indicator.

The quantity of each acid site was calculated using the following Eq. 4.3 to Eq. 4.5:

$$\text{Carboxylic groups} = V_{\text{NaHCO}_3} \quad 4.3$$

$$\text{Lactonic groups} = V_{\text{Na}_2\text{CO}_3} - V_{\text{NaHCO}_3} \quad 4.4$$

$$\text{Phenolic groups} = V_{\text{NaOH}} - V_{\text{Na}_2\text{CO}_3} \quad 4.5$$

where V is the volume of the titration solution used on the samples neutralized by the solutions indicated (mL).

#### 4.3.4 Point of zero charge

The point of zero charge (PZC) or the point of zero charge pH (pH<sub>PZC</sub>) is the pH where the adsorbent surface charge is equal to zero<sup>19,106</sup>.

This value was found by taken eleven samples of 0.15 g of pine bark and put them into 50 mL of NaCl, adjusting pH from 2 to 12 with 0.1 mol L<sup>-1</sup> of HCl and 0.1 mol L<sup>-1</sup> of NaOH. The mixtures were agitated in a shaker P SELECTA model UNITRONIC-OR C, for 48 h at room temperature. After that, the suspensions were filtered and pH of each solution was measured. The point of zero charge pH is the point when the initial pH is equal to final pH.

## 4.4 Adsorption studies

The capacity of adsorption (q) (mg g<sup>-1</sup>) and the removal efficiency (R<sub>eff</sub>) of the adsorbent were calculated with Eq. 4.6 and 4.7.

$$\text{Adsorption capacity (q)} = \frac{(C_0 - C_f)}{m} \times V_S \quad 4.6$$

$$R_{eff}(\%) = \frac{(C_0 - C_f)}{C_f} \times 100 \quad 4.7$$

where **C<sub>0</sub>** is the initial concentration of the adsorbate (mg L<sup>-1</sup>), **C<sub>f</sub>** is the final concentration of adsorbate (mg L<sup>-1</sup>), **m** mass of the adsorbent (g) and **V<sub>S</sub>** the volume of the solution (L).

The adsorption studies involved the analysis of equilibrium conditions as well as the influence of contact time and pH.

#### 4.4.1 Adsorption equilibrium isotherms

Adsorption isotherms were obtained with 500 ppm of Cr(III) solution at pH 2, 3 and 5 (pH adjusted using 0.1 mol L<sup>-1</sup> of NaOH solution and 0.1 mol L<sup>-1</sup> of HCl solution). In each batch adsorption experiments, it was used 30 mL of aliquots of Cr(III) solution with the

adsorbent dosage ranging from 15 to 140 mg L<sup>-1</sup>. The suspensions were put on a thermostatic water bath shaker for 3 h at 25°C and then filtrated and analyzed by FAAS.

#### 4.4.2 Effect of contact time

The influence of time was tested by taking 0.3 g of pine bark into contact with 30 mL of a 500 ppm solution of Cr(III). The mixtures were agitated in a thermostatic water bath shaker for 3 h at 25 °C (room temperature). Aliquots were taken from time to time (each 2, 4, 10, 15, 20, 25, 30, 40, 50, 60, 90, 120, 150 and 180 min) and filtrated with a FILTER-LAB filter with pore size of 0.45 µm.

#### 4.4.3 Effect of initial pH

The effect of pH was studied putting 0.3g of pine bark (raw and mercerized) in contact with 30 mL of 300 ppm Cr(III) solution. The initial pH of the different samples was adjusted from 2 to 5.5 using 0.1 mol L<sup>-1</sup> of NaOH solution or 0.1 mol L<sup>-1</sup> of HCl. Mixtures were put on a thermostatic water bath shaker for 3 h at 25°C. After that time, the solid particles were separated from liquid by filtration.

#### 4.4.4 FAAS – Flame Atomic Absorption Spectroscopy

Cr(III) concentration was determined using a Flame Atomic Absorption Spectrometer (FAAS) Analytickjena – Contra 300, with a wavelength of 357 nm and a flame of acetylene/air. The calibration curve involved 1 ppm to 6 ppm of Cr(III) solutions. Standards were prepared by adding 0.1 mL of a buffer (Cesium Chloride Lanthanum buffer, Fluka Analytical) and 1 mL HCl (37%) in 100 mL flasks.

### 4.5 Modeling adsorption data

#### 4.5.1 Equilibrium isotherms

The Matlab toolbox *cftool* was used to modeling equilibrium data. The parameters that allow the best fitting was obtained when the fitting error is low. It was also developed a model to describe the adsorption process with initial pH variations.

#### 4.5.2 Design of experiments (DOE)

Design of Experiments (DOE) was used to understand which factor (initial concentration, pH, temperature and liquid-to-solid ratio (L/S)) would have a major impact on adsorption processes and how these parameters would interact between them. This method was also used in order to optimize some parameters and try to develop a mathematical model to describe the adsorption process<sup>107,108</sup>.

The experiments were designed based on Box-Benken Design (BBD). This model is an incomplete three-level factorial where the coefficients of a second-order model are estimated by experimental point chosen a priori. The inputs for the BBD are presented in Table 4.1<sup>108</sup>.

Table 4.1: Inputs for the Box-Benken design

Factor	-1	0 (middle point)	1
Initial concentration (ppm)	137.3	364.7	466.3
pH	2.3	3.4	4.8
Temperature (°C)	25	40	55
L/S	66.6	100	200

Thus, 27 experiments were generated on Statistica 7 program as indicated in Table D.1, in the Appendix D. These tests were made using 25 mL of Cr(III) solution in the conditions indicated in Table 4.2., for 3 h of contact.

## 5. Results and discussion

### 5.1 Surface chemical modification

#### 5.1.1 Effect of particle size

Particle size of the adsorbent is an important factor that affects the adsorption process. The sorption capacity as well as the time required to reach equilibrium conditions may be determined by the particle size of the adsorbent tested. Therefore, a particle size fraction must be chosen in order to ensure the best performance of the adsorbent before proceeding with its characterization and modification. It is desirable that the adsorbent exhibits a small particle sizes thus implying a larger superficial area and less resistance to mass transfer<sup>47</sup>.

The effect of particle size on Cr(III) uptake by raw pine bark is illustrated in Fig. 5.1. From the obtained results, it can be concluded that the adsorption capacity slightly decreases with increasing particle size.

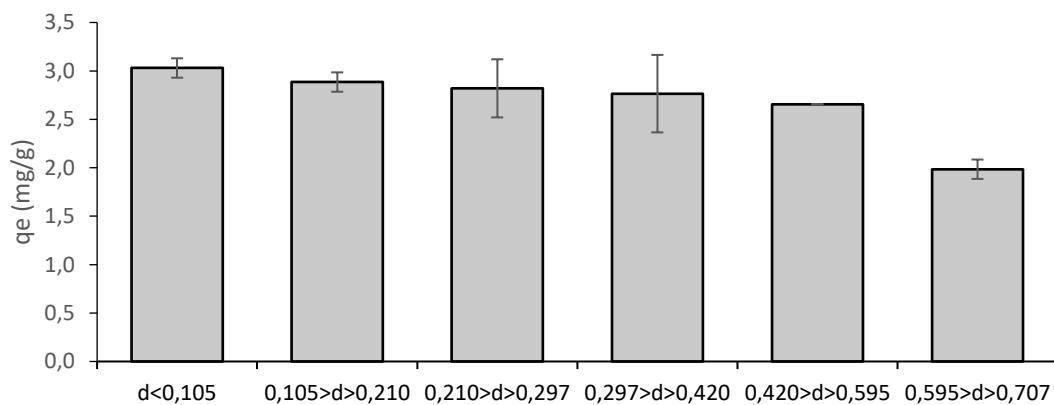


Fig. 5.1: Adsorption test to raw pine bark with different particle sizes (d in mm). ( [Cr(III)] = 500 ppm, pH = 3.2, T = 25°C (room temperature), t = 6 h, L/S = 100 )

Raw pine bark is a lignocellulosic residue with potential to be used as low cost adsorbent in the removal of heavy metals. Low amounts of adsorbed Cr(III) were obtained by using this residue without any treatment as shown in Fig. 5.1. The small capacity of adsorption of the adsorbent in its native form is due to the few active groups present on its surface and its high crystallinity of the material that keeps the heavy metal from other active sites<sup>97,106</sup>. Chemical treatment of pine bark using NaOH (mercerization) and acids to enhance its adsorption capacity will be analyzed in the next sections. A particle size adsorbent fraction varying between 0.21 and 0.60 mm was selected for the subsequent studies.

#### 5.1.2 Effect of chemical treatment – NaOH (mercerization)

In the previous results, it was observed that untreated pine bark has small capacity for adsorption of Cr(III). However, it was reported by Demirbas et al.<sup>56</sup> that this capacity could be

enhanced through a chemical modification of the adsorbent. One of its modifications is using an alkali solution as Ofomaja et al.<sup>106</sup> (2009) suggested.

Therefore, in order to chemically modify a sample of raw pine bark to obtain a better adsorption capacity and removal efficiency, different concentrations of sodium hydroxide were tested. The results can be seen in Fig. 5.2 (a) and (b). These figures show that raw pine bark has the lower adsorption capacity for Cr(III) when compared with samples of pine bark modified with concentrated NaOH solution. For example, the adsorption capacity of the raw adsorbent was doubled when it was treated with 10 % NaOH.

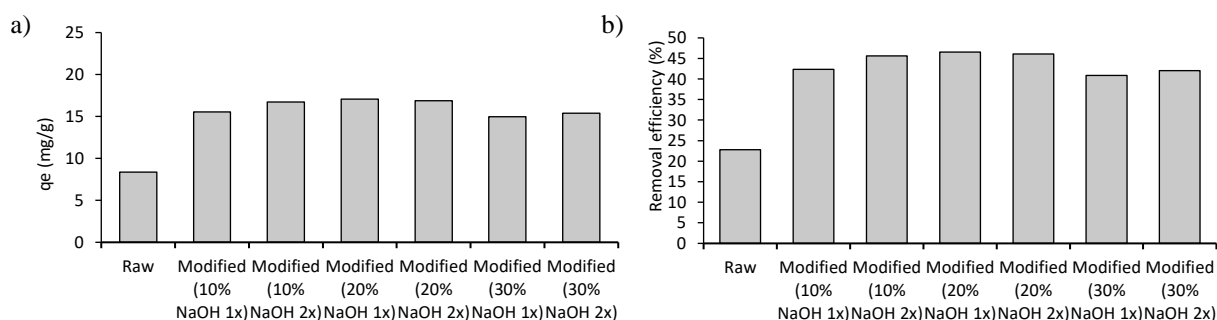


Fig. 5.2: Effect of concentration of NaOH solution for pine bark modification in its adsorption capacity (a) and in its efficiency (b) (Alkali modification: L/S = 30, T= 25 °C (room temperature), t= 16 h. Adsorption tests: L/S= 100, [Cr(III)] = 300 ppm, pH= 3.2, t= 6 h)

In Fig. 5.2 (a) and (b) it can also be seen that there is pine bark treated two times (2x) with the NaOH solution. This second treatment was made subjecting the sample to the same treatment conditions for a second time. It can be concluded that a second treatment does not introduce any enhancement in the adsorption capacity after the first time.

The mercerization process is characterized by the transformation of cellulose I into cellulose II. The latter have hydroxyl groups more accessible turning the material more reactive, what will make the adsorption process to be more efficient. The modification of cellulose I to cellulose II is an irreversible process, due to the fact that cellulose II is thermodynamically more stable than cellulose I. So, during the first treatment with NaOH (1x), cellulose structure will transform from parallel chains (cellulose I) to antiparallel chains (cellulose II). The second treatment (2x), with the same modifying agent, will only transform cellulose I that did not react the first time, not causing changes on the structure already treated and not increasing any further the adsorption capacity<sup>62,63,67,73</sup>.

It is also very interesting to notice that there is a little increasing on adsorption capacity when the concentration of the modifying solution increased from 10% to 20%, as

already observed by Oudiani et al.<sup>73</sup>. However, after that, the adsorption capacity tends to diminish. This was expected because after 10-15% of NaOH solution concentration, degradation starts to happen<sup>63,73</sup>.

In mercerization, the NaOH solution penetrates into the amorphous parts of cellulosic material. After the ideal concentration mentioned above, cellulose II is predominant and, so it is expected more swelling and dissolution to happen from this type of cellulose amorphous. Because the concentration is higher, more sodium ions are expected to penetrate in the structure of the material. As referred by Oudiani et al.<sup>73</sup>, the solvation sphere of sodium hydroxide ions acts to separate cellulose chains, so more than ideal sodium ions on the structure will sever inter and intramolecular bonds, and the material starts degrade<sup>62,73</sup>.

Having those results, it was concluded that the best alkali treatment for further studies was using a solution of 10% (v/v) sodium hydroxide and only applying the treatment once.

### 5.1.3 Effect of chemical treatment – Acids

Another chemical treatment tested was to use of organic and inorganic acid solutions also with the purpose of increasing efficiency metal adsorption. This acid solution will react with the hydroxyl groups presents on cellulose of the lignocellulosic residue and form an ester (reaction of esterification). This reaction will increase the content of carboxylic groups leading to an increase of adsorption.

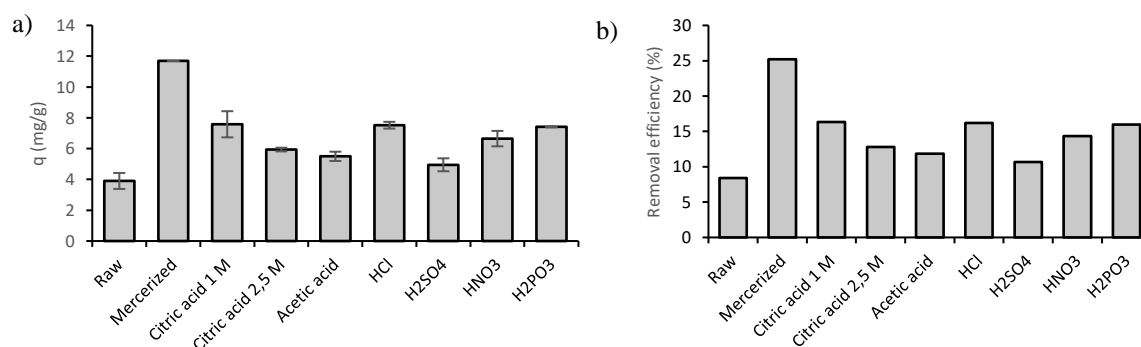


Fig. 5.3: Effect of acid treatment in the adsorption capacity of Cr(III) (a) and in its removal efficiency (b) (Acid modifications: all acids have concentration 1 M (except those indicated), L/S = 30, T= 60 °C, t= 2 h. Adsorption tests: L/S = 100, T = 25 °C (room temperature), t= 6 h, [Cr(III)] = 500 ppm, pH = 5)

Fig. 5.3 (a) and (b) shows an improvement in the adsorption capacity when the native material is treated with an acid solution. This occurred because considering that the adsorption capacity is proportional to the concentration of carboxylic groups present on the adsorbent, the acid treatment should increase its content<sup>97</sup>.

During the acid treatment, for example citric acid, it was necessary to provide heat to turn the acid to its anhydride form through a dehydration reaction. The anhydride reacts with the hydroxyl groups present in cellulose of the material and adds carboxyl groups to the structure. The increment of carboxyl groups enhances the adsorption capacity, like reported by Leyva-Ramos et al.<sup>97</sup> and Pehlivan et al.<sup>9</sup>.

The adsorption capacities, however, did not increase significantly. As Salazar-Rabago et al.<sup>96</sup> stated, inorganic acids used in treatments, such HCl, usually destroy the molecular structures of lignin and polysaccharides (cellulose and hemicellulose) to form the active site where adsorption will occur.

Organic acids also didn't improve significantly the adsorption capacity. This could be due to the fact that during the treatment, those acids may have had secondary reactions with the lignocellulosic material, as it was suggested by Velazquez-Jimenez et al.<sup>95</sup> or the quantity of carboxyl groups created is not sufficient to increase the efficiency of the adsorbent.

In conclusion, the acid treatment only enhanced from 3.9 mg g<sup>-1</sup> to 7.59 mg g<sup>-1</sup>. This is due to the introduction of only one or two carboxylic groups by organic acid, or there is a solubilizing of some components of the residue, using inorganic acids, that allows a re-adjustment of cellulose and turning the hydroxyl groups more accessible for adsorption<sup>95-97</sup>.

The mercerized pine bark (with 10% NaOH) led to the best result in terms of adsorption capacity of Cr(III). Moreover, the treatment with sodium hydroxide also solubilized some components of pine bark, like inorganic acids, besides promoting the changes in the structure, turning the hydroxyl groups more accessible. Therefore, the sorption studies for evaluating the performance of the adsorbent for uptaking Cr(III) were performed with mercerized pine bark using 10% NaOH.

## **5.2 Characterization of adsorbent**

Some tests were made to characterize raw and mercerized pine bark samples in order to assess the effect of chemical treatment on surface and morphological features of the adsorbent. Suitable analytical techniques previously described were used to perform that characterization.

### **5.2.1 BET surface area, porosity and density**

The adsorbent was characterized in terms of its surface properties (surface area and porosity) and density. The results obtained for untreated and treated pine bark are shown in - Table 5.1 Laboratory reports can be seen in the Appendix I.



Table 5.1: Physical properties of raw pine bark and mercerized pine bark

<b>Parameter</b>	<b>Raw material</b>	<b>Modified pine bark</b>
Surface area (m <sup>2</sup> g <sup>-1</sup> )	4.95	8.74
Average pore diameter (nm)	4.97	16.64
Pore volume (cm <sup>3</sup> g <sup>-1</sup> )	0.01	0.04
Density (g cm <sup>-3</sup> )	1.01	0.81

The surface area of the adsorbent increased 1,5 - 2 times after the treatment with sodium hydroxide solution, in accordance with studies reported by Ngah e Hanafiah<sup>21</sup>. This happened due to the fact that some components of the lignocellulosic residue may have solubilized during the mercerization process increasing the porosity and thus the surface area. The same result was also obtained by Gurgel et al.<sup>10</sup> with the mercerization, where the surface area of lignocellulosic biomass was increased after treatment making the hydroxyl groups of the cellulose macromolecules more accessible. This is an important advantage when designing a new low-cost adsorbent because, as Farooq et al.<sup>19</sup> mentioned, a greater surface area will increase the adsorption capacity, due to the fact that the active sites are more available and providing that all other parameters are kept constant.

Table 5.1 also shows that the density of the material also decreased, as result of dissolution of some components. This tendency was also noted by Brás et al.<sup>109</sup> who obtained a decrease on density of the material after mercerization.

In short, it can be said that the alkali treatment changed the morphologic characteristics of pine bark increasing the surface area, average pore diameter as well as pore volume, and caused the decrease of density.

### 5.2.2 Scanning Electronic Microscopy and Energy Dispersive Spectroscopy (SEM-EDS)

Scanning electronic microscopy (SEM) is a very useful tool in the characterization of the material because it allows the visualization of the physical structures on the surface of it. This technique was applied to raw pine bark and alkali modified to better understand the difference between them.

In the Fig. 5.4 are depicted two SEM microscopic pictures from the raw pine bark (Fig.5.4 a) and mercerized pine bark (Fig.5.4 b). Other pictures are shown in Appendix E.

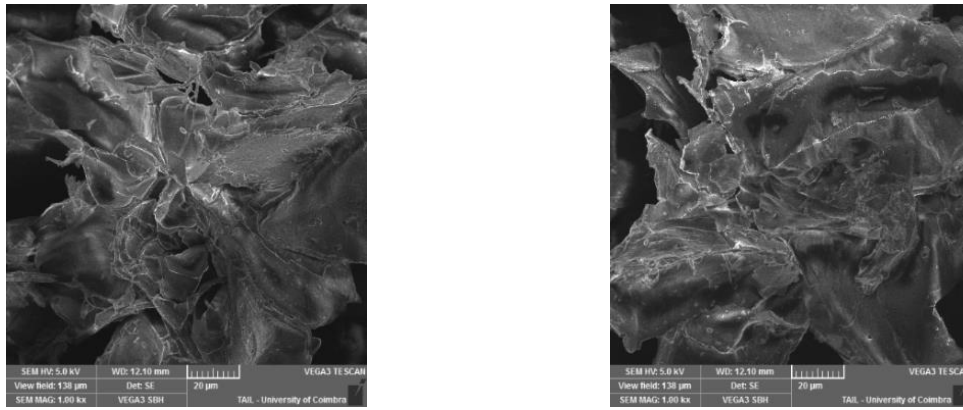


Fig. 5.4: Images obtained by SEM of pine bark (*Pinus pinaster*) raw (a) and mercerized (b) (1000x)

Through those images, it is noticeable that the pine bark is a very heterogeneous material, have complex surface structures and is only slightly porous. Those pores have a basic structure and seem to have low depth, as was also comproved by Brás et al.<sup>109</sup>. This can become a problem for adsorption process which requires a highly porous material of large superficial area. Comparing the raw bark with the mercerized bark, it is observable that the structure of modified pores is slightly smaller.

It was also done an energy dispersive spectroscopy (EDS) after SEM to the raw pine bark and mercerized. This technique, as explained in section 4.3.2, gives an approximated elemental composition of the sample and a relative concentration of them. The spectrums can be seen in Figs. 5.5 and 5.7. The approximate concentration of each element is shown in Table E.1 (Appendix E).

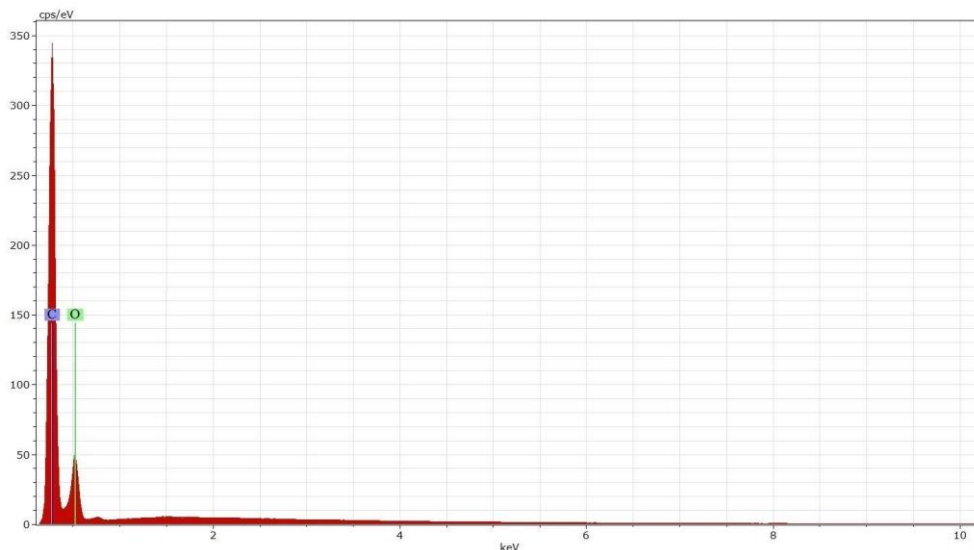


Fig. 5.5: EDS of raw pine bark

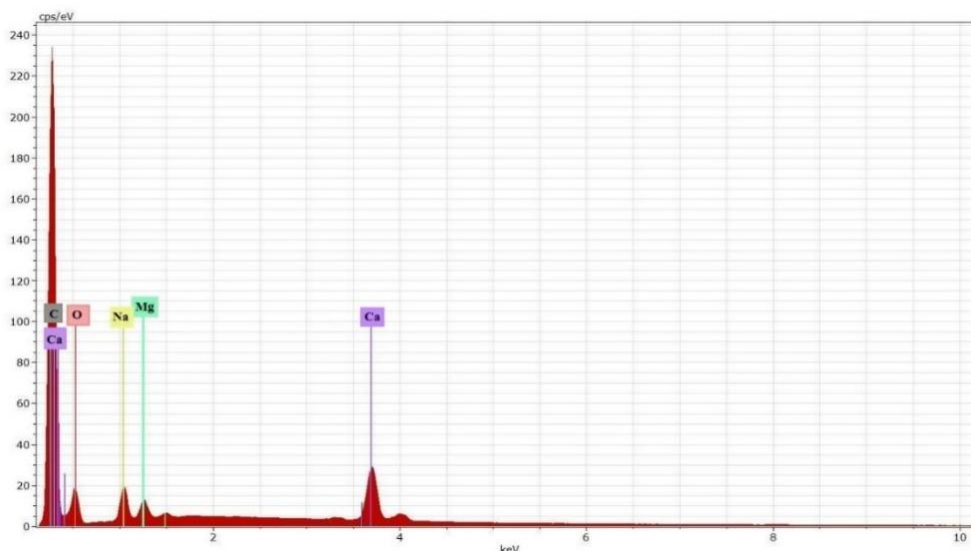


Fig. 5.6: EDS of mercerized pine bark

In Figs 5.5 and 5.6, it is visible that the pine bark is composed of carbon and oxygen as expected for a lignocellulosic residue. After the chemical treatment, it appears on EDS analysis, the presence of sodium on pine bark. This is due to the treatment with sodium hydroxide where there is the formation of Na-cell (ternary complexes of cellulose-sodium-water).

In the mercerized pine bark, there is also noted the presence of other elements such as calcium and magnesium. Those metals appeared because, after mercerization process, the sample was washed with tap water before the ultrapure water until pH constant. Following the quarterly report of “Águas de Coimbra”, the supply company of water, the tap water has in its composition calcium and magnesium (report on Appendix F) and thus some ions may have entered in the structure of the material.

It was also done an EDS analysis on mercerized pine bark after an adsorption of Cr(III) being the result illustrated in Fig. 5.7. This result shows that Cr(III) was indeed adsorbed by the adsorbent appearing in this approximate elemental analysis. It is also noticed that the sodium quantity has diminished. This could be a result of adsorption of this heavy metal on pine bark.

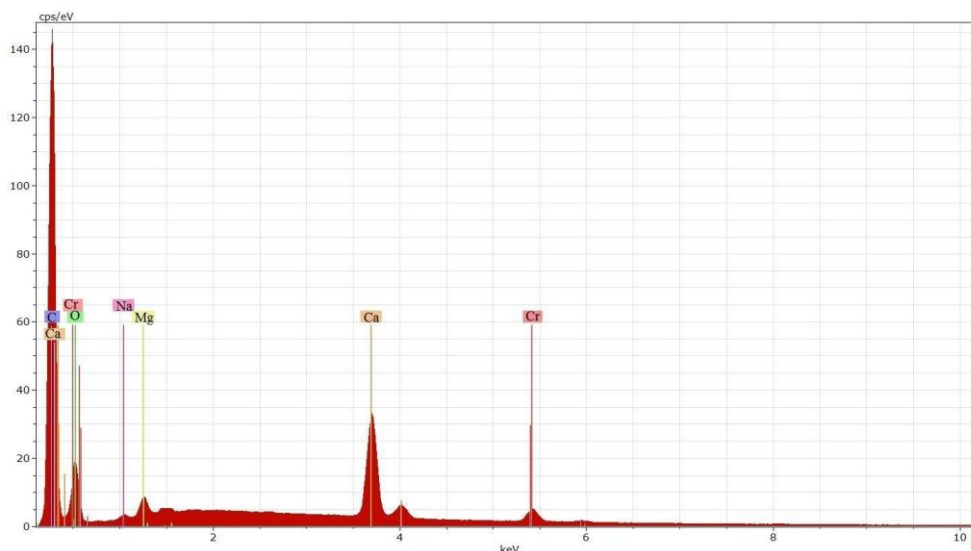


Fig. 5.7: EDS of mercerized pine bark after adsorption of Cr(III)

### 5.2.3 Determination of surface active sites by Boehm Titration method

Metal adsorption is a complex process in which components present on a fluid phase are selectively retained by the adsorbent. This process can be affected by many factors and the mechanisms can involve chemical adsorption, complexation, adsorption-complexation on surface and pores, ion exchange, microprecipitation, heavy metal hydroxide condensation onto the surface and surface adsorption<sup>44,52,56</sup>.

The active sites, like carboxylic, lactonic and phenolic groups, play an important role on adsorption process. So, in order to understand how Cr(III) is going to be adsorbed on pine bark, it is essential to identify and quantify the functional groups involved in the adsorption process. The quantification of the different active sites was determined by Boehm titration methods for the raw and mercerized pine bark being the results depicted in Fig. 5.8<sup>56,110,111</sup>.

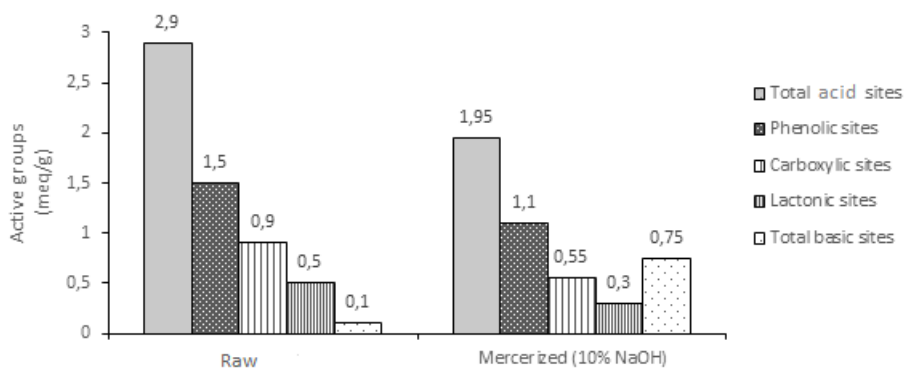


Fig. 5.8: Active sites on raw and mercerized pine bark

In Fig. 5.8 it can be noted that the quantity of total acid sites decreased while the total of basic sites increased. This result is to be expected because it was used a basic solution in order to undergo the pine bark to a chemical treatment. The solution neutralized some acid

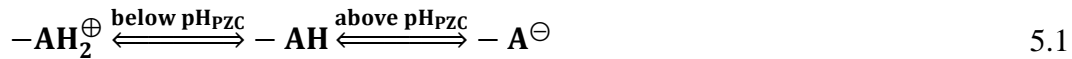
sites (phenolic, carboxylic and lactonic sites) while increasing the basic content. Ofomaja et al. <sup>106</sup> also justified the decreasing of carboxylic groups to the extraction of resin acids that are converted to their sodium salts and the phenolic decreasing to the slight solubility of lignin that contains phenolic compounds.

#### 5.2.4 Point of zero charge

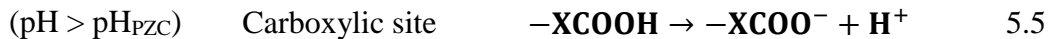
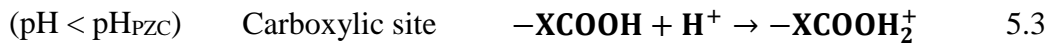
The pH at point of zero charge ( $pH_{PZC}$ ) is the pH at which the adsorbent surface charge is equal to zero, this is, the negative charges on the material surface is equal to the amount of positive charges on the solution<sup>7,102,106,112</sup>.

The point of  $pH_{PZC}$  also indicates the ionization of functional groups on the material and is very helpful when assessing for the ideal pH for the process of metal adsorption. In most cases, adsorption on charged surfaces is strongly influenced by electrostatic attraction and repulsion forces, so pH of the medium is an important parameter to have into attention<sup>19,51</sup>.

When the pH of the solution is higher than the  $pH_{PZC}$ , the functional groups deprotonates and act as a negative specie. However, when the medium pH is lower than the  $pH_{PZC}$  it occurs the inverse, some functional groups suffers protonation and the material acts as positively charged. The Eq. 5.1 illustrates the relation between pH of the medium and the  $pH_{PZC}$ , where  $-AH$  represents the adsorbent with zero charge<sup>19,51,106</sup>.



Leyva-Ramos et al. <sup>97</sup> suggested in his report what would happen to hydroxyl and carboxyl sites when the pH is lower (protonation) and higher (deprotonation) than the  $pH_{PZC}$ , being represented by Eq. 5.2 to 5.5



Considering the importance of  $pH_{PZC}$ , it was evaluated the point of zero charge for the raw and mercerized pine bark whose the results are presented in Fig. 5.9.

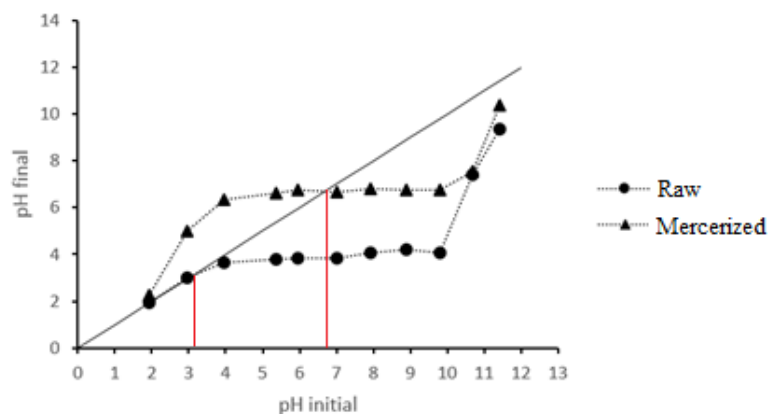


Fig. 5.9: Point of zero charge pH for pine bark raw and mercerized

The  $pH_{PZC}$  is shown at the Fig. 5.9 as the point where the line of the linear function ( $y = x$ ) intersects the data. Therefore, the point of zero charge is, approximately, 3,2 for raw pine bark and for mercerized pine bark is 6,8.

The obtained result means that, when the pH of the solution is below 3,2, the surface of raw pine bark will be charged positively and the adsorption of Cr(III) would not be favored, because the ion of this heavy metal is charged positively and would cause repulsion. However, if the pH of the solution is increased, higher than 3,2, then the pine bark will be charged negatively and the adsorption capacity should likely increase.

The same happens for the mercerized pine bark. Fig. 5.9 shows that it has always a  $pH_{final}$  higher than the  $pH_{initial}$  of the raw pine bark. This could have happened due to some sodium hydroxide still in the sample that would increase the pH and because of the characteristics of the bark after the treatment.

To use the mercerized pine bark for adsorption of Cr(III), the pH of the solution must be close to 6,5 for better results. For pH 6,5 or higher there would be too much  $OH^-$  on the solution and the heavy metal would react with it and precipitate as chromium hydroxide, thus the adsorption would not be favored. However, if the pH of the solution is near the pH of precipitation, the surface charge of residue will not be so positive charged and the adsorption can be favored<sup>19,106</sup>.

Brás et al.<sup>109</sup> also verified that mercerized pine bark has a point of zero charge pH higher than raw pine bark because the treatment increases the polarity of the material surface and thus the surface total energy.

### 5.3 Adsorption studies

After analyzing the physical and chemical relevant characteristics of the pine bark, it can be stated that this lignocellulosic residue has the possibilities to become a good low-cost adsorbent if treated previously with a 10% (v/v) sodium hydroxide solution.

Based on results on the selection of the particle size adsorbent, the best modification treatment to obtain an enhanced adsorption capacity and its chemical and physical characteristics, the subsequent studies were performed to optimize the adsorption process of Cr(III) onto mercerized pine bark.

#### 5.3.1 Effect of contact time

The effect of contact time should be one of the first issues to investigate when studying adsorption processes. This study allows to obtain information on the kinetics and the time required for the system to reach equilibrium conditions, where a maximum uptake of adsorbate is achieved for the tested conditions.

In this test, all the parameters were kept constant (pH, temperature, liquid-to-solid ratio, initial concentration of metal in solution), being the time the only parameter that was varied. The result can be seen in Fig. 5.10.

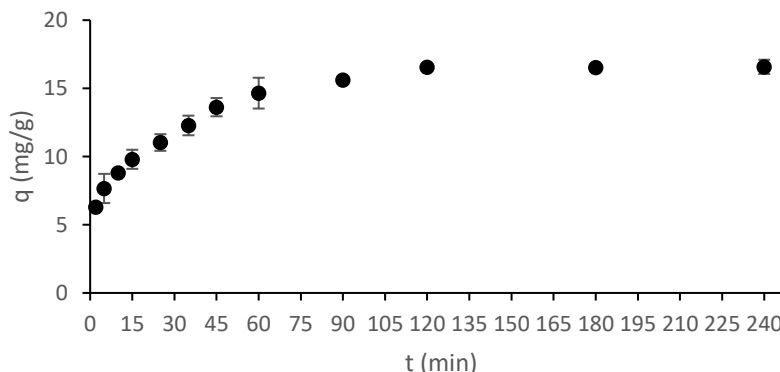


Fig. 5.10: Effect of contact time on Cr(III) removal. (L/S= 100, T= 25°C (room temperature), t= 4 h, [Cr(III)]= 500 ppm, pH= 3.2)

It is observed from Fig. 5.10 that the adsorption of Cr(III) by mercerized pine bark is very fast on the first minutes, becoming slower with the lapse of time and reaching an equilibrium after 180 min (3 h). Parab et al.<sup>84</sup> also observed this behavior in the study on adsorption of Cr(III) onto coir pit where an equilibrium time of 3 h was found.

A similar trend in kinetic studies involving the adsorption of heavy metals on lignocellulosic residues was also reported by other researchers. As Pehlivan et al.<sup>9</sup>, Sen et al.<sup>112</sup>, Parab et al.<sup>84</sup> e Hokkanen et al.<sup>57</sup> explained, the quick uptake of metal on the first minutes occurred due to the fact that there were many functional groups (active sites) on the

adsorbent surface that could bind the metal. After that time, it was achieved an equilibrium between the adsorbent and the adsorbate, this is, the active sites were saturated with heavy metal and the maximum uptake was reached.

Based on these results, the contact time was set to 3h in all further adsorption experiments.

### 5.3.2 Effect of initial pH

The pH of the solution is an important factor to be controlled in the adsorption process. This parameter will not only affect the adsorbate (speciation of the same), but will also influence the adsorbent (its active sites).

To find the optimum pH for Cr(III) removal using a modified pine bark, adsorption tests with the initial pH of the solution varying from 2 to 5,5 were performed. It was not tested pH higher than 5,5 because Cr(III) precipitates in the form of metal hydroxide. The effect of initial pH on the sorption capacity is illustrated in Fig. 5.11.

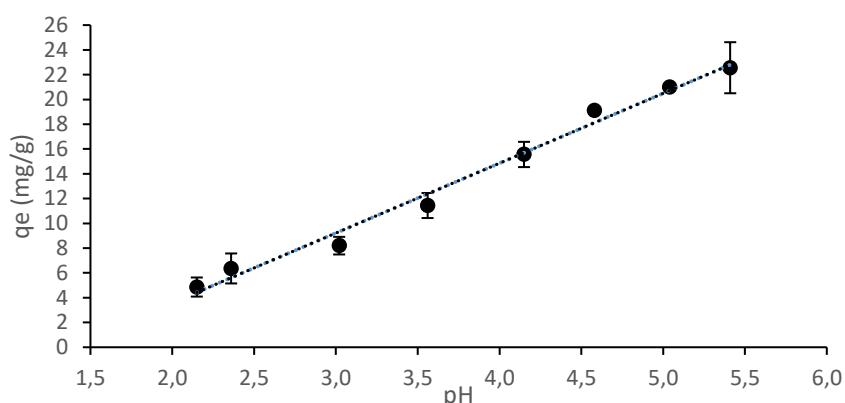


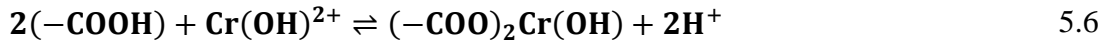
Fig. 5.11: Effect on pH on Cr(III) removal. (L/S= 100, T= 25 °C (room temperature), t= 4 h, [Cr(III)]= 500 ppm)

The adsorption of Cr(III) on mercerized pine bark increased approximately from 4 mg g<sup>-1</sup> to 22 mg g<sup>-1</sup>, with the increase of pH from 2 to 5,5, respectively. The pH of the solution, as said before, it will influence the active sites present in the adsorbent surface. At low pH, the binding sites will be, most likely, protonated resulting in poor heavy metal binding and there will be a higher concentration of H<sup>+</sup> on the solution that will compete with Cr(III) ions, as it was suggested by Anirudhan et al.<sup>4</sup> and Pehlivan et al.<sup>4,9</sup>.

Gardea-Torresday et al.<sup>3</sup> reported that the trend in pH dependency suggests the metal ion binding to the functional groups present in the adsorbent by ion-exchange mechanism. For example, the carboxylic groups have the ionization constants (pKa) reported to be between pH 3 and 4, therefore, at pH higher than 4 the hydroxyl group is deprotonated and could bind



Cr(III) cations. This binding could be represented through Eq. 5.6 knowing that, at pH 5, Cr(III) appears in the form of Cr(OH)<sup>2+</sup> (see Fig. 2.1 for the speciation of chromium)<sup>4</sup>.



This tendency occurs not only for carboxylic groups, but for the others as well. At higher pH the deprotonation increases, there are lower H<sup>+</sup> to compete with Cr(III) cation and thus the adsorption capacity will increase<sup>9</sup>.

A limiting pH value of 5 for the adsorption of Cr(III) on mercerized pine bark was then considered. It was not used pH 5,5, even though it obtained a higher adsorption capacity than at pH 5, to guarantee that the Cr(III) ions do not precipitate.

### 5.3.3 Equilibrium adsorption isotherms

Equilibrium studies are important to understand the relationship between the amount of metal ion adsorbed and the metal ion concentration of the aqueous phase, as well as to develop models to compare the performance of different adsorbents. Moreover, equilibrium data are crucial to design and optimize operations in fixed-bed.

Data obtained were modeled with the Langmuir and Freundlich isotherms. The Langmuir model is represented by the Eq. 5.7.

$$q_e = \frac{Q_{\max} \cdot K_L \cdot C_e}{1 + K_L \cdot C_e} \quad 5.7$$

where  $q_e$  is the equilibrium adsorption capacity (mg g<sup>-1</sup>),  $Q_{\max}$  is the maximum adsorption capacity of the adsorbent (mg g<sup>-1</sup>),  $C_e$  is the equilibrium concentration of the adsorbate (ppm) and the  $K_L$  is the Langmuir constant related to the heterogeneity of the adsorbent surface (L mg<sup>-1</sup>)<sup>19,97</sup>.

This model is based on the following assumptions (Parab et al.<sup>84</sup> and Bulut et al.<sup>42</sup>): (i) the adsorbent in study has finite number of identical sites on its surface being them energetically equals; (ii) there is no transmigration of the adsorbate turning the energy of adsorption constant; (iii) the maximum adsorption capacity is when the adsorbent surfaces reaches saturation (monolayer); (iv) the molecules adsorbed in those sites have no interactions between neighboring sites.

The Freundlich isotherm, on the other hand, have different assumptions like considering a heterogeneous surface energies, multilayer adsorption and interaction between adsorbed molecules. This model can be described by Eq 5.8<sup>42,84,113</sup>.

$$q_e = K_f \cdot C_e^{1/n} \quad 5.8$$

where  $q_e$  is the equilibrium adsorption capacity ( $\text{mg g}^{-1}$ ),  $K_f$  is the Freundlich constant that considers multilayer adsorption which related to bond strength ( $\text{mg}^{1-(1/n)} \text{L}^{1/n} \text{g}^{-1}$ ),  $C_e$  is equilibrium concentration of adsorbate (ppm) and  $n$  is the adsorption intensity and indicative of bond energies between metal ion and the adsorbent.

The results of the fitting of both models to experimental data are shown in Fig. 5.12 and 5.13. The values found for the Langmuir and Freundlich model's parameters are presented in Table 5.2. Determination coefficients ( $R^2$ ) of 0,98-0,99 shown in Table 5.2 suggest that the adsorption of Cr(III) on treated pine bark can be well explained by the Langmuir model. Results corresponding to the fitting of the equilibrium data with other isotherm models can be seen on Appendix B (Table B.1).

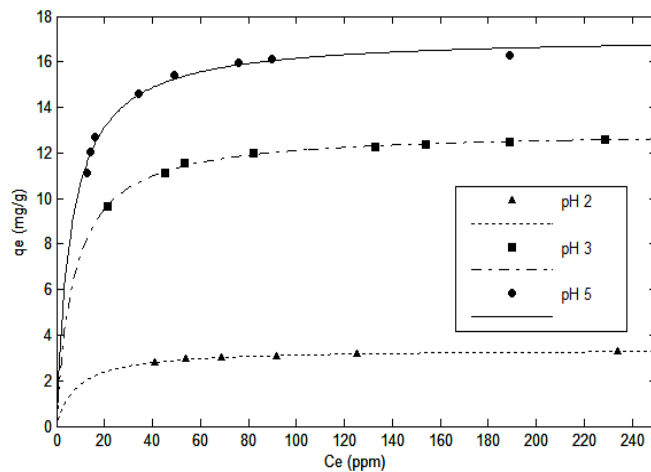


Fig. 5.12: Adsorption isotherms of Cr(III) on mercerized pine bak at 25 °C, for different initial pH values. Symbols represent the experimental data and the lines Langmuir model. ( $L/S= 100$ ,  $t= 4\text{h}$ ,  $[\text{Cr(III)}]= 500 \text{ ppm}$ , adsorbent dosage:20 – 150  $\text{mg/L}$ )

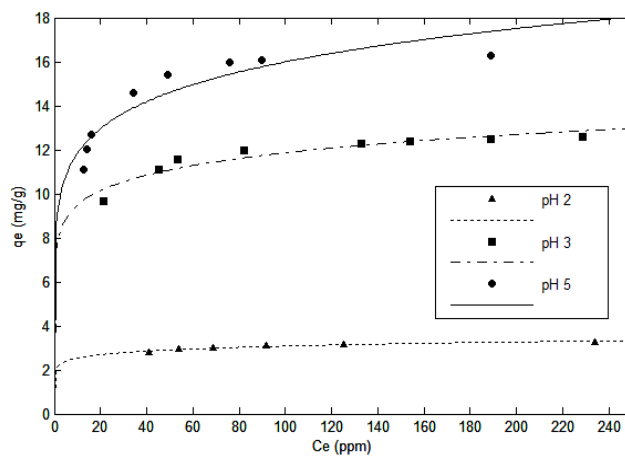


Fig. 5.13: Adsorption isotherms of Cr(III) on mercerized pine bark, at 25 °C, for different initial pH values. Symbols represent the experimental data and the lines Freundlich model. ( $L/S= 100$ ,  $t= 4\text{h}$ ,  $[\text{Cr(III)}]= 500 \text{ ppm}$ , adsorbent dosage:20 – 150  $\text{mg/L}$ )

Table 5.2: Langmuir and Freundlich model and adjust parameters

pH	Langmuir model					Freundlich model				
	$K_L$ (L mg <sup>-1</sup> )	$Q_{max}$ (mg g <sup>-1</sup> )	SSE	R <sup>2</sup>	RMSE	$K_f$ (mg <sup>1-(1/n)</sup> L <sup>1/n</sup> g <sup>-1</sup> )	n	SSE	R <sup>2</sup>	RMSE
2.0	0.12	3.39	0.003	0.977	0.029	2.09	11.82	0.011	0.924	0.053
3.2	0.14	12.99	0.039	0.994	0.080	7.56	10.23	0.716	0.895	0.346
5.0	0.16	17.15	0.418	0.986	0.264	8.76	7.64	4.124	0.859	0.829

As previously mentioned when it was analyzed the effect of pH on the adsorption of Cr(III) on pine bark, an increasing pH will favor the adsorption process. In this study, it was observed an increase of maximum adsorption capacity from 3,39 mg g<sup>-1</sup> for pH 2,0 to 17,15 mg g<sup>-1</sup> for pH 5,0. This result confirms the results obtained for the influence of pH and for the study of point of zero charge pH. During those studies it was concluded that at a lower pH, the surface charge of the material is positively charged repelling the chromium cation. With the increase of pH, the functional groups become less positive and thus obtaining a higher adsorption capacity. So, it can be concluded that the best pH for the adsorption system Cr(III)/mercerized pine bark is approximately 5.

In order to understand if this adsorption process is favorable ( $0 < R_L < 1$ ) or irreversible ( $R_L = 0$ ) was determined the equilibrium parameter  $R_L$  of the Langmuir isotherm trough Eq. 5.9<sup>50,84</sup>.

$$R_L = \frac{1}{1 + K_L \cdot C_0} \quad 5.9$$

where  $K_L$  is the Langmuir constant and  $C_0$  is the initial concentration (500 ppm). For pH 2,3 and 5,  $R_L$  values of 0,02, 0,01 and 0,01 (values near 0), respectively, were found, which means that, even though the process is favorable, is almost irreversible.

During the equilibrium adsorption isotherms, it was also studied the effect of adsorbent dosage. It was noted that higher dosage will lead to a lower adsorption capacity and thus a higher efficiency. Appendix J This happens because with the increase of the amount of adsorbent, it will also increase the number of active sites available for metal binding, as Vankateswarlu et al.<sup>114</sup> and Argun et al.<sup>115</sup> mentioned, and thus the quantity of Cr(III) adsorbed per mass of adsorbent will be lower.

It was noticed that the adsorption capacity has a high dependency on the pH of the medium. So it was proposed the development of a model that would describe the adsorption process as function of initial solution pH. For the development of the model, it was assumed, as starting point, the Langmuir model because it was the model that best fitted the

experimental data. In this model, a polynomial equation was used for explaining the dependence of the parameter corresponding to maximum adsorption capacity ( $Q_{\max}$ ) with initial pH. In the Table 5.3 are listed the  $Q_{\max}$  values for the three pH levels tested.

Table 5.3: Data information for the new model proposal

pH	$Q_{\max}$
2	3.39
3	12.99
5	17.15

The fitting process using the Matlab software led to a quadratic model with a determination coefficient ( $R^2$ ) of 1 (Eq. 5.10).

$$Q_{\max} = -2,51(\text{pH})^2 + 22,13.\text{pH} - 30,85 \quad 5.10$$

Replacing Eq. 5.10 in the Langmuir model yields to Eq. 5.11:

$$q_e = \frac{[-2,51.(\text{pH})^2 + 22,13.\text{pH} - 30,85].K_L.C_e}{1 + K_L.C_e} \quad 5.11$$

For the case in study, with pH,  $C_e$  and  $q_e$  values known, it was only necessary to define the window of search to determine the value of  $K_L$ . For that it was necessary to find the limits of the window and they are expressed in Table 5.4. It was chosen those limiting cases of pH because above pH 5, Cr(III) tends to precipitate and below pH 2 the adsorption of Cr(III) is not favorable. For  $C_e$  and  $q_e$  variables, the limits were stipulated based on data obtained from the equilibrium adsorption isotherms.

Table 5.4: Limits of the window of search

Parameter	Lower limit	Upper limit
pH	2	5
$C_e$	12.66	234.15
$Q_e$	2.78	16.29

The parameter  $K_L$  was calculated for the case limit where pH is equal to 5 obtaining the value of 0,169 L mg<sup>-1</sup>. However, for the other case limit, when the pH is equal to 2, it was not possible to obtain a value, possibly it would need more points for the adjust. Considering only the  $K_L$  obtained, the model equation would be Eq. 5.12 and the plot of values observed as function of values predicted is visible in Fig. 5.14, 5.15 and 5.16 to different pH data from equilibrium isotherms. From these figures it is possible to observe that the model describes well the equilibrium data because the determination coefficient is approximately 1 and the observed values are close to the predicted values.

$$q_e = \frac{[-2,51 \cdot (\text{pH})^2 + 22,13 \cdot \text{pH} - 30,85] \cdot 0,17 \cdot C_e}{1 + 0,17 \cdot C_e} \quad 5.12$$

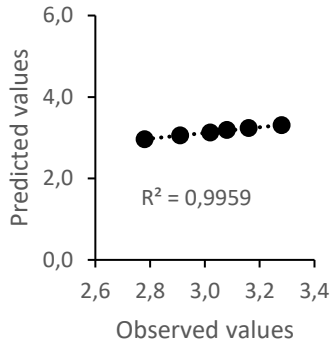


Fig. 5.14: Predicted values of  $q_e$  in function of observed values of  $q_e$  for the new model pH2

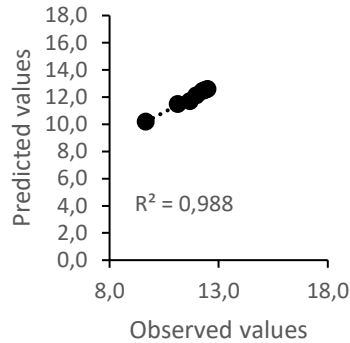


Fig. 5.15: Predicted values of  $q_e$  in function of observed values of  $q_e$  for the new model pH3

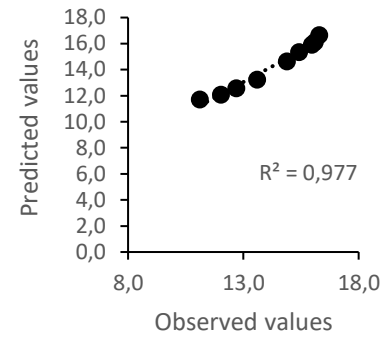


Fig. 5.16: Predicted values of  $q_e$  in function of observed values of  $q_e$  for the new model pH5

### 5.3.4 Design of experiments (DOE)

The design of experiments (DOE) was used in order to reduce the number of experiments, to understand which operational variable would have a major impact on adsorption process, how they interact between each other and develop a mathematical model<sup>107</sup>.

After the screening of the principal effects that could affect the process, it could be applied a more complex and efficient experimental design like Box-Benken for the optimization of those factors, instead of a simpler full factorial.

As variable response was chosen the removal efficiency of Cr(III) while the factors were the initial solution pH, initial concentration of the adsorbate ( $C_0$ ), liquid-to-solid ratio (L/S) and temperature. One advantage of this type of design is the fact that it does not contain combinations in which all factors are simultaneously under extreme conditions and, as mentioned by Ferreira et al.<sup>107</sup>, is the design used for various sorption processes.

The total number of experiments were estimated using Eq. 5.13 and the combination of factors were given by the software Statistica7 and can be consulted on Appendix D.

$$N = 2f(f - 1) + CP \quad 5.13$$

where N is the number of experiments, f is the number of factors and CP is the number of central points. In Fig. 5.17 were represented the Pareto chart of standardized effects at  $p = 0.05$ .

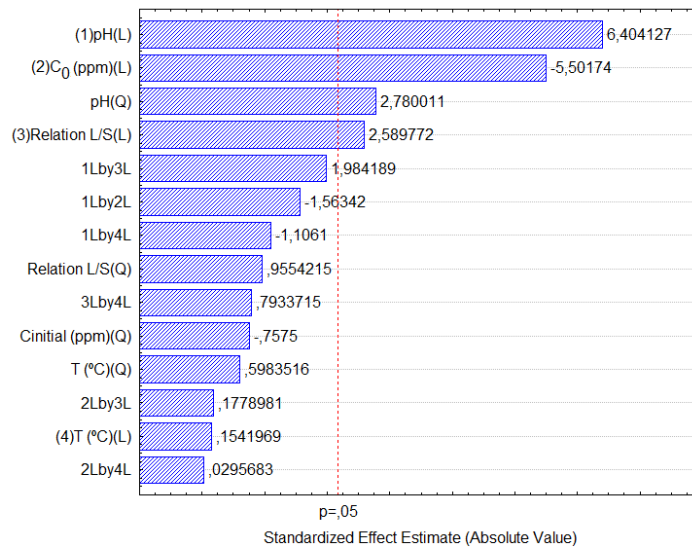


Fig. 5.17: Pareto chart obtained after Box-Benken Design results

Analysing the results plotted in Fig. 5.17 it can be inferred that the pH is the most significant effect on the removal efficiency of Cr(III). There is a linear dependence between the pH and the adsorbent performance, this is, the removal efficiency increases with the increase of pH. Another parameter that affects adsorption, also in a linear relation, is the initial concentration of the adsorbate. However, temperature does not affect the process as much as expected has a negligible effect.

The predictive model obtained is represented by Eq. 5.14 and Fig. 5.18 shows the values observed as function of predicted values. As it can be seen, the values observed are very close to the predicted ones in which the R<sup>2</sup> value found was of 0,906.

$$y = -210,363 + 120,553pH - 11,570pH^2 - 0,120C_0 - 0,036(L/S) \quad 5.14$$

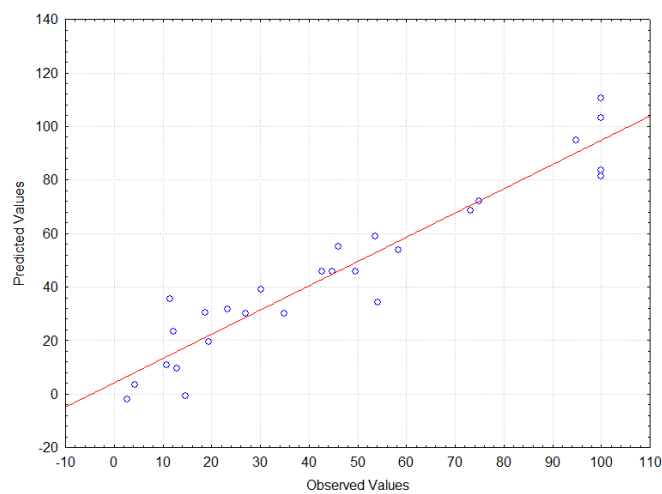


Fig. 5.18: Observed values in function of predicted values

From the surface responses, Fig. 5.19 (a) and (b), it can be observed that the highest removal efficiency of Cr(III) occurs for high pH values as suggested by Pareto chart results.

Lower  $C_0$  values favors the removal efficiency because there is less Cr(III) ions to uptake with the same adsorbent mass, obtaining a higher removal efficiency. Temperature will not influence the removal efficiency as it can be seen on Fig. 5.20 (a) and (b). In Fig. 5.21 it can be seen that higher removal efficiency values are obtained for low initial concentration of Cr(III) and high liquid/solid ratios.

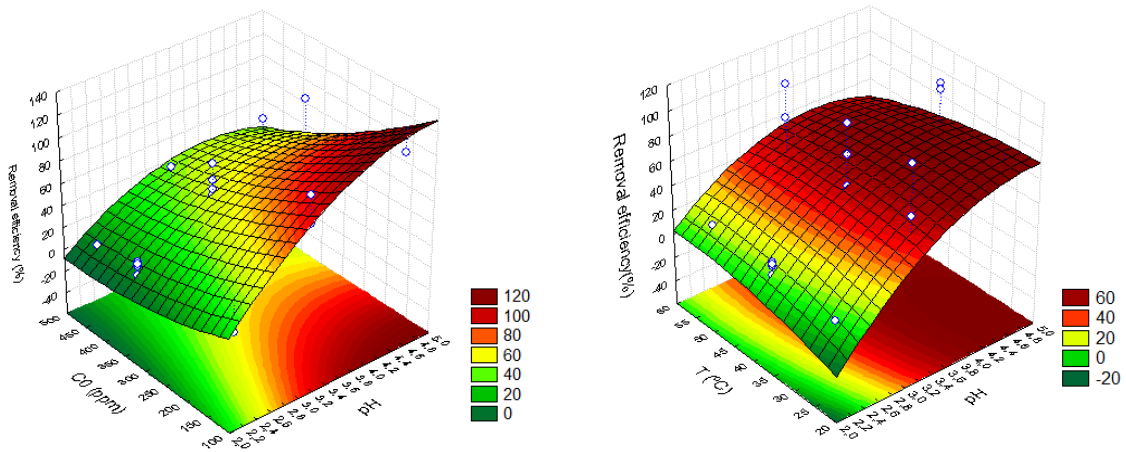


Fig. 5.19: Surface response of the Box-Benken Design (a) the influence of  $C_0$  and pH (b) the influence of temperature and pH

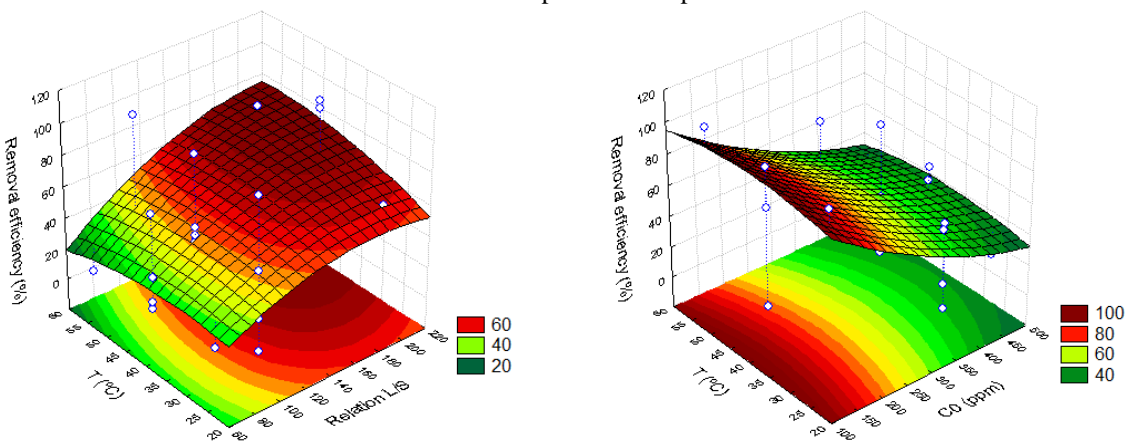


Fig. 5.20: Surface response of the Box-Benken design (a) influence of T and L/S relation (b) influence of T and  $C_0$

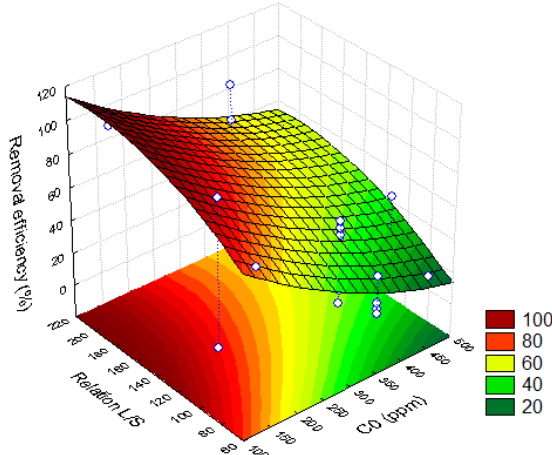


Fig. 5.21: Surface response of the Box-Benken Design. Influence of L/F and  $C_0$  on removal efficiency

## 6. Conclusion and future work

The capacity of raw pine bark for adsorption of Cr(III) ions from aqueous solutions is low and the adsorption capacity is little affected by the particle size before the chemical treatment. The alkali treatment of the adsorbent enabled to improve the uptake of Cr(III) being the most successful treatment when it is used a 10 % (v/v) of sodium hydroxide once. Acid treatment did not provide significant improvements of the adsorption capacity, so it was not studied further.

During the physical characterization of the adsorbent it was noticed that either raw pine bark or mercerized pine bark is not very porous. However the surface area increased after the alkaline treatment. After quantification of active sites of the adsorbent, it was observed that the total acid sites decreased while the basic sites increased when the mercerization was applied, however the acid sites were still a majority. The  $pH_{PZC}$  of raw pine bark is approximately 3,2 while in the mercerized pine bark is 6,5.

In the adsorption studies on mercerized pine bark, the metal uptake reached the equilibrium after 3 h and the optimum pH is 5 being the maximum adsorption equilibrium of 17,15 mg g<sup>-1</sup>. The adsorption isotherms of Cr(III) onto mercerized pine bark, at 25 °C, at different initial pH value are well described by the Langmuir model. It was developed a model, having as reference the Langmuir isotherm, in which the maximum adsorption capacity ( $Q_{max}$ ) depends on pH according to quadratic polynomial. This model provided a good agreement between the observed equilibrium data and predicted ones.

A Box-Benken design for optimization of the batch adsorption of Cr(III) using mercerized pine bark was studied. According to the significance effect obtained in variance analysis, the initial pH was found to have a significant effect on the adsorption of Cr(III) and the temperature had a weak influence on the removal efficiency. Experimental removal efficiencies of Cr(III) were well predicted by a quadratic model where the independent variables were the tested factors (initial pH, initial concentration of Cr(III) and temperature).

The results have demonstrated that mercerized pine bark is a promising adsorbent for removing Cr(III) ions from aqueous solutions.

For future work, the following studies should be implemented:

- It was concluded that before chemical treatment (mercerization and/or acid treatment) the particle size did not influence the adsorption process. One suggestion is to test different particle sizes after the chemical treatment to see if this parameter do not influence the adsorption process.



- Determine the chemical composition of the material (cellulose, hemicellulose, lignin, ashes).
- FTIR before and after adsorption to verify the effect of adsorption of Cr(III) on the functional groups.
- Test the particle size distribution (LDS) and prove the surface charge with zeta potential.
- Realize kinetic studies (study the effect of pH, initial concentration, test models like the pseudo-first and second order).
- Study the effect of the contaminant.
- Study the regeneration of adsorbent.
- Test another modification methods (for example: grafting).

## Bibliography

1. Rengaraj, S., Yeon, K.-H. and Moon, S.-H. (2001). "Removal of chromium from water and wastewater by ion exchange resins". *Journal of Hazardous Materials*. **87**, 273–287.
2. Tchounwou, P. B., Yedjou, C. G., Patlolla, A. K., Sutton, D. J. (2012) "Heavy Metals Toxicity and the environment" in Luch, A. (ed) *Molecular, Clinical and Environmental Toxicology: Volume 2: Clinical Toxicology*. Springer eBooks, 365–396 (doi: 10.1007/978-3-7643-8338-1).
3. Gardea-Torresdey, J. L., Tiemann, K. J., Armendariz, V., Bess-Oberto, L., Chianelli, R. R., Rios, J., Parsons, J. G., Gamez, G. (2000) "Characterization of Cr(VI) binding and reduction to Cr(III) by the agricultural byproducts of *Avena monida* (Oat) biomass". *Journal of Hazardous Material*. **80**, 175–188.
4. Anirudhan, T. S. and Radhakrishnan, P. G. (2007). "Chromium(III) removal from water and wastewater using a carboxylate-functionalized cation exchanger prepared from a lignocellulosic residue". *Journal of Colloid Interface Science*. **316**, 268–276.
5. Sawalha, M. F., Gardea-Torresdey, J. L., Parsons, J. G., Saupe, G. and Peralta-Videa, J. R. (2005) "Determination of adsorption and speciation of chromium species by saltbush (*Atriplex canescens*) biomass using a combination of XAS and ICP-OES". *Microchemical Journal*. **81**, 122–132.
6. Kurniawan, T. A., Chan, G. Y. S., Lo, W. H. and Babel, S. (2006). "Physico-chemical treatment techniques for wastewater laden with heavy metals". *Chemical Engineering Journal*. **118**, 83–98.
7. Salman, M., Athar, M. and Farooq, U. (2015). "Biosorption of heavy metals from aqueous solutions using indigenous and modified lignocellulosic materials" in Lens, P. (ed) *Reviews in Environmental Science Bio/Technology*. **14**, 211–228.
8. O'Connell, D. W., Birkinshaw, C. & O'Dwyer, T. F. (2008). "Heavy metal adsorbents prepared from the modification of cellulose: A review". *Bioresource Technology*. **99**, 6709–6724.
9. Pehlivan, E., Altun, T. and Parlayici, S. (2012) "Modified barley straw as a potential biosorbent for removal of copper ions from aqueous solution". *Food Chemistry*. **135**, 2229–2234.

10. Gurgel, L. V. A., Júnior, O. K., Gil-Freitas, R. P. and Gil, L. F. (2008). "Adsorption of Cu(II), Cd(II), and Pb(II) from aqueous single metal solutions by sugarcane bagasse and mercerized sugarcane bagasse chemically modified with succinic anhydride". *Bioresource Technology*. **99**, 3077-3083.
11. Oliveira, A. (1999). "Boas Práticas Florestais para o Pinheiro Bravo". Centro Pinus - Associação para a Valorização da Floresta.
12. Knapic, S.; Glória, A.; Pereira, H. (2003). "Rendimentos industriais de pinheiro bravo em serração". Centro de Estudos Florestais, Instituto superior de Agronomia, Lisboa.
13. Baral, A. and Engelken, R. D. (2002). "Chromium-based regulations and greening in metal finishing industries in the USA". *Environmental Science Policy*. **5**, 121–133.
14. Mudhoo, A., Garg, V. K., Wang, S. (2012). "Removal of heavy metals by biosorption". *Environmental Chemistry Letters*. **20**, 109-117. (doi:10.1007/s10311-011-0342-2)
15. Förstner, U., Wittmann, G. (1979). *Metal pollution in the aquatic environment*. Springer. (doi: 10.1007/978-3-642-96511-1).
16. Jaramillo, J., Gómez-Serrano, V. and Álvarez, P. M. (2009). "Enhanced adsorption of metal ions onto functionalized granular activated carbons prepared from cherry stones". *Journal of Hazardous Materials*. **161**, 670–676. (doi:10.1016/j.jhazmat.2008.04.009)
17. Argun, M. E. and Dursun, Ş. (2008) "Cadmium removal using activated pine bark". *Journal International Environmental Application and Science*. **3**, 37–42.
18. Lichtfouse, E., Schwarzbauer, J., Robert, D. (2014) "*Environmental Chemistry for a Sustainable World: Volume 2: Remediation of Air and Water Pollution*". Springer. (doi: 10.1007/978-94-007-2439-6)
19. Farooq, U., Kozinski, J. A., Khan, M. A. and Athar, M. (2010). "Biosorption of heavy metal ions using wheat based biosorbents - A review of the recent literature". *Bioresource Technology*. **101**, 5043–5053. (doi: 10.1016/j.biortech.2010.02.030)
20. Abdolali, A., Guo, W. S., Ngo, H. H., Chen, S. S., Nguyen, N. C. and Tung, K. L. (2014). "Typical lignocellulosic wastes and by-products for biosorption process in water and wastewater treatment: A critical review". *Bioresource Technology*. **160**, 57–66 (2014). (doi: 10.1016/j.biortech.2013.12.037)
21. Ngah, W. S. and Hanafiah, M. A. K. M. (2008) "Removal of heavy metal ions from wastewater by chemically modified plant wastes as adsorbents: a review". *Bioresource Journal*. **99**, 3935-3948. (doi: 10.1016/j.biortech2007.06.011)
22. Buasri, A., Chaiyut, N., Tapang, K., Jaroensin, S. and Panphrom, S. (2012). "Biosorption of Heavy Metals from Aqueous Solutions Using Water Hyacinth as a

- Low Cost Biosorbent". *Civil and Environmental Research*. **2**, 17–25.
23. Mohan, D. and Jr. Pittman, C. U. (2006). "Activated carbons and low cost adsorbents for remediation of tri- and hexavalent chromium from water". *Journal of Hazardous Materials*. **137**, 762–811. (doi: 10.1016/j.jhazmat.2006.06.060)
  24. Zayed, A. M. and Terry, N. (2003). "Chromium in the environment: Factors affecting biological remediation". *Plant and Soil*. **249**, 139–156.
  25. Dakiky, M., Khamis, M., Manassra, A. and Mer'eb, M. (2002). "Selective adsorption of chromium(VI) in industrial wastewater using low-cost abundantly available adsorbents". *Advances in Environmental Resources*. **6**, 533–540.
  26. Reddad, Z., Gerente, C., Andres, Y. and Cloirec, P. L. (2003). "Mechanisms of Cr(III) and Cr(VI) removal from aqueous solutions by sugar beet pulp". *Environmental Technology*. **24**, 257–264.
  27. Ying, L. Y., Jiang, H. L., Zhou, S. and Zhou, Y. (2011). "Ionic liquid as a complexation and extraction medium combined with high-performance liquid chromatography in the evaluation of chromium(VI) and chromium(III) speciation in wastewater samples". *Microchemical Journal*. **98**, 200–203. (doi:10.1016/j.microc.2011.01.010)
  28. Patlolla, A. K., Barnes, C., Yedjou, C., Velma, V. R., Tchounwou, P. B. (2009). "Oxidative stress, DNA damage, and antioxidant enzyme activity induced by hexavalent chromium in Sprague-Dawley rats". *Environmental Toxicology*. **24**, 66–73.
  29. Fawell, J. K. and Lund, U. (1996). "Chromium in Drinking-water". *Guidelines for Drinking-water Quality - World Health Organization*. **2**, 1–13.
  30. Sengupta, A. K. and Clifford, D. (1986). "Important process variables in chromate ion exchange". *Environmental Science Technology*. **20**, 149–55.
  31. Kotaś, J. and Stasicka, Z. (2000). "Chromium occurrence in the environment and methods of its speciation". *Environmental Pollution*. **107**, 263–283.
  32. Kumral, E. (2007). "Speciation of Chromium in Waters Via Sol-Gel Preconcentration Prior To Atomic Spectrometric Determination". Master thesis submitted to School of engineering and Sciences of İzmir Institute of Technology.
  33. Barnhart, J. (1997). "Chromium chemistry and implications for environmental fate and toxicity". *Journal of Soil and Sediment Contamination*. **6**, 561–568. (doi: 10.1080/15320389709383589)
  34. Beverskog, B. (1997). "Revised Pourbaix diagrams for Chromium at 25-300 °C". *Corrosion Science*. **39**, 43–57.

35. Bhatnagar, A. and Sillanpää, M. (2010). "Utilization of agro-industrial and municipal waste materials as potential adsorbents for water treatment — A review". *Chemical Engineering Journal*. **157**, 277–296.
36. Sekhar, K. C., Subramanian, S., Modak, J. M. and Natarajan, K. A. (1998). "Removal of metal ions using an industrial biomass with reference to environmental control". *International Journal of Mineral Processing*. **53**, 107–120.
37. Kurniawan, T. A., Chan, G. Y. S., Lo, W. H. and Babel, S. (2006). "Comparisons of low-cost adsorbents for treating wastewaters laden with heavy metals". *Science of the Total Environment*. **366**, 409–426. (doi: 10.1016/j.scitotenv.2005.10.001)
38. Fu, F. and Wang, Q. (2011). "Removal of heavy metal ions from wastewaters: A review". *Journal of Environmental Management*. **92**, 407–418. (doi: 10.1016/j.envman.2010.11.011)
39. Dermentzis, K. (2010). "Removal of nickel from electroplating rinse waters using electrostatic shielding electro dialysis/electrodeionization". *Journal of Hazardous Materials*. **173**, 647–652. (doi: 10.1016/j.hazmat.2009/08/133)
40. Harker, J. H., Coulson, J. M., Backhurst, J. R., Richardson, J. F. (2002) *Chemical Engineering 2*. 5<sup>th</sup> Edition. Great Britain: Butterworth-Heinemann Ltd. (ISBN: 978-0-7506-4445-7)
41. McCabe, W., Smith, J., Harriott, P. (2005) *Unit Operations of Chemical Engineering*. 7<sup>th</sup> Edition. USA: McGraw-Hill Education. (ISBN: 978-0-07-124710-6)
42. Bulut, Y. and Tez, Z. (2007). "Adsorption studies on ground shells of hazelnut and almond". *Journal of Hazardous Materials*. **149**, 35–41. (doi: 10.1016/j.jhazmat.2007.03.044)
43. J. D. Seader, Ernest J. and Henley, D. K. R. (2013) *Separation Process Principles*. 3<sup>rd</sup> Edition. John Wiley & Sons. (ISBN: 978-0-470-48183-7)
44. Ruthven, D. M. (1984) *Principles of Adsorption and Adsorption Processes*. Canada: John Wiley & Sons. (ISBN: 0-471-86606-7)
45. Snyder, L. R. (1968) *Principles of adsorption chromatography*. New York: Marcel Dekker, Inc.
46. Mohapatra, P. K. (2008) *Textbook of Environmental Microbiology*. New Delhi: I K International Publishing House. (ISBN: 978-81-90656-67-2)
47. Park, D., Yun, Y.-S. and Park, J. M. (2010). "The past, present, and future trends of biosorption". *Biotechnology and Bioprocess Engineering*. **15**, 86–102. (doi:10.1007/s12257-009-0199-4)

48. Vandebossche, M., Jimenez, M., Casetta, M. and Traisnel, M. (2015). "Remediation of Heavy Metals by Biomolecules: A Review". *Critical Reviews in Environmental Science and Technology*. **45**, 1644–1704. (doi: 10.1080/10643389.2014.966425)
49. Green, D. W., Perry, R. H. (2007). *Perry's Chemical Engineers' Handbook*. 8<sup>th</sup> Edition. McGraw-Hill Education. (ISBN: 978-0071422949)
50. Rangabhashiyam, S., Anu, N., Nandagopal, M. S. G. and Selvaraju, N. (2014). "Relevance of isotherm models in biosorption of pollutants by agricultural byproducts". *Journal of Environmental Chemical Engineering*. **2**, 398–414. (doi: 10.1016/j.jece.2014.01.014)
51. Worch, E. (2012) *Adsorption Technology in Water Treatment: Fundamentals, Processes, and Modeling*. Germany: De Gruyter (ISBN: 978-3-11-024022-1)
52. Suzuki, M. (1990) *Adsorption engineering*. Tokyo: Kodansha and Elsevier (ISBN: 4-06-201485-8)
53. He, J. and Chen, J. P. (2014). "A comprehensive review on biosorption of heavy metals by algal biomass: Materials, performances, chemistry, and modeling simulation tools". *Bioresource Technology*. **160**, 67–78. (doi: 10.1016/j.biortech.2014.01.068)
54. Electrocorp: Industrial Air Purification Systems and IAQ concerns. (29<sup>th</sup> June 2010) "Why activated carbon works so well" <https://electrocorpairpurification.wordpress.com/2010/06/29/why-activated-carbon-works-so-well/> [18<sup>th</sup> August 2016].
55. Kula, I., Ugurlu, M., Karaoglu, H. and Çelik, A. (2008). "Adsorption of Cd(II) ions from aqueous solutions using activated carbon prepared from olive stone by ZnCl<sub>2</sub> activation". *Bioresource Technology*. **99**, 492–501. (doi: 10.1016/j.biortech.2007.01.015)
56. Demirbas, A. (2008). "Heavy metal adsorption onto agro-based waste materials: A review". *Journal of Hazardous Materials*. **157**, 220–229. (10.1016/j.jhazmat.2008.01.024)
57. Hokkanen, S., Repo, E. and Sillanpaa, M. (2013). "Removal of heavy metals from aqueous solutions by succinic anhydride modified mercerized nanocellulose". *Chemical Engineering Journal*. **223**, 40–47. (doi: 10.1016/j.cej.2013.02.054)
58. Argun, M. E. and Dursun, Ş. (2007). "Activation of pine bark surface with NaOH for lead removal". *Journal International of Environmental Application and Science*. **2**, 5–10.
59. Sarin, V. and Pant, K. K. (2006). "Removal of chromium from industrial waste by using eucalyptus bark". *Bioresource Technology*. **97**, 15–20. (doi: 10.1016/j.biortech.2006.01.015)

- 10.1016/j.biortech.2005.02.010)
60. Dias, J. M., Alvim-Ferraz, M. C. M., Almeida, M. F., Rivera-Utrilla, J. and Sánchez-Polo, M. (2007). "Waste materials for activated carbon preparation and its use in aqueous-phase treatment: A review". *Journal of Environmental Management*. **85**, 833–846. (doi: 10.1016/j.jenvman.2007.07.031)
  61. Miranda, I., Gominho, J., Mirra, I. and Pereira, H. (2012). "Chemical characterization of barks from *Picea abies* and *Pinus sylvestris* after fractioning into different particle sizes". *Industrial Crops Products*. **36**, 395–400. (doi: 10.1016/j.indcrop.2011.10.035)
  62. Rowell, R. (2005) *Handbook of Wood Chemistry and Wood Composites*. USA: CRC Press Taylor & Francis Group. (ISBN: 0-8493-1588-3)
  63. Sjötröm, E. (1993). *Wood chemistry, fundamentals and applications*. 2<sup>nd</sup> Edition. USA: Academic Press (ISBN: 0-12-647481-8)
  64. Harkin, J. M. and Rowe, J. W. (1973) *Bark and its possible uses*. U.S. Department of Agriculture, Forest Service, Forest Products Laboratory. (*FLP-091*).
  65. Miretzky, P. and Cirelli, A. F. (2010). "Cr(VI) and Cr(III) Removal from Aqueous Solution by Raw and Modified Lignocellulosic Materials: A Review". *Journal of Hazardous Materials*. **180**, 1-19. (doi:10.1016/j.jhazmat.2010.04.060)
  66. Suhas, P. J. M., Carrott, M. M. L. and Carrott, R. (2007) "Lignin - from natural adsorbent to activated carbon: A review". *Bioresource Technology*. **98**, 2301–2312. (doi: 10.1016/j.biortech.2006.08.008)
  67. Hill, C. A. S. (2006) *Wood modification: Chemical, Thermal and Other Processes*. England: John Wiley & Sons, Inc. (ISBN: 978-0-470-02172-9)
  68. Bergman, R., Ellman, J., Nichols, J., Bishop, L., Volkman, J., Toste, D., Son, S., Hartwig, J., Sergeev, A. (2011) *Catalytic disproportionation and catalytic reduction of carbon-carbon and carbon-oxygen bonds of lignin and other organic substrates*. US: WO/2011/003029
  69. Sud, D., Mahajan, G. and Kaur, M. P. (2008). "Agricultural waste material as potential adsorbent for sequestering heavy metal ions from aqueous solutions - A review". *Bioresource Technology*. **99**, 6017–6027. (doi: 10.1016/j.biortech.2007.11.064)
  70. RSC Advancing the Chemical Sciences: Chemistry for Biologists. *Carbohydrates*. <http://www.rsc.org/Education/Teachers/Resources/cfb/carbohydrates.htm> [18th August 2016]
  71. IUFRO. (2010). "Global change and mediterranean pines: alternatives for management". *Joint International Meeting*. University of Valladolid at Palencia. 1–92.

72. Kim, B., Gulati, I., Park, J. and Shin, J. S. (2012). "Pretreatment of cellulosic waste sawdust into reducing sugars using mercerization and etherification". *BioResources*. **7**, 5152–5166.
73. Oudiani, A. E., Chaabouni, Y., Msahli, S. and Sakli, F. (2011). "Crystal transition from cellulose I to cellulose II in NaOH treated *Agave americana* L. fibre". *Carbohydrate Polymers*. **86**, 1221–1229. (doi: 10.1016/j.carbpol.2011.06.037)
74. Borysiak, S. and Doczekalska, B. (2005). "X-ray diffraction study of pine wood treated with NaOH". *Fibres and Textiles in Eastern Europe*. **13**, 87–89.
75. Xie, H., King, A., Kilpelainen, I., Granstrom, M. and Argyropoulos, D. S. (2007). "Thorough Chemical Modification of Wood-Based Lignocellulosic Materials in Ionic Liquids". *Biomacromolecules*. **8**, 3740–3748.
76. Eyley, S. S. and Thielemans, W. (2014). "Surface modification of cellulose nanocrystals". *Nanoscale*. **6**, 7764–79. (doi: 10.1039/c4nr01756k)
77. Kaushik, V. K., Kumar, A. and Kalia, S. (2012). "Effect of Mercerization and Benzoyl Peroxide Treatment on Morphology, Thermal Stability and Crystallinity of Sisal Fibers". *International Journal of Textile Science*. **1**, 101–105. (doi: 10.5923/j.textile.20120106.07)
78. Wertz, J. L., Bédué, O. and Mercier, J. P. (2010). *Cellulose Science and Technology*. Lausanne: EPFL Press. (ISBN 978-1-4398-0799-6)
79. Larson, R. A. and Weber, E. J. (1994) *Reaction mechanisms in environmental organic chemistry*. USA: Lewis Publishers.
80. Kirk-Othmer (1990) *Kirk-Othmer Encycl. Chem. Technology: Esterification*. 4th Edition. **9**, 1–37.
81. Pantze, A. (2006) *Studies of Ester Formation on a Cellulose Matrix*. Licentiate thesis in Lulea University of Technology, LTU Skelleftea, Division of Wood Science and Technology.
82. Spurlin, H. M. (1938). "Mechanism of Cellulose Reactions". *Trans. Electrochem. Soc.* **73**, 95.
83. Credou, J. and Berthelot, T. (2014). "Cellulose: from biocompatible to bioactive material". *Journal of Materials Chemistry B*. **2**, 4767–4767. (doi: 10.1039/c4tb00431k)
84. Parab, H., Joshi, S., Shenoy, N., Lali, A., Sarma, U.S., Sudersanan, M. (2006). "Determination of kinetic and equilibrium parameters of the batch adsorption of Co(II), Cr(III) and Ni(II) onto coir pith". *Process Biochemistry*. **41**, 609–615. (doi: 10.1016/j.procbio.2005.08.006)



85. Bellú, S., García, S., González, J. C., Atria, A. M., Sala, L. F., Signorella, S. (2008). "Removal of Chromium (VI) and Chromium (III) from Aqueous Solution by Grain-less Stalk of Corn".
86. Dean, S. A. and Tobin, J. M. (1999). "Uptake of chromium cations and anions by milled peat". *Resources, Conservation and Recycling*. **27**, 151–156.
87. Gardea-Torresdey, J. L., Gonzalez, J. H., Tiemann, K. J., Rodriguez, O. and Gamez, G. (1998). "Phytofiltration of hazardous cadmium, chromium, lead and zinc ions by biomass of *Medicago sativa* (Alfalfa)". *Journal Hazardous Materials*. **57**, 29–39.
88. Li, Y. S., Liu, C. C. and Chiou, C. S. (2004). "Adsorption of Cr(III) from wastewater by wine processing waste sludge". *Journal of Colloid and Interface Science*. **273**, 95–101. (doi: 10.1016/j.jcis.2003.12.051)
89. Ma, W. and Tobin, J. M. (2004). "Determination and modelling of effects of pH on peat biosorption of chromium, copper and cadmium". *Biochemical Engineering Journal*. **18**, 33–40.
90. Nasernejad, B., Zadeh, T. E., Pour, B. B., Bygi, M. E. and Zamani, A. (2005). "Comparison for biosorption modeling of heavy metals (Cr (III), Cu (II), Zn (II)) adsorption from wastewater by carrot residues". *Process Biochemistry*. **40**, 1319–1322. (doi: 10.1016/j.procbio.2004.06.010)
91. Fonseca-correa, R., Giraldo, L. and Moreno-Piraján, J. C. (2013) "Trivalent chromium removal from aqueous solution with physically and chemically modified corncob waste". *Journal of Analytical Applied Pyrolysis*. **101**, 132–141. (doi: 10.1016/j.jaap.2013.01.019)
92. Machado, R., Carvalho, J. R. and Correia, M. J. N. (2002). "Removal of trivalent chromium(III) from solution by biosorption in cork powder". *Journal of Chemical Technology and Biotechnology*. **77**, 1340–1348. (doi: 10.1002/jctb.724)
93. Kumar, A., Rao, N. N. and Kaul, S. N. (2000). "Alkali-treated straw and insoluble straw xanthate as low cost adsorbents for heavy metal removal - preparation, characterization and application". *Bioresource Technology*. **71**, 133–142.
94. Farajzadeh, M. A. and Monji, A. B. (2004). "Treated Rice Bran for Scavenging Cr ( III ) and Hg ( II ) from Acidic Solution". *Journal of the Chinese Chemical Society*. **51**, 751–759.
95. Velazquez-Jimenez, L. H., Pavlick, A. and Rangel-Mendez, J. R. (2013). "Chemical characterization of raw and treated agave bagasse and its potential as adsorbent of metal cations from water". *Industrial Crops Products*. **43**, 200–206. (doi:

- 10.1016/j.indcrop.2012.06.049)
96. Salazar-Rabago, J. J. and Leyva-Ramos, R. (2016). "Novel biosorbent with high adsorption capacity prepared by chemical modification of white pine (*Pinus durangensis*) sawdust. Adsorption of Pb(II) from aqueous solutions". *Journal of Environmental Management*. **169**, 303–312. (doi: 10.1016/j.jenvman.2015.12.040)
  97. Leyva-Ramos, R., Landin-Rodriguez, L. E., Leyva-Ramos, S. and Medellin-Castillo, N. A. (2012). "Modification of corncob with citric acid to enhance its capacity for adsorbing cadmium(II) from water solution". *Chemical Engineering Journal*. **180**, 113–120. (doi: 10.1016/j.cej.2011.11.021)
  98. Oatley, C. W., Nixon, W. C. and Pease, R. F. W. (1965). "Scanning Electron Microscopy". *Adv. Electron. Electron Phys.* **21**, 181–247.
  99. Kutchko, B. G. and Kim, A. G. (2006). "Fly ash characterization by SEM-EDS". *Fuel*. **85**, 2537–2544. (doi: 10.1016/j.fuel.2006.05.016)
  100. Fidel, R. B., Laird, D. A. and Thompson, M. L. (2013). "Evaluation of Modified Boehm Titration Methods for Use with Biochars". *Journal of Environmental Quality*. **42**, 1771–1778. (doi: 10.2134/jeq2013.07.0285)
  101. Goertzen, S. L., Thériault, K. D., Oickle, A. M., Tarasuk, A. C. and Andreas, H. A. (2010). "Standardization of the Boehm titration. Part I. CO<sub>2</sub> expulsion and endpoint determination". *Carbon N. Y.* **48**, 1252–1261. (doi: 10.1016/j.carbon.2009.11.050)
  102. Boehm, H. P. (2002). "Surface oxides on carbon and their analysis: A critical assessment". *Carbon N. Y.* **40**, 145–149.
  103. Boehm, H. P., Diehl, E., Heck, W. and Sappok, R. (1964). "Surface Oxides of Carbon". *Angewandte Chemie International Edition English*. **3**, 669–677.
  104. Boehm, H. P., Setton, R. and Stumpp, E. (1994). "Nomenclature and terminology of graphite intercalation compounds (IUPAC Recommendations 1994)". *Pure Applied Chemistry*. **66**, 1893–1901.
  105. Boehm, H. P. (1994). "Some aspects of the surface chemistry of carbon blacks and other carbons". *Carbon N. Y.* **32**, 759–769.
  106. Ofomaja, A. E., Naidoo, E. B. and Modise, S. J. (2009). "Removal of copper(II) from aqueous solution by pine and base modified pine cone powder as biosorbent". *Journal of Hazardous Materials*. **168**, 909–917. (doi: 10.1016/j.jhazmat.2009.02.106)
  107. Ferreira, S. L. C., Bruns, R. E., Ferreira, H. S., Matos, G. D., David, J. M., Brandão, G. C., Silva, E. G. P., Portugal, L. A., Reis, P. S., Souza, A. S., Santos, W. N. L. (2007). "Box-Behnken design: An alternative for the optimization of analytical methods".

- Analytica Chimica Acta*. **597**, 179–186. (doi: 10.1016/j.aca.2007.07.011)
108. Box, G., Hunter, J. S. and Hunter, W. (2009). *Statistics for Experimenters: Design, Innovation, and Discovery*. New Jersey: John Wiley & Sons. (ISBN 978-0471-71813-0)
  109. Brás, I. P. L. (2005). *Utilização de casca de pinheiro como adsorvente para remoção de pentaclorofenol de águas contaminadas*. Tese de Doutorado em Ciências de Engenharia pela Faculdade de Engenharia da Universidade do Porto.
  110. Lyubchik, S. I., Lyubchik, A. I., Galushko, O. L., Tikhonova, L. P., Vital, J., Fonseca, I. M., Lyubchik, S. B. (2004). "Kinetics and thermodynamics of the Cr(III) adsorption on the activated carbon from co-mingled wastes". *Colloids Surfaces A Physicochemistry Engineering Aspects*. **242**, 151–158. (doi: 10.1016/j.colsurfa.2004.04.066)
  111. Webb, P. A. (2003). "Introduction to Chemical Adsorption Analytical Techniques and their Applications to Catalysis". *MIC Tech. Publ.* **13**, 1–4.
  112. Sen, A., Pereira, H., Olivella, M. A. and Villaescusa, I. (2015). "Heavy metals removal in aqueous environments using bark as a biosorbent". *International Journal of Environmental Science and Technology*. **12**, 391–404. (doi:10.1007/s13762-014-0525-z)
  113. Karniba, M., Kabbani, A., Holail, H. and Olama, Z. (2014). "Heavy metals removal using activated carbon, silica and silica activated carbon composite". *Energy Procedia*. **50**, 113–120. (doi: 10.1016/j.egypro.2014.06.014)
  114. Venkateswarlu, P., Ratnam, M. V., Rao, D. S. and Rao, M. V. (2007). "Removal of chromium from an aqueous solution using *Azadirachta indica* (neem) leaf powder as an adsorbent". *International Journal of Physical Science*. **2**, 188–195.
  115. Argun, M. E., Dursun, S., Ozdemir, C. and Karatas, M. (2007). "Heavy metal adsorption by modified oak sawdust: Thermodynamics and kinetics". *Journal of Hazardous Materials*. **141**, 77–85. (doi: 10.1016/j.jhazmat.2006.06.095)
  116. Krishnani, K. K., Meng, X. and Dupont, L. (2009). "Metal ions binding onto lignocellulosic biosorbent". *Journal of Environmental Science and Health, Part A*. **44:7**, 688–99. (doi: 10.1080/10934520902847810)
  117. Argun, M. E., Dursun, S., Gur, K., Ozdemir, C., Karatas, M. and Dogan, S. (2005). "Nickel adsorption on the modified pine tree materials". *Environmental Technology*. **26:5**, 479–87. (doi: 10.1080/09593332608618532)
  118. Aksas, H., Bouregghda, M. Z., Babaci, H. and Louhab, K. (2015). "Kinetics and

- Thermodynamics of Cr ions Sorption on Mixed Sorbents prepared from Olive Stone and Date pit from Aqueous Solution". *International Journal of Food and Biosystem Engineering*. **1**, 1–8.
119. Argun, M. E. and Dursun, Ş. (2006). "Removal of heavy metal ions using chemically modified adsorbents". *Journal International Environmental Application Science*. **1**, 27–40.
120. Gode, F., Atalay, E. D. and Pehlivan, E. (2008). "Removal of Cr(VI) from aqueous solutions using modified red pine sawdust". *Journal of Hazardous Materials*. **152**, 1201–1207. (doi: 10.1016/j.jhazmat.2007.07.104)
121. Yang, J., Park, Y., Baek, K. and Choi, J. (2010). "Removal of metal ions from aqueous solutions using sawdust modified with citric acid or tartaric acid". *Separation Science and Technology*. **45**, 1963–1974. (doi: 10.1080/01496395.2010.493782)

## 7. Appendixes

### Appendix A - Different adsorption isotherm models and their assumptions

As explained on 2.3.3. Adsorption Isotherms, there are different types of equilibrium adsorption isotherms models that are normally grouped by the three fundamental approaches: kinetic considerations, thermodynamics and potential theory. The most known isotherms are Langmuir and Freundlich. However, there are another isotherms that are derivation of each one, a combination of the two, or try to explain an entirely new approach to adsorption<sup>44,50-52</sup>.

In Table A.1, there are the isotherm models used in this work, as well as their assumptions, being  $q_e$  the equilibrium adsorption capacity ( $\text{mg g}^{-1}$ ) and  $C_e$  equilibrium adsorbate concentration ( $\text{mg L}^{-1}$  or ppm)<sup>50</sup>.

Table A.1: Adsorption isotherm models, their parameters and assumptions<sup>50</sup>

Models	Equation	Parameters	Assumptions
Langmuir	$q_e = \frac{Q_0 \cdot K_L \cdot C_e}{1 + K_L \cdot C_e}$	<p><math>Q_0</math> Maximum adsorption capacity (<math>\text{mg g}^{-1}</math>)</p> <p><math>K_L</math> Langmuir isotherm constant (<math>\text{L mg}^{-1}</math>)</p>	There is a fixed number of well-defined localized sites on the adsorbent where the adsorbate is adsorbed. Each site can only hold one molecule of adsorbate (monolayer adsorption). All sites are energetically equivalent. The adsorbed molecules have no interaction with molecules on neighboring sites. The strength of the intermolecular attractive force decreases with the increase of distance.
Freundlich	$q_e = K_f \cdot C_e^{1/n}$	<p><math>K_f</math> Freundlich isotherm constant (<math>\text{mg}^{1-(1/n)} \text{L}^{1/n} \text{g}^{-1}</math>)</p> <p><math>n</math> Adsorption intensity</p>	Heterogeneous adsorption surfaces. Uniform energy distribution. Reversible adsorption.

Table A.1: Adsorption isotherm models, their parameters and assumptions<sup>50</sup> (continuation)

Models	Equation	Parameters	Assumptions
<b>Redlich-Peterson</b>	$q_e = \frac{K_{RP} \times C_e}{1 + A_{RP} \times C_e^g}$	$K_{RP}$ Redlich-Peterson model isotherm constant (L g <sup>-1</sup> )	Includes features of Langmuir and Freundlich model
<b>Henry's law</b>	$q_e = \frac{K_{RP} \times C_e}{1 + A_{RP}}$	$A_{RP}$ Redlich-Peterson model constant (mg L <sup>-1</sup> ) <sup>g</sup> $g$ Redlich-Peterson model exponent	Special case of Redlich-Peterson model when g=0
<b>Toth</b>	$q_e = \frac{K_T \times C_e}{(A_T + C_e^{T_t})^{1/T_t}}$	$K_T$ Toth equilibrium constant $A_T$ - $T_t$ Toth model exponent	Langmuir modified. Reduce the error between experimental and predictive data. Multilayer adsorption. Liquid-solid adsorption.
<b>Sips</b>	$q_e = \frac{q_{ms} \times K_s \times C_e^{m_s}}{1 + K_s \times C_e^{m_s}}$	$q_{ms}$ Sips maximum adsorption capacity (mg g <sup>-1</sup> ) $K_s$ Sips equilibrium constant (L mg <sup>-1</sup> ) <sup>m<sub>s</sub></sup> $m_s$ Sips model exponent	Freundlich modified. At high adsorbate concentration, it predicts a monolayer adsorption.
<b>Temkin</b>	$q_e = \frac{R \cdot T}{B} \cdot \ln(A_T \cdot C_e)$ $B = \frac{R \cdot T}{b_T}$	$R$ Universal gas constant (8,314 J (mol K) <sup>-1</sup> ) $T$ Temperature (K) $A_T$ Temkin isotherm equilibrium binding constant (L mg <sup>-1</sup> ) $b_T$ Temkin isotherm constant	The decline of the heat of adsorption, as function of temperature, is linear. Predicts the gas equilibria. Good for predict adsorption of heavy metals on liquids. Does not take into account complex phenomenon in liquid adsorption.
<b>Hill</b>	$q_e = \frac{q_{s_H} \cdot C_e^{n_H}}{K_D + C_e^{n_H}}$	$q_{s_H}$ Hill isotherm maximum uptake saturation (mg L <sup>-1</sup> ) $n_H$ Hill cooperativity coefficient of the binding interaction $K_D$ Hill constant	Non-ideal competitive adsorption model. Explain about the binding of different species onto homogeneous substrates. Adsorption as a cooperative phenomenon with the ligand binding ability at one site on the macromolecule, may influence the different binding sites on the same molecule.

Table A.1: Adsorption isotherm models, their parameters and assumptions<sup>50</sup> (continuation)

Models	Equation	Parameters	Assumptions
<b>Fritz-Schlunder</b>	$q_e = \frac{q_{m_{FS}} \cdot K_{FS} \cdot C_e}{1 + q_{m_{FS}} \cdot C_e^{m_{FS}}}$	<p><math>q_{m_{FS}}</math> Fritz-Shlunder maximum adsorption capacity (mg g<sup>-1</sup>)</p> <p><math>K_{FS}</math> Fritz-Shlunder equilibrium constant (L mg<sup>-1</sup>)</p> <p><math>m_{FS}</math> Fritz-Shlunder model exponent</p>	
<b>Koble-Corrigan</b>	$q_e = \frac{a \cdot C_e^n}{1 + b \cdot C_e^n}$	<p><math>a</math> Koble-corrigan parameters L<sup>n</sup> mg<sup>1-n</sup> g<sup>-1</sup></p> <p><math>b</math> (L mg<sup>-1</sup>)<sup>n</sup></p> <p><math>n</math> -</p>	Based on Langmuir and Freundlich. Applied to heterogeneous sorbent surface.
<b>Liu</b>	$q_e = \frac{Q_{max} \cdot K_g \cdot C_e^{n_L}}{1 + K_g \cdot C_e^{n_L}}$	<p><math>Q_{max}</math> Maximum adsorption capacity (mg g<sup>-1</sup>)</p> <p><math>K_g</math> Liu equilibrium constant (L mg<sup>-1</sup>)</p> <p><math>n_L</math> Dimensionless expoente of Liu equation</p>	
<b>Khan</b>	$q_e = \frac{q_s \cdot b_K \cdot C_e}{(1 + b_K \cdot C_e)^{n_K}}$	<p><math>q_s</math> Theoretical isotherm saturation capacity (mg g<sup>-1</sup>)</p> <p><math>b_K</math> Khan isotherm model constant</p> <p><math>n_K</math> Khan model expoent</p>	Generalized isotherm for the bi-solute adsorption from dilute aqueous solution. Derives from Langmuir and Freundlich isotherms.
<b>Dubinin-Radushkevich</b>	$q_e = Q_m \cdot e^{-K\varepsilon^2}$ $\varepsilon = R \cdot T \ln \left( 1 + \frac{1}{C_e} \right)$	<p><math>Q_m</math> Theoretical isotherm saturation capacity (mg g<sup>-1</sup>)</p> <p><math>K</math> Dubinin-Radushkevich isotherm constant related to the adsorption energy (mol<sup>2</sup> (kJ<sup>2</sup>)<sup>-1</sup>)</p> <p><math>\varepsilon</math> Polanyi potential</p> <p><math>T</math> Temperature (K)</p> <p><math>R</math> Gas constant (8,314 J (mol K)<sup>-1</sup>)</p>	Is often applied for the estimation of apparent free energy and characteristics of adsorption. Temperature dependent.

## Appendix B – Isotherm models adjust to adsorption data

With the data information of the equilibrium adsorption isotherm, it was able to test several isotherm models using the program Matlab. After the introduction of the Data on the script, it was used the tool *cftool* where it was introduced the equation of the model (listed in Table A.1) and the adjusted to the data.

The models adjustment parameters are present in Table B.1 where it can be seen similarities between models. This happens because some isotherms constants turn the model equal to another.

Table B.1: Model adjust for isotherm models using Matlab

Particle size	30-70 mesh					
pH	5.0		3.2		2.0	
Model	R <sup>2</sup>	SSE	R <sup>2</sup>	SSE	R <sup>2</sup>	SSE
Langmuir	0.986	0.418	0.994	0.039	0.977	0.003
Freundlich	0.859	4.124	0.895	0.716	0.924	0.011
Redlich-Peterson	0.986	0.418	0.994	0.039	0.977	0.003
Toth	0.986	0.418	0.994	0.039	0.977	0.003
Sips	0.986	0.418	0.994	0.039	0.977	0.003
Temkin	0.892	3.155	0.914	0.588	0.933	0.010
Hill	0.993	0.192	0.995	0.033	0.977	0.003
Fritz- Schlunder	0.993	0.219	0.995	0.033	0.977	0.003
Koble-Corrigan	0.993	0.192	0.995	0.032	0.977	0.003
Liu	0.993	0.192	0.995	0.033	0.977	0.003
Khan	0.992	0.222	0.995	0.033	0.977	0.003
Dubinin-Radushkevich	0.991	0.279	0.995	0.033	0.978	0.003



## Appendix C - State of the art (for other heavy metals)

There are several studies about adsorption of heavy metals onto lignocellulosic residues. On the following tables there are information about adsorption of heavy metals on lignocellulosic residues raw or that received chemical treatment. There is also information on operational conditions for the adsorption of the adsorbate as well as the maximum adsorption capacity of each residue.

Table C.1: Adsorption of other heavy metals besides Cr(III) on lignocellulosic residues without pre-treatment

Adsorbent	Modifying agent	Adsorbate	Q <sub>max</sub> (mg/g)	pH	T (°C)	C <sub>0</sub> (ppm)	L/S (mL/g)	Ref.
Wool	Raw	Cr(VI)	41.15	2	30	100	125	25
Olive cake			4.70					
Sawdust			15.82					
Pine needles			21.50					
Almond shells			10.62					
Cactus leaves			6.78					
Coal			7.08					
Bagasse from sugarcane	Raw	Pb(II)	24.22	6.5	30	20	333.3	116
		Hg(II)	14.0					
		Cu(II)	7.6					
		Cd(II)	3.36					
		Zn(II)	3.27					
		Ni(II)	2.64					
Hazelnut shells	Raw	Ni(II)	3.83	-	25	10-200	100	42
Almond shells			3.11					
		Cd(II)	5.42					
			3.18					
		Pb(II)	16.23					
			5.48					
Neem leaf ( <i>Azadirachta indica</i> )	Raw	Cr(VI)	49.15	7	-	25-125	50	114

Table C.2: Adsorption of other heavy metals besides Cr(III) on lignocellulosic residues alkali pre-treated

Adsorbent	Modifying agent	Adsorbate	Q <sub>max</sub> (mg/g)	pH	T (°C)	C <sub>0</sub> (ppm)	L/S (mL/g)	Ref.
Pine tree cones	NaOH	Cu(II)	17.47	4	24	50	125	106
Pine bar ( <i>Pinus nigra</i> )	NaOH	Pb(II)	49	8	-	100	10	58
Pine bark ( <i>Pinus nigra</i> )	NaOH	Cd(II)	9.6	7	-	35	400	17

Table C.3: Adsorption of other heavy metals besides Cr(III) on lignocellulosic residues with acid pre-treatment

Adsorbent	Modifying agent	Adsorbate	Q <sub>max</sub> (mg/g)	pH	T (°C)	C <sub>0</sub> (ppm)	L/S (mL/g)	Ref.	
Oak sawdust ( <i>Quercus coccifera</i> )	HCl	Cu(II)	3.22	4	40	0.1-150	25	115	
		Ni(II)	3.29	8			33		
		Cr(VI)	1.70	3			17		
Cellulose	Succinic acid	Cu(II)	123.5	-	-	120-540	1	10	
		Cd(II)	164.0						
		Pb(II)	294.1						
Eucalyptus bark	Formaldehyde +HCl	Cr(VI)	7.88	3.41	-	44.5	2	59	
Corncob	Citric acid	Cd(II)	42.88	7	25	20-300	90	97	
Barley straw	Citric acid	Cu(II)	31.71	7	120	63.55	200	9	
Pine bark ( <i>Pinus nigra</i> ) Pine cone	HCl	Ni(II)	20.58	6	-	1-150	20	117	
			1.67						
Olive stones Date pits	H <sub>3</sub> PO <sub>4</sub>	Cr(VI)	56.50	5.6	25	1007- 1246	75	118	
			56.18						
Pine bark ( <i>Pinus nigra</i> )	HCl	Cd(II) Pb(II)	9.54	6	-	30	10	119	
	H <sub>2</sub> SO <sub>4</sub>		10.6						
		8.5	5						
	HNO <sub>3</sub>	9.12	5						
		8.4	5						
		9.24							
	NaOH		11.2	7					
			11.9						
	KOH		10.9	7					
			11.7						
Red pine sawdust ( <i>Pinus nigra</i> )	NaOH	Cr(VI)	15.2	3	25	5.2-52	200	120	
	Tartaric acid		22.6						
Agave bagasse	NaOH	Cd(II) Pb(II) Zn(II)	18.32	5	25	60	1000- 500	95	
									50.12
									20.54
	HCl		12.50						
			42.31						
			12.40						
HNO <sub>3</sub>		7.58							
		32.01							
		10.56							
Sawdust ( <i>Pinus densiflora</i> )	Citric acid	Cd(II)	12.81	4.5	25	34	1200	121	
									11.80
	Tartaric acid	Cu(II)	15.06			19			
							11.19		
		Ni(II)	9.80			18			
							7.63		
		Pb(II)	48.49			62			
							38.33		
	Zn(II)	9.16			20				
			9.22						

## Appendix D – Design of Experiments (DOE)

In the Design of Experiments (DOE), it was studied the influence of diverse factors on the adsorption processes. It was used the program Statistica 7 to design this study, using Box-Benken design, where it was introduced the factors present in Table D.1. The result of the combination is present at Table D.2.

Table D.1: Inputs for the Box-Benken design

Factor	-1	0 (middle point)	1
Initial concentration (ppm)	137.3	364.7	466.3
pH	2.3	3.4	4.8
Temperature (°C)	25	40	55
L/S	66.6	100	200

Table D.2: Result of Box-benken design from DOE using the values of Table 4.A as inputs

	pH	Co (mg/L)	R (L/S)	T (°C)	Efic. Remoção%
1	2,3	137,3	100	40	11,43
2	2,3	364,75	66,6	40	14,71
3	2,3	364,75	100	25	2,67
4	2,3	364,75	100	55	10,71
5	2,3	364,75	200	40	12,87
6	2,3	466,3	100	40	4,31
7	3,4	137,3	66,6	40	74,85
8	3,4	137,3	100	25	100
9	3,4	137,3	100	55	100
10	3,4	137,3	200	40	100
11	3,4	364,75	66,6	25	18,68
12	3,4	364,75	66,6	55	12,13
13	3,4	364,75	100	40	42,67
14	3,4	364,75	100	40	44,89
15	3,4	364,75	100	40	49,55
16	3,4	364,75	200	25	58,33
17	3,4	364,75	200	55	73,1
18	3,4	466,3	66,6	40	19,37
19	3,4	466,3	100	25	23,35
20	3,4	466,3	100	55	27
21	3,4	466,3	200	40	45,96
22	4,8	137,3	100	40	100
23	4,8	364,75	66,6	40	35,02
24	4,8	364,75	100	25	53,69
25	4,8	364,75	100	55	30,23
26	4,8	364,75	200	40	94,79
27	4,8	466,3	100	40	54,15

## Appendix E – SEM-EDS results

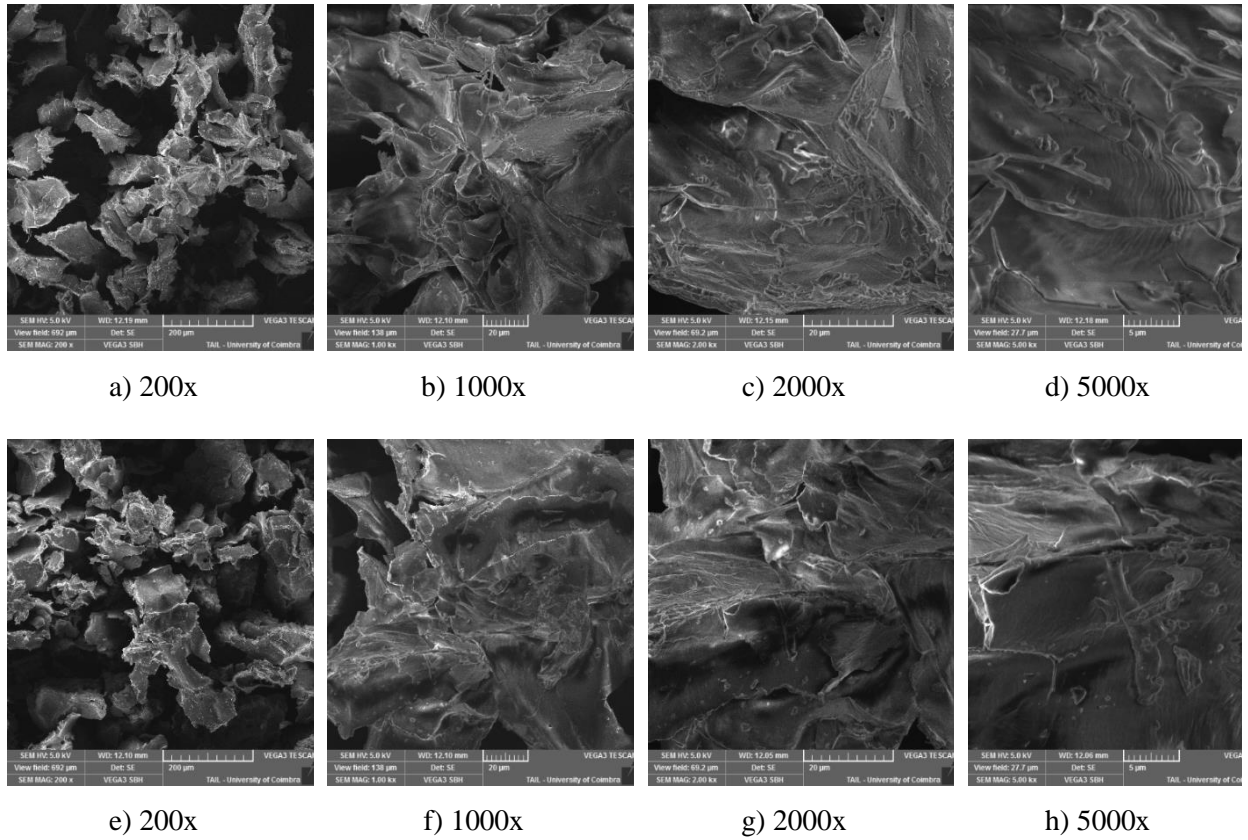


Fig. E.7.1: Results of SEM for raw pine bark (a-b) and for mercerized pine bark (e-h)

Table E.1: EDS results for raw, mercerized and after adsorption pine bark

	Raw		Mercerized		After adsorption	
	(wt. %)	(at.%)	(wt. %)	(at.%)	(wt. %)	(at.%)
<b>Oxygen</b>	22.86	22.47	18.92	15.74	21.97	18.78
<b>Carbon</b>	72.13	77.52	73.0	80.88	68.36	77.85
<b>Sodium</b>			2.19	1.27	0.22	0.13
<b>Aluminium</b>	0.02	0.01			0.19	0.10
<b>Calcium</b>			4.99	1.66	7.11	2.43
<b>Magnesium</b>			0.77	0.42	0.48	0.27
<b>Potassium</b>			0.13	0.04		
<b>Chromium</b>			0	0	1.67	0.44
<b>Total</b>	100	100	100	100	100	100

# Appendix F - Quarterly report of “Águas de Coimbra”



## Controlo de qualidade da água destinada ao consumo humano Município de Coimbra - Zona de Abastecimento Boavista - 1º trimestre 2016

Divulgação dos resultados de qualidade da água distribuída pela AC, Águas de Coimbra, E.M. obtidos na zona de abastecimento de Boavista, segundo o Programa de Controlo de Qualidade de Água (PCQA) aprovado pela autoridade competente (ERSAR - Entidade Reguladora dos Serviços de Águas e Resíduos) e de acordo com o Decreto-Lei n.º 306/2007, de 27 de Agosto.

Parâmetro	Unidades	Nº de análises previstas (PCQA)	% análises realizadas	Valor Paramétrico (VP) fixado pelo DL n.º 306/2007	Valores Obtidos		% análises que cumprem o VP
					Mínimo	Máximo	
<b>CR1 - Controlo de Rotina 1</b>							
Cloro Residual Livre	mg/L Cl	100	100	---	<0,1	0,8	---
Coliformes Totais	N/100 mL	100	100	0	0	5	98,00
Escherichia Coli	N/100 mL	100	100	0	0	1	99,00
<b>CR2 - Controlo de Rotina 2</b>							
Azoto Amoniacal	mg/L NH4	26	100	0,50	<0,02	<0,02	100
Cheiro, a 25°C	Fator diluição	26	100	3	<1	<1	100
Condutividade	µS/cm a 20°C	26	100	2500	86	350	100
Cor	mg/L Pt-Co	26	100	20	<2	<2	100
Manganês	µg/L Mn	26	100	50	<15	20	100
Microrganismos 22°C	N/mL	26	100	sem alteração anormal	0	41	---
Microrganismos 37°C	N/mL	26	100	sem alteração anormal	0	63	---
(*) Nitratos	mg/L NO <sub>3</sub>	27	100	50	2,5	4,3	100
Oxidabilidade	mg/L O <sub>2</sub>	26	100	5	<1,0	1,2	100
pH	Esc. Sorensen	26	100	6,5 - 9	6,8	8,5	100
Sabor, a 25°C	Fator diluição	26	100	3	<1	<1	100
Turvação	NTU	26	100	4	<0,5	0,75	100
<b>CI - Controlo de Inspeção</b>							
(*) 1,2-Dicloroetano	µg/L	1	100	3,0	<0,5	<0,5	100
Alumínio	µg/L Al	2	100	200	32	56	100
(*) Antimónio	µg/L Sb	1	100	5,0	<2	<2	100
(*) Arsénio	µg/L As	1	100	10	<1	<1	100
(*) Benzeno	µg/L	1	100	1,0	<0,5	<0,5	100
Benzo(a)pireno	µg/L	2	100	0,010	<0,005	<0,005	100
(*) Boro	mg/L B	1	100	1,0	<0,10	<0,10	100
(*) Brometos	µg/L BrO <sub>3</sub>	1	100	10	<5	<5	100
(*) Cádmio	µg/L Cd	1	100	5,0	<1,0	<1,0	100
Cálcio	mg/L Ca	2	100	---	5	8	---
Carbono Orgânico Total	mg/L C	2	100	sem alteração anormal	<1,0	2,6	---
Chumbo	µg/L Pb	2	100	10	<3	<3	100
(*) Cianetos	µg/L Cn	1	100	50	<10	<10	100
(*) Cloretos	mg/L Cl	1	100	250	10,5	10,5	100
Clostridium Perfringens	N/100 mL	2	100	0	0	0	100
(*) Tetracloroetano e Tricloroetano	µg/L	1	100	10	<3	<3	100
(*) Tetracloroetano	µg/L	1	100	---	<3	<3	---
(*) Tricloroetano	µg/L	1	100	---	<0,5	<0,5	---
Cobre	mg/L Cu	2	100	2,0	<0,01	<0,01	100
(*) Crómio	µg/L Cr	1	100	50	<5	<5	100
Dureza Total	mg/L CaCO <sub>3</sub>	2	100	---	<17	26	---
Enterococos	N/100 mL	2	100	0	0	0	100
Ferro	µg/L Fe	2	100	200	<50	149	100
(*) Fluoretos	mg/L F	1	100	1,5	0,08	0,08	100
Hidrocarbonetos Aromáticos Policíclicos (HAP)	µg/L	2	100	0,10	<0,010	<0,010	100
HAP Benzo(b)fluoranteno	µg/L	2	100	---	<0,010	<0,010	---
HAP Benzo(ghi)perileno	µg/L	2	100	---	<0,010	<0,010	---
HAP Benzo(k)fluoranteno	µg/L	2	100	---	<0,010	<0,010	---
HAP Indeno(1,2,3-cd)pireno	µg/L	2	100	---	<0,010	<0,010	---
Magnésio	mg/L Mg	2	100	---	<1,0	1,4	---
(*) Mercúrio	µg/L Hg	1	100	1	<0,30	<0,30	100
Níquel	µg/L Ni	2	100	20	<5	<5	100
Nitritos	mg/L NO <sub>2</sub>	2	100	0,5	<0,02	<0,02	100
(*) Pesticidas (PEST) Total	µg/L	1	100	0,50	< 0,014	< 0,014	100
(*) PEST Alacloro	µg/L	1	100	0,10	< 0,014	< 0,014	100
(*) PEST Atrazina	µg/L	1	100	0,10	< 0,014	< 0,014	100
(*) PEST Desetilatrazina	µg/L	1	100	0,10	< 0,014	< 0,014	100
(*) PEST Desetilterbutazina	µg/L	1	100	0,10	< 0,014	< 0,014	100
(*) PEST Diurão	µg/L	1	100	0,10	< 0,014	< 0,014	100
(*) PEST Linurão	µg/L	1	100	0,10	< 0,014	< 0,014	100
(*) PEST Terbutilazina	µg/L	1	100	0,10	< 0,014	< 0,014	100
Radão	Bq/L Rn	2	---	500	<6,6	<7,3	100
(*) α-Total	Bq/L	1	---	0,1	< 0,05	< 0,05	100
(*) β-Total	Bq/L	1	---	1,0	< 0,10	< 0,10	100
(*) Selénio	µg/L Se	1	100	10	< 1	< 1	100
(*) Sódio	mg/L Na	1	100	200	8,8	8,8	100
(*) Sulfatos	mg/L SO <sub>4</sub>	1	100	250	6,8	6,8	100
Trihalometanos (THM) Total	µg/L	2	100	100	<5	11	100
THM Bromodichlorometano	µg/L	2	100	---	<5	6	---
THM Bromofórmio	µg/L	2	100	---	<5	<5	---
THM Clorodibromometano	µg/L	2	100	---	<5	<5	---
THM Clorofórmio	µg/L	2	100	---	<5	5	---

Ensaios e coleta de amostras realizados pelo Laboratório Pró-Qualidade (acreditado pelo IPAC, segundo a NP EN ISO/IEC 17025, e considerado apto para o controlo da qualidade da água para consumo humano pela autoridade competente-ERSAR)

(\*) Parâmetros (conservativos) analisados pela entidade gestora em alta (Águas do Centro Litoral, S.A.)

Informação complementar relativa à averiguação das situações de incumprimento dos Valores Paramétricos (VP):

As não conformidades do parâmetro Coliformes Totais e Escherichia Coli detetadas tratam-se de situações localizadas e pontuais e estão associadas a contaminações com origem na rede predial dos clientes e sem implicações para a saúde pública. Foram tomadas medidas para regularizar estas situações.

O Vogal do Conselho de Administração (Victor Manuel Carvalho dos Santos)

Data  
23 de maio de 2016

## Appendix G – Script of MATLAB used for the adsorption isotherm fitting

For the adjust of the adsorption isotherm models, it was used Matlab. With the data obtained with FAAS, it was determined the equilibrium concentration and the adsorption capacity. That data was introduced on the script and then it was used the Matlab toolbox *cftool* for the adjusts.

On the panel from the toolbox, it was introduced the equation of the model, the limits of search of the parameters and the starting point. Then it was said to apply the model to Data information through iterations. The starting point was changed several times to obtain the best adjust.

The toolbox *cftool* also allowed the creation of a m-file (script) for each adjustment. Below there is the original script where it was introduced the data information of the adsorption process followed by an example of an m-file created after de adjustment of one model.

```
%-----  
% Script for the adjust of isotherms  
%-----  
clc;  
clear all;  
%-----  
% DATA  
%-----  
% Effect of pH  
% 30-60 mesh  
%-----  
pH_5 = [ 188.95    16.29  
        89.75    16.10  
        75.99    15.97  
        49.28    15.42  
        34.20    14.60  
        16.14    12.69  
        14.07    12.02  
        12.66    11.11];  
Ce_pH5 = pH_5 (:,1);  
qe_pH5 = pH_5 (:,2);  
pH_3 = [ 228.60    12.59  
        188.95    12.48  
        153.75    12.38  
        133.10    12.26  
        81.96     11.97  
        53.18     11.58  
        45.38     11.11  
        21.40     9.65];  
Ce_pH3 = pH_3 (:,1);  
qe_pH3 = pH_3 (:,2);  
pH_2 = [234.15    3.28  
        125.10    3.16  
        91.64     3.08
```

```

        68.83    3.02
        53.90    2.97
        41.08    2.78];
Ce_pH2 = pH_2 (:,1);
qe_pH2 = pH_2 (:,2);
%-----
% Effect of particle size
% 140 - 170 mesh
%-----
pH_5_new = [239.95    29.72
            230.51    29.66
            176.75    29.58
             96.70    29.58
             75.75    28.50
             59.90    27.38
             33.30    25.35
             23.73    23.38
             20.36    20.71];
Ce_pH5_new = pH_5_new (:,1);
qe_pH5_new = pH_5_new (:,2);
%-----
% For adjust the isotherm models to Data information it was used cftool
where it was introduced the isotherm models and applied to Data
%-----

cftool

%-----
% Script generated by cftool for the adjustment of Langmuir model to given
data
%-----
% Set up figure to receive data sets and fits
f_ = clf;
figure(f_);
set(f_,'Units','Pixels','Position',[695 95 680 481]);

% Limits of the x-axis.
xlim_ = [Inf -Inf];

% Axes for the plot.
ax_ = axes;
set(ax_,'Units','normalized','OuterPosition',[0 0 1 1]);
set(ax_,'Box','on');
axes(ax_);
hold on;
% --- Plot data that was originally in data set "30 - 60 mesh"
Ce_pH5 = Ce_pH5(:);
qe_pH5 = qe_pH5(:);
h_ = line(Ce_pH5,qe_pH5,'Parent',ax_,'Color',[0.333333 0 0.666667],...
          'LineStyle','none', 'LineWidth',1,...
          'Marker','.', 'MarkerSize',12);
xlim_(1) = min(xlim_(1),min(Ce_pH5));
xlim_(2) = max(xlim_(2),max(Ce_pH5));

% --- Plot data that was originally in data set "140 - 170 mesh"
Ce_pH5_new = Ce_pH5_new(:);
qe_pH5_new = qe_pH5_new(:);
h_ = line(Ce_pH5_new,qe_pH5_new,'Parent',ax_,'Color',[0.333333 0.666667
0],...
          'LineStyle','none', 'LineWidth',1,...
          'Marker','.', 'MarkerSize',12);
xlim_(1) = min(xlim_(1),min(Ce_pH5_new));

```

```

xlim_(2) = max(xlim_(2),max(Ce_pH5_new));

% Nudge axis limits beyond data limits
if all(isfinite(xlim_))
    xlim_ = xlim_ + [-1 1] * 0.01 * diff(xlim_);
    set(ax_,'XLim',xlim_)
else
    set(ax_,'XLim',[10.3871, 242.22289999999998]);
end

% --- Create fit "Langmuir_1"
ok_ = isfinite(Ce_pH5) & isfinite(qe_pH5);
if ~all(ok_)
    warning('GenerateMFile:IgnoringNansAndInfs',...
        'Ignoring NaNs and Infs in data. ');
end
st_ = [0.100000000000000001 15 ];
ft_ = fitttype('(qmax*kl*x)/(1+(kl*x))',...
    'dependent',{'y'},'independent',{'x'},...
    'coefficients',{'kl','qmax'});

% Fit this model using new data
cf_ = fit(Ce_pH5(ok_),qe_pH5(ok_),ft_,'Startpoint',st_);

% Plot this fit
h_ = plot(cf_,'fit',0.95);
set(h_(1),'Color',[1 0 0],...
    'LineStyle','-','LineWidth',2,...
    'Marker','none','MarkerSize',6);
% Turn off legend created by plot method.
legend off;

% --- Create fit "Langmuir_2"
ok_ = isfinite(Ce_pH5_new) & isfinite(qe_pH5_new);
if ~all(ok_)
    warning('GenerateMFile:IgnoringNansAndInfs',...
        'Ignoring NaNs and Infs in data. ');
end
st_ = [0.100000000000000001 15 ];
ft_ = fitttype('(qmax*kl*x)/(1+(kl*x))',...
    'dependent',{'y'},'independent',{'x'},...
    'coefficients',{'kl','qmax'});

% Fit this model using new data
cf_ = fit(Ce_pH5_new(ok_),qe_pH5_new(ok_),ft_,'Startpoint',st_);

% Plot this fit
h_ = plot(cf_,'fit',0.95);
set(h_(1),'Color',[0 0 1],...
    'LineStyle','-','LineWidth',2,...
    'Marker','none','MarkerSize',6);
% Turn off legend created by plot method.
legend off;

% --- Finished fitting and plotting data. Clean up.
hold off;

% Remove labels from x- and y-axes.
xlabel(ax_,'');
ylabel(ax_,'');

```



## Appendix H – mm to Mesh

The unit mesh refers to the number of openings in one inch of screen (in the U.S.). For example, a 4-mesh screen means that there are four little squares across one linear inch of screen. As the size of particles decreases, the number of mesh size increases.

Table H.1: Table of conversion between mesh and millimeters

<b>U.S. Mesh</b>	<b>Millimeters (mm)</b>
3	6,730
4	4,760
5	4,000
6	3,360
7	2,830
8	2,380
10	2,000
12	1,680
14	1,410
16	1,190
18	1,000
20	0,841
25	0,707
30	0,595
35	0,500
40	0,420
45	0,354
50	0,297
60	0,250
70	0,210
80	0,177
100	0,149
120	0,125
140	0,105
170	0,088
200	0,074
230	0,063
270	0,053
325	0,044
400	0,037

# Appendix I - Physical properties of pine bar

## Particle diameter

### Raw pine bark

UGRAN - LED&MAT

ASAP 2000 V2.04

PAGE 1

SAMPLE DIRECTORY/NUMBER: DATA2016/134	START 12:08:13
07/28/16	
SAMPLE ID: NaOH	COMPL 14:45:50
07/28/16	
SUBMITTER: DEQ	REPRT 15:07:19
07/30/16	
OPERATOR: VR	SAMPLE WT:
0.2080 g	
UNIT NUMBER: 1	FREE SPACE:
88.3572 cc	
ANALYSIS GAS: Nitrogen	EQUIL INTRVL:
5 sec	

### ANALYSIS LOG

RELATIVE SATURATION PRESSURE (mmHg)	PRESSURE (mmHg)	VOL ADSORBED (cc/g STP)	ELAPSED TIME (HR:MN)
			1:19
760.986			
0.0012	0.879	-0.0234	1:21
0.0033	2.482	0.0533	1:22
0.0055	4.189	0.0799	1:24
0.0091	6.930	0.1163	1:26
0.0114	8.688	0.1212	1:27
0.0569	43.337	0.4035	1:29
0.0916	69.712	0.5850	1:30
0.1148	87.398	0.6570	1:32
0.1378	104.878	0.7569	1:33
0.1595	121.375	0.8418	1:34
0.1794	136.528	0.9254	1:36
0.1995	151.835	0.9882	1:37
0.2196	167.091	1.0347	1:39
0.2493	189.742	1.1269	1:40
0.2792	212.497	1.2050	1:41
0.2994	227.856	1.2646	1:43
0.3193	243.009	1.3140	1:44
0.3687	280.554	1.4236	1:46
0.5645	429.545	1.8096	1:47
0.7620	579.880	2.1037	1:49
0.8646	657.970	2.2721	1:50
0.9168	697.635	2.4699	1:52
0.9571	728.354	2.6473	1:53
0.9781	744.334	2.8538	1:54
0.9967	758.504	3.9777	2:05
0.9686	737.094	2.7873	2:07
0.9422	716.977	2.5690	2:08

0.9216	701.359	2.4089	2:10
0.9005	685.275	2.3549	2:11
0.8427	641.266	2.2271	2:13
0.8016	610.030	2.1358	2:15
0.7520	572.278	2.0299	2:16
0.7019	534.113	1.9455	2:18
0.6519	496.050	1.8223	2:19
0.6016	457.833	1.7377	2:21
0.5515	419.719	1.6521	2:22
0.5015	381.605	1.5525	2:24
0.4514	343.491	1.4234	2:25
0.4009	305.067	1.3229	2:27
0.3509	267.056	1.1858	2:28
0.1554	118.220	0.6032	2:32

UGRAN - LED&MAT

ASAP 2000 V2.04

PAGE 2

SAMPLE DIRECTORY/NUMBER: DATA2016/134	START 12:08:13
07/28/16	
SAMPLE ID: NaOH	COMPL 14:45:50
07/28/16	
SUBMITTER: DEQ	REPRT 15:07:19
07/30/16	
OPERATOR: VR	SAMPLE WT:
0.2080 g	
UNIT NUMBER: 1	FREE SPACE:
88.3572 cc	
ANALYSIS GAS: Nitrogen	EQUIL INTRVL:
5 sec	

ANALYSIS LOG

RELATIVE SATURATION PRESSURE (mmHg)	PRESSURE (mmHg)	VOL ADSORBED (cc/g STP)	ELAPSED TIME (HR:MN)
0.1034	78.659	0.3681	2:34
0.0489	37.235	0.1310	2:38

UGRAN - LED&MAT

ASAP 2000 V2.04

PAGE 3

SAMPLE DIRECTORY/NUMBER: DATA2016/134	START 12:08:13
07/28/16	
SAMPLE ID: NaOH	COMPL 14:45:50
07/28/16	
SUBMITTER: DEQ	REPRT 15:07:19
07/30/16	
OPERATOR: VR	SAMPLE WT:
0.2080 g	
UNIT NUMBER: 1	FREE SPACE:
88.3572 cc	
ANALYSIS GAS: Nitrogen	EQUIL INTRVL:
5 sec	

BET SURFACE AREA REPORT

BET SURFACE AREA:	4.9481	0.1397	sq. m/g
SLOPE:	0.775857	0.024345	

Y-INTERCEPT: 0.103922 0.004928  
 C: 8.465768  
 VM: 1.136649 cc/g STP  
 CORRELATION COEFFICIENT: 9.98037E-01

RELATIVE PRESSURE	VOL ADSORBED (cc/g STP)	1/[VA(Po/P - 1)]
0.0569	0.4035	0.149673
0.1148	0.6570	0.197484
0.1595	0.8418	0.225414
0.1995	0.9882	0.252226
0.2493	1.1269	0.294751
0.3193	1.3140	0.357031

UGRAN - LED&MAT

ASAP 2000 V2.04  
 PAGE 5  
 SAMPLE DIRECTORY/NUMBER: DATA2016/134 START 12:08:13  
 07/28/16  
 SAMPLE ID: NaOH COMPL 14:45:50  
 07/28/16  
 SUBMITTER: DEQ REPRT 15:07:19  
 07/30/16  
 OPERATOR: VR SAMPLE WT:  
 0.2080 g  
 UNIT NUMBER: 1 FREE SPACE:  
 88.3572 cc  
 ANALYSIS GAS: Nitrogen EQUIL INTRVL:  
 5 sec

SUMMARY REPORT  
 AREA

BET SURFACE AREA: 4.9481  
 sq. m/g  
 SINGLE POINT SURFACE AREA AT P/Po 0.3193: 3.8936  
 sq. m/g

VOLUME

SINGLE POINT TOTAL PORE VOLUME OF PORES LESS THAN  
 5915.0317 A DIAMETER AT P/Po 0.9967:  
 0.006153 cc/g

PORE SIZE

AVERAGE PORE DIAMETER (4V/A BY BET): 49.7385  
 A

**Mercerized pine bark**

UGRAN - LED&MAT

ASAP 2000 V2.04  
 PAGE 1  
 SAMPLE DIRECTORY/NUMBER: DATA2016/135 START 14:37:23  
 07/29/16  
 SAMPLE ID: IN NATURA COMPL 17:14:26  
 07/29/16

SUBMITTER: DEQ  
 07/30/16  
 OPERATOR: VR  
 0.1250 g  
 UNIT NUMBER: 1  
 54.1044 cc  
 ANALYSIS GAS: Nitrogen  
 5 sec

REPRT 15:09:27  
 SAMPLE WT:  
 FREE SPACE:  
 EQUIL INTRVL:

ANALYSIS LOG

RELATIVE SATURATION PRESSURE (mmHg)	PRESSURE (mmHg)	VOL ADSORBED (cc/g STP)	ELAPSED TIME (HR:MN)
			1:28
764.399			
0.0015	1.138	0.0279	1:30
0.0032	2.431	0.0798	1:31
0.0055	4.241	0.1125	1:33
0.0089	6.775	0.1210	1:35
0.0112	8.585	0.1533	1:36
0.0570	43.544	0.5790	1:38
0.0915	69.919	0.8374	1:39
0.1146	87.605	1.0053	1:40
0.1378	105.343	1.1614	1:42
0.1595	121.944	1.2910	1:43
0.1796	137.252	1.4246	1:45
0.1996	152.559	1.5437	1:46
0.2193	167.660	1.6617	1:47
0.2492	190.518	1.8312	1:49
0.2793	213.480	2.0076	1:50
0.2990	228.580	2.1109	1:51
0.3194	244.147	2.1705	1:53
0.3688	281.898	2.4027	1:54
0.5652	432.027	3.1871	1:56
0.7635	583.604	3.7754	1:57
0.8657	661.745	4.0560	1:59
0.9173	701.204	4.2398	2:00
0.9576	732.026	4.4878	2:01
0.9785	747.954	4.6506	2:03
0.9943	760.055	8.1032	2:04
0.9950	760.573	23.4957	2:06
0.9889	755.918	4.8854	2:08
0.9525	728.095	4.3468	2:09
0.9219	704.669	4.1636	2:11
0.8999	687.913	4.0651	2:12
0.8420	643.645	3.8601	2:14
0.8011	612.357	3.7168	2:16
0.7514	574.398	3.5491	2:17
0.7012	536.026	3.3529	2:19
0.6511	497.705	3.1975	2:20
0.6012	459.539	3.0198	2:22
0.5513	421.426	2.8076	2:23
0.5010	382.950	2.6561	2:25
0.4508	344.629	2.4519	2:26
0.4006	306.205	2.2284	2:28
0.3506	267.987	1.9995	2:29

UGRAN - LED&MAT

ASAP 2000 V2.04  
 PAGE 2  
 SAMPLE DIRECTORY/NUMBER: DATA2016/135 START 14:37:23  
 07/29/16  
 SAMPLE ID: IN NATURA COMPL 17:14:26  
 07/29/16  
 SUBMITTER: DEQ REPRT 15:09:27  
 07/30/16  
 OPERATOR: VR SAMPLE WT:  
 0.1250 g  
 UNIT NUMBER: 1 FREE SPACE:  
 54.1044 cc  
 ANALYSIS GAS: Nitrogen EQUIL INTRVL:  
 5 sec

ANALYSIS LOG

RELATIVE SATURATION PRESSURE (mmHg)	PRESSURE (mmHg)	VOL ADSORBED (cc/g STP)	ELAPSED TIME (HR:MN)
0.1503	114.859	0.8926	2:32
0.0986	75.349	0.5611	2:34
0.0480	36.718	0.1690	2:37

UGRAN - LED&MAT

ASAP 2000 V2.04  
 PAGE 3  
 SAMPLE DIRECTORY/NUMBER: DATA2016/135 START 14:37:23  
 07/29/16  
 SAMPLE ID: IN NATURA COMPL 17:14:26  
 07/29/16  
 SUBMITTER: DEQ REPRT 15:09:27  
 07/30/16  
 OPERATOR: VR SAMPLE WT:  
 0.1250 g  
 UNIT NUMBER: 1 FREE SPACE:  
 54.1044 cc  
 ANALYSIS GAS: Nitrogen EQUIL INTRVL:  
 5 sec

BET SURFACE AREA REPORT

BET SURFACE AREA: 8.7378 0.1914 sq. m/g  
 SLOPE: 0.418323 0.010693  
 Y-INTERCEPT: 0.079879 0.002164  
 C: 6.236923  
 VM: 2.007218 cc/g STP  
 CORRELATION COEFFICIENT: 9.98696E-01

RELATIVE PRESSURE	VOL ADSORBED (cc/g STP)	1/[VA(Po/P - 1)]
0.0570	0.5790	0.104332
0.1146	1.0053	0.128756
0.1595	1.2910	0.147022
0.1996	1.5437	0.161529
0.2492	1.8312	0.181297

0.3194

2.1705

0.216210

UGRAN - LED&MAT

ASAP 2000 V2.04

PAGE 5

SAMPLE DIRECTORY/NUMBER: DATA2016/135  
07/29/16

START 14:37:23

SAMPLE ID: IN NATURA  
07/29/16

COMPL 17:14:26

SUBMITTER: DEQ  
07/30/16

REPRT 15:09:27

OPERATOR: VR  
0.1250 g

SAMPLE WT:

UNIT NUMBER: 1  
54.1044 cc

FREE SPACE:

ANALYSIS GAS: Nitrogen  
5 sec

EQUIL INTRVL:

SUMMARY REPORT

AREA

BET SURFACE AREA: 8.7378  
sq. m/g

SINGLE POINT SURFACE AREA AT P/P<sub>0</sub> 0.3194: 6.4308  
sq. m/g

VOLUME

SINGLE POINT TOTAL PORE VOLUME OF PORES LESS THAN  
3868.1121 A DIAMETER AT P/P<sub>0</sub> 0.9950:  
0.036343 cc/g

PORE SIZE

AVERAGE PORE DIAMETER (4V/A BY BET): 166.3717  
A

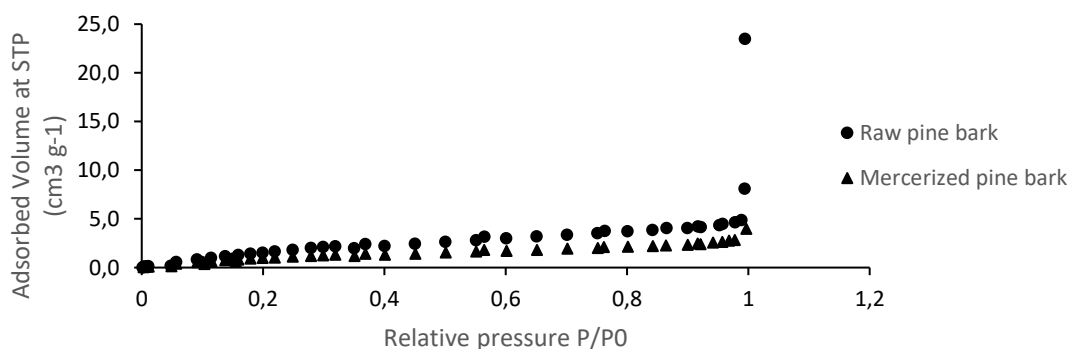


Fig. I.1: Result of BET

# Density

Page 1

AccuPyc 1330 V2.01  
Serial Number: 0  
Density and Volume Report

Sample ID: *NATURA*  
Sample Weight: 0.1940 g  
Temperature: 22.6 C  
Number of Purges: 0  
Cell Volume: 12.2339 cm<sup>3</sup>

Started: 09/09/16 14:05:43  
Completed: 09/09/16 15:04:13  
Equilibration Rate: 0.0500 psig/min  
Expansion Volume: 8.2969 cm<sup>3</sup>

Run#	Volume cm <sup>3</sup>	Deviation cm <sup>3</sup>	Density g/cm <sup>3</sup>	Deviation g/cm <sup>3</sup>	Elapsed Time (h:m:s)
1	0.2031	0.0097	0.9553	-0.0502	0:11:30
2	0.2011	0.0078	0.9646	-0.0410	0:23:14
3	0.1786	-0.0147	1.0661	0.0806	0:35:01
4	0.1926	-0.0007	1.0071	0.0015	0:46:42
5	0.1912	-0.0021	1.0147	0.0091	0:58:22

Average Volume: 0.1933 cm<sup>3</sup>  
Average Density: 1.0056 g/cm<sup>3</sup>

Standard Deviation: 0.0097 cm<sup>3</sup>  
Standard Deviations: 0.0519 g/cm<sup>3</sup>

Page 1

AccuPyc 1330 V2.01  
Serial Number: 0  
Density and Volume Report

Sample ID: *NaOH*  
Sample Weight: 0.1560 g  
Temperature: 23.0 C  
Number of Purges: 0  
Cell Volume: 12.2338 cm<sup>3</sup>

Started: 08/09/16 14:12:52  
Completed: 08/09/16 15:20:59  
Equilibration Rate: 0.0500 psig/min  
Expansion Volume: 8.2969 cm<sup>3</sup>

Run#	Volume cm <sup>3</sup>	Deviation cm <sup>3</sup>	Density g/cm <sup>3</sup>	Deviation g/cm <sup>3</sup>	Elapsed Time (h:m:s)
1	0.1843	-0.0095	0.8467	0.0366	0:12:08
2	0.1829	-0.0108	0.8528	0.0427	0:24:19
3	0.2238	0.0300	0.6971	-0.1130	0:35:45
4	0.1958	0.0021	0.7966	-0.0134	0:47:18
5	0.1820	-0.0117	0.8571	0.0470	1:07:59

Average Volume: 0.1938 cm<sup>3</sup>  
Average Density: 0.8100 g/cm<sup>3</sup>

Standard Deviation: 0.0177 cm<sup>3</sup>  
Standard Deviations: 0.0677 g/cm<sup>3</sup>

XX



## Appendix J - Effect of adsorbent dosage

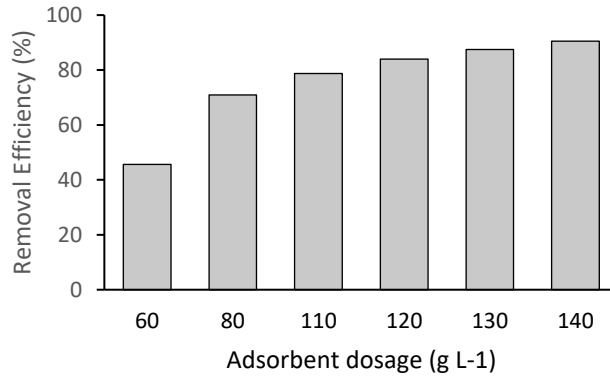


Fig. J.1: Effect of adsorbent dosage for removal of Cr(III) for pH 2

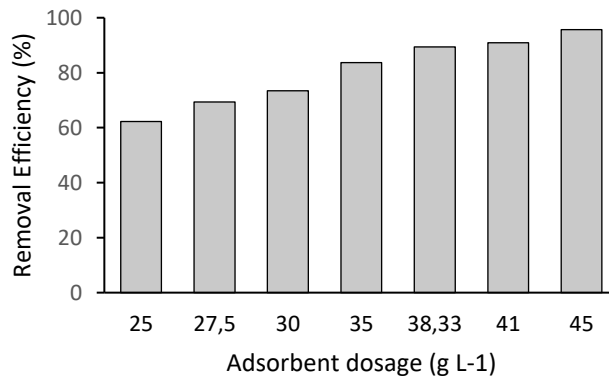


Fig.J.2: Effect of adsorbent dosage for removal of Cr(III) for pH 3

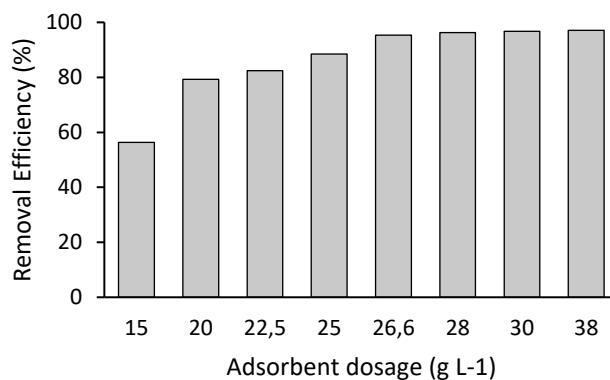


Fig.J.3: Effect of adsorbent dosage for removal of Cr(III) for pH 5

Fig. J.1, J.2 and J.3 reveal that it is necessary more adsorbent for obtain high removal efficiency. With increase of pH, the adsorption of Cr(III) is favored and so it's necessary less adsorbent to obtain high removal efficiency.

This relation, between the adsorbent dosage and removal efficiency ( $R_{\text{eff}}$ ) can be illustrated by Eq. J.1

$$\text{Adsorbent dosage (g L}^{-1}\text{)} = R_{\text{eff}} \left[ \frac{C_0}{K_L \cdot Q_{\text{max}} \cdot C_e} + \frac{C_0}{Q_{\text{max}}} \right]$$

J.1

where  $R_{\text{eff}}$  is the removal efficiency,  $C_0$  is the initial concentration (ppm),  $Q_{\text{max}}$  is the maximum adsorption capacity ( $\text{mg g}^{-1}$ ),  $C_e$  is the equilibrium concentration of the adsorbate (ppm) and  $K_L$  is the Langmuir constant.

- Development of equation J.1

- From the mass balance:

$$\begin{aligned} C_0 \cdot V &= C \cdot V + m \cdot q \\ V(C_0 - C) &= m \cdot q \\ \frac{V}{m} &= \frac{q}{(C_0 - C)} \\ \frac{m}{V} &= \frac{1}{q} \cdot (C_0 - C) \end{aligned}$$

- Langmuir equation:

$$\begin{aligned} q &= \frac{Q_{\text{max}} \cdot K_L \cdot C}{1 + K_L \cdot C} \\ \frac{1}{q} &= \frac{1}{K_L \cdot Q_{\text{max}}} \cdot \frac{1}{C} + \frac{1}{Q_{\text{max}}} \end{aligned}$$

- Substituting  $1/q$  in the mass balance:

$$\frac{m}{V} = (C_0 - C) \cdot \left[ \frac{1}{K_L \cdot Q_{\text{max}}} \cdot \frac{1}{C} + \frac{1}{Q_{\text{max}}} \right]$$

$$\frac{1}{C_0} \cdot \frac{m}{V} = \frac{(C_0 - C)}{C_0} \cdot \left[ \frac{1}{K_L \cdot Q_{\text{max}}} \cdot \frac{1}{C} + \frac{1}{Q_{\text{max}}} \right]$$

$$\frac{m}{V} = \frac{(C_0 - C)}{C_0} \cdot \left[ \frac{1}{K_L \cdot Q_{\text{max}}} \cdot \frac{C_0}{C} + \frac{C_0}{Q_{\text{max}}} \right]$$

$$\text{Adsorbent dosage} = \text{Removal efficiency} \cdot \left[ \frac{1}{K_L \cdot Q_{\text{max}}} \cdot \frac{C_0}{C} + \frac{C_0}{Q_{\text{max}}} \right]$$